LIQUID CRYSTALLINE PROPERTIES OF ETHYL CELLULOSE

by

Derek Richard Budgell

A thesis submitted to the Faculty of Graduate Studies and Research in partial fulfillment of the requirements for the degree of Doctor of Philosophy

Department of Chemistry
McGill University
Montreal, Quebec, Canada

September, 1989

Abstract

The formation and chiroptical properties of liquid crystals of ethyl cellulose (EC) and some related polymers are investigated to determine which features affect the mesophase behaviour.

The onset of mesophase formation is studied by employing literature data on the viscosity / molar mass relationship of several cellulose derivatives, including EC in several solvents, to calculate their molecular dimensions by a recent hydrodynamic theory. The phase separation behaviour is compared with the predictions of theories for both freely-jointed and wormlike chains.

The effects of solvent and degree of substitution (DS) on the cholesteric structure are assessed by studying the chiroptical properties using Circular Reflectance and Optical Rotatory Dispersion (ORD) techniques. The DS strongly influences the helicoidal twist sense, reflection wavelength and response of the reflection wavelength to changes in temperature. Mesophases and cholesteric films of the methyl and n-butyl derivatives of EC are also investigated. The ORD spectra of isotropic EC solutions are found to be strongly influenced by the solvent employed.

Résumé

La formation et les proprietés optiques chirales des cristaux liquides d'ethyl cellulose (EC) et autres polymères voisins sont étudiées afin de déterminer les facteurs qui affectent le comportement mésophasiques.

Pour étudier la formation de la mésophase nous avons employé des données de la littérature concernant les relations viscosité / masse moléculaire de plusiers dérivés - cellulosiques y compris l'EC dans différents solvants. Une théorie hydrodynamique récente a permis de calculer leurs dimensions moléculaires. La séparation de phase est compareé avec les prédictions obtenues selon les théories des chaînes "freely-jointed" et des chaînes en forme de ver.

Les effets du solvant et degré de substitution (DS) sur la structure cholestérique sont étudiés en utilisant des techniques de dichoïsme circulaire apparent et de dispersion rotatoire optique (DRO). Le DS influe fortement sur le sens de l'hélicité, sur la longueur d'onde de la réflection et sur la dépendance de cette longueur d'onde en fonction de la température. Les mésophasee et les films cholestériques de dérivés methyl et n-butyl de l'EC sont également étudiés. Les spectra DRO des solutions isotropes d'EC dépendent fortement du solvant employé.

Foreword

The structure of the thesis requires a note of explanation. The option provided by section 7 of the Guidelines Concerning Thesis Preparation has been utilized.

> "The candidate has the option, subject to the approval of the Department, of including as part of the thesis the text, or duplicated published text (see below), of an original paper, or papers. In this case the thesis must conform to all other requirements explained in Guidelines Concerning Thesis Preparation. Additional material (procedural and design data as well as descriptions of equipment) must be provided in sutficient detail (e.g. in appendices) to allow a clear and precise judgement to be made of the importance and originality of the research reported. The thesis should be more than a mere collection of manuscripts published or to be published. *It must include a general abstract, a full introduction and literature review and a final overall conclusion.* Connecting texts which provide logical bridges between different manuscripts are usually desirable in the interests of cohesion.
>
> It is acceptable for theses to include as chapters authentic copies of papers already published, provided these are duplicated clearly on regulation thesis stationary and bound as an integral part of the thesis. Photographs or other materials which do not duplicate well must be included in their original form. *In such instances, connecting texts are mandatory* and supplementary explanatory material is almost always necessary.
>
> The inclusion of manuscripts co-authored by the candidate and others is acceptable but the candidate is required to make an explicit statement on who contributed to such work and to what extent, and supervisors must attest to the accuracy of the claims, e.g. before the Oral Committee. Since the task of the Examiners is made more difficult in these cases, it is in the candidate's interest to make the responsibilities of authors perfectly clear. Candidates following this option must inform the Department before it submits the thesis for review."

The dissertation is presented in six chapters. Chapters 2, 3, 4 and 5 each describe a unique aspect of the thesis and so have been written in a paper format. Each of these chapters contains an introduction, experimental, results and discussion, conclusion, and reference section. Chapters 1 and 6 present a general introduction and overall conclusion to the thesis. The only co-author on all publications will be the thesis director, Dr. D.G. Gray.

Acknowledgements

The author wishes to express his gratitude to Dr. Derek G. Gray for his support and patience throughout this degree.

The author also thanks:

Mr. B. Harkness and Mr. C. Williams for their assistance in obtaining NMR spectra.

Drs. A.S. Perlin and R.S. Werbowyj for their interest and advice.

Dr. M.A. Whitehead for the use of the statistical analysis program.

Dr. J.-F. Revol for translating the abstract.

Hercules Inc. for supplying product information.

The Natural Sciences and Engineering Research Council of Canada for a Postgraduate Scholarship, the Pulp and Paper Research Institute of Canada for the Otto Maass Memorial Fellowship and the Paper Industries Management Association for the Bernadette du Maulin Memorial Award.

Table of Contents

List of Tables

List of Figures

List of Polymer and Solvent Abbreviations

Cellulose Derivative	Abbreviation
Ethyl cellulose	EC
Triethyl cellulose	TEC
(Ethyl)(methyl)cellulose	EMC
(n-Butyl)(ethyl)cellulose	BEC
(Hydroxypropyl)cellulose	HPC
(Acetoxypropyl)cellulose	APC
Benzoic acid ester of HPC	BzPC
Cellulose acetate	CA
Cellulose triacetate	CTA
Cellulose tricarbanilate	CTC
(Cyanoethoxylpropyl)cellulose	CEPC
Methyl cellulose	MC
Nitrocellulose	NC
Polybenzyl-L-glutamate	PBLG

Solvent	Abbreviation
Dichloroacetic acid	DCA
Dichloromethane	DCM
Dimethylacetamide	DMAC
Dimethylphthalate	DMP
Ethyl methyl ketone	EMK
Monochloroacetic acid	MCA
Tetrachloroethane	TCE
Tetrahydrofuran	THF
Trichloromethane	TCM
Trifluoroacetic acid	TFA

CHAPTER 1

INTRODUCTION

Liquid crystals have traditionally had two main applications: optical display devices such as watches and televisions which are based on low molar mass components and high strength fibres such as Kevlar ® which are manufactured from polymeric liquid crystalline solutions and melts. Polymer liquid crystals capable of functioning as permanent (1, 2), reversible and holographic (3) optical data storage systems have been developed and low molar mass liquid crystals have been polymerized to give systems with macromolecular liquid crystalline properties (4). The discovery that cellulose, an abundantly available biological polymer, and its derivatives are also capable of forming liquid crystals has led to numerous investigations to determine the factors controlling their liquid crystalline properties and potential end-uses. The study of liquid crystal chemistry and physics is essential to an understanding of all these phenomena and further innovations in the field.

1.1 CLASSIFICATION OF LIQUID CRYSTALS

Reflection colours, which are now a recognized trait of certain types of liquid crystals, were first observed in 1861 by Planer in a cholesteryl chloride melt (5), but the publication acknowledged as the true beginning of the liquid crystal field is the report by Reinitzer (6) in 1888 that cholesteryl benzoate exhibits iridescent colours and double refraction when cooled from the melt. Initially called flowing crystals or crystalline liquids the term *flussige kristalle*, meaning liquid crystal, was given to these types of systems in 1904 by Lehmann (7) due to the unusual combination of crystal-like optical properties in a fluid. Another term commonly used to describe these systems is mesophase; it was introduced in 1922 by Freidel (8) to indicate that the phase is a stable one with an order that is intermediate between the unoriented and constantly changing structure of liquids and the long-range permanent order of solid crystals.

Within a few years of the initial liquid crystal discovery so many other compounds had been found which exhibited different mesomorphic properties that a classification system had to be introduced. At an elementary physical level two general categories of liquid crystals are recognized: lyotropic and thermotropic. A lyotropic substance requires

the presence of a solvent as part of the matrix with the liquid crystal forming when, at some critical concentration, the solution changes from an isotropic or disordered state to an anisotropic or ordered one. Thermotropic liquid crystals are formed by the action of heat alone on the pure compound and exist within specific ranges of temperature. While the first low molar mass liquid crystals to be found were thermotropic and the first polymeric liquid crystals were lyotropic, both types of mesophase have been found for low and high molar mass compounds. However, given the vast number of organic compounds that can form lyotropic and / or thermotropic structures (9), a more comprehensive classification system is required.

Freidel (8) originated the modern classification system that differentiates liquid crystals based on their optical properties. The two major categories of liquid crystals are smectics and nematics. These are illustrated in Figure 1.1 along with an isotropic fluid. Smectic mesophases are composed of layers of molecules in which the long axis of each constituent molecule is at an angle to the plane of the layer. Several subgroups of smectics have been classified on the basis of differing optical textures and x-ray diffraction patterns (10). In nematic structures the major axes of the constituent molecules generally point in the same direction but the centres of mass are randomly disposed throughout the mesophase. A special form of the nematic structure is the cholesteric phase which is sometimes called a twisted nematic. Even a small chiral component in the molecular arrangement can cause the twisting one "layer" relative to the next (11). The result is a supramolecular helicoidal network that is represented in a simplified form by Figure 1.2. The name cholesteric is applied to this type of structure because most of the early cholesteric mesophases were derivatives of cholesterol. An important attribute of the cholesteric structure is the rotation of each layer relative to its neighbour. Two layer rotations are possible: left-handed and right-handed. When the rotation of a successive numbers of layers from any given layer is such that the layer director has rotated 360°, the distance between the two layers is called the pitch. For a layer director rotation of 180° the distance is called the half-pitch; this is illustrated in Figure 1.2 as P / 2.

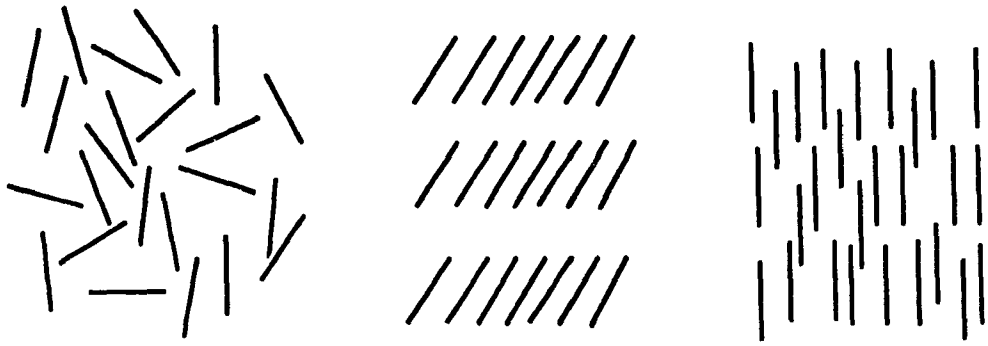

Isotropic Smectic Nematic

Figure 1.1 Isotropic and anisotropic ordering of molecules. In an isotropic solution there is no ordering of the molecules. Smectic liquid crystals are composed of layers of ordered molecules where the molecules are at an angle to the layer while in nematic mesophases the orientations of the molecules are correlated but the centres of mass are randomly distributed.

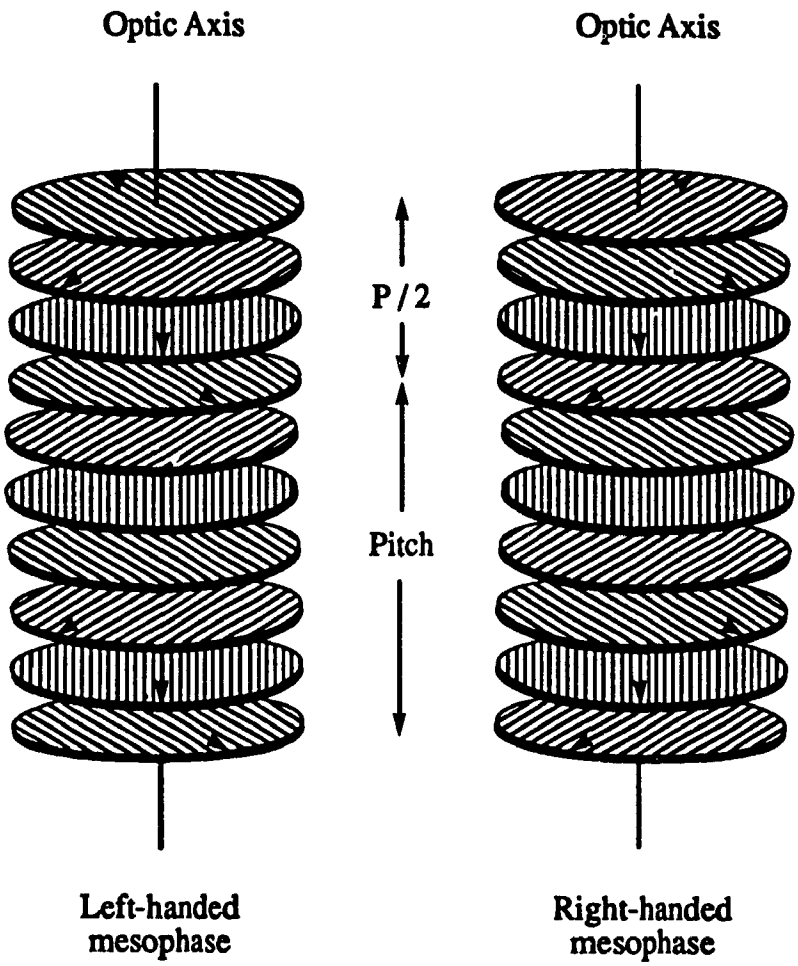

Figure 1.2 A simplified schematic of a cholesteric liquid crystal. Each layer has nematic ordering but is twisted at an angle relative to its neighbour. The pitch, P, is defined as the distance between two layers separated by a 360° rotation of the layer directors. P / 2 represents the half-pitch.

1.2 POLYMER LIQUID CRYSTALS

Interest in liquid crystals was further heightened in 1937 when the first polymeric mesophase was discovered. Bawden and Pirie (12) first demonstrated that suspensions of the tobacco mosaic virus were liquid crystalline and in the 1950's it was found that polypeptides would also form anisotropic phases (13, 14). The development of liquid crystalline polymer phases was of tremendous interest to industry. The first process for the production of a fibre from a liquid crystal was described in 1964 by Ballard et al. (15). Since this time several processes for the production of high strength, low weight fibres have been developed (16). An understanding of the polymer mesophase, either in the melt or the solution, has predictably taken on major importance.

Models for the formation of low molar mass mesophases are based on molecular anisotropy and this is also true of polymer mesophase formation. However, the modelling of a polymer molecule as an anisotropic entity for use in any theory has taken several routes in the attempt to find a mathematical description that best reflects reality. A reliable model is particularly important for polymer hydrodynamic theories where the shape of the macromolecule is closely related to the movement of the molecule in a solvent.

1.2.1 Models of Polymers in Solution

The dimension of a linear polymer is frequently expressed as the mean square end-to-end distance, $< r^2 >$. This distance is a function of short range interactions such as hindrance to internal rotations and long range interactions such as excluded volume effects between remote parts of the chain. In the absence of both types of interactions a freely-jointed chain is obtained and the dimension of the chain is expressed as $< r_f^2 >$. If short range effects are considered then the chain dimension is changed, but the proportionality between the end-to-end distance and the number of bonds remains the same. In this case the average dimension of the chain is called the unperturbed dimension, $< r_0^2 >$. If long range interactions are also considered then not only the restriction of the angle between and rotation about each bond must be considered, but also the concept of excluded

volume must be included. The excluded volume is the volume each segment of a real polymer chain occupies from which all other segments must be excluded (17). This refined model describes a random flight chain and the end-to-end distance is no longer proportional to the number of bonds but rather is related to the linear expansion factor, α, through Equation [1.1].

$$\langle r^2 \rangle^{0.5} = \alpha \langle r_0^2 \rangle^{0.5}. \qquad [1.1]$$

Kuhn (18) introduced a model in which a real chain with n bond segments of length l is replaced by a freely-jointed conceptual chain of $n' = n / m$ vectors of average length l', called the Kuhn length, where m is the number of bond segments of the real chain contained in a vector. The chain is modelled by assembling the termini of all the freely-jointed bond vectors such that there is less correlation between successive steps than in the real chain, but the model chain still has the same end-to-end distance and contour length, L, which is equal to nl. The value of m is chosen such that the directions of the first and m^{th} units are uncorrelated and still obeys Gaussian statistics. As the molar mass increases, the resulting freely-jointed chain asymptotically approaches the random flight conformation.

In some real chain structures such as polysaccharides, nucleic acids and helical polypeptides L is no longer very large compared to the Kuhn segment length except, hypothetically, at molar masses that are unobtainably high (19). This type of chain structure is described as stiff or semiflexible. The random flight chain no longer is as reasonable a model for these types of polymers, but an alternative has been proposed by Kratky and Porod (20). In this method a persistent or wormlike chain model can take stiff behaviour into account. The main advantage of this model is that it permits a continuous description of chain character ranging from the highly flexible to the rodlike states. The basis of the model is that free rotation with a fixed angle, θ, of nearly 180^o is permitted each of n segments of length l. The direction of the chain persists in the direction of the first vector and the cosine of the angle between the first and last segments decreases as $\exp(-L/q)$, where q, the persistence length, is equal to $-l / \ln \langle -\cos\theta \rangle$. In this model the mean square end-to-end distance is given by Equation [1.2].

$$\langle r^2 \rangle = 2q\{L - q[1 - \exp(-L/q)]\}. \qquad [1.2]$$

The persistence length thus becomes a measure of chain stiffness. Two extreme cases are possible: $L << q$ and $L >> q$. In the former case the mean square end-to-end distance is described by Equation [1.3] while for the latter condition Equation [1.4] holds.

$$\langle r^2 \rangle = L^2 \qquad [1.3]$$

$$\langle r^2 \rangle \sim 2qL. \qquad [1.4]$$

Equation [1.4] means that at the limit of infinite molar mass, where L is very large compared to q, the Kratky-Porod model adopts random flight statistics and behaves as a random coil. Under these conditions twice the persistence length of the Kratky-Porod model takes on the value of the segment length, l, in the Kuhn freely-jointed model. When l is applied to the wormlike chain model it is called the "equivalent Kuhn segment length", k_W. This adaptation has been used in hydrodynamic theories that attempt to explain polymer mesophase formation on the basis of chain dimensions (21, 22).

For most polymers the nearly free intramolecular rotation about each bond means that an extended structure is not obtained. However, there are a variety of effects that can restrict the rotation and cause the polymer to adopt an extended structure. Two of the major sources of restriction are hydrogen bonding and steric hindrance. The first effect is seen in polymers such as polypeptides and is the product of hydrogen bonding between the amide and the carbonyl groups in the backbone. The result is a helical conformation for the backbone which induces an extremely extended structure in the polymer. The second effect can sometimes be seen in polymers that contain cyclic groups in the backbone such as aromatic polyesters and amides or any of the cellulose derivatives. These polymers are therefore considered to be semiflexible.

1.2.2 Polypeptide Liquid Crystals

The most widely researched polypeptide in the liquid crystal field is polybenzyl-L-glutamate (PBLG) (Figure 1.3). This polymer was first shown to exhibit mesomorphic properties in the 1950's by Elliot and Ambrose (13) and Robinson (14). The polymer was invented as part of a program designed to produce a synthetic silk based on polypeptides. The attractiveness of the PBLG system for experimental purposes is the well defined nature of the molecule and the fact that it shows a variety of properties in the liquid crystalline phase (23, 24, 25). Most theories that have attempted to explain the cholesteric twist sense and pitch response to temperature of a polymeric mesophase have employed PBLG and its derivatives as models (26, 27). As mentioned in Section 1.2.1, the source of the rigidity is the helical structure of the backbone. If this helical structure is destroyed by the addition of a hydrogen bonding inhibitor (28) or heating the sample to above the helix-coil transition temperature (29) then the rigidity is lost and mesophase formation will not occur. While the role of the helical backbone of polypeptides in the isotropic / anisotropic phase transition has been discussed (30, 31), the role conformation plays in determining the cholesteric mesophase properties is still uncertain.

1.2.3 Cellulose Derivatives

Another major class of polymers that has been found to exhibit liquid crystalline properties is the cellulose derivatives. Cellulose is a naturally occurring polymer that is composed of a series of 1,4-β linked anhydroglucopyranose monomer units (Figure 1.4). The possibility that cellulosic compounds might be capable of forming ordered phases was first postulated by Flory in 1956 (32), but it was not until 1976 that the first paper and patents on cellulose derivative mesophases began to appear (33 - 36). The first cellulosic to be extensively studied in the liquid crystalline state was (hydroxypropyl) cellulose (33), an ether derivative of cellulose.

Cellulose, which can be considered a carbohydrate polymer, has been known to form oriented suspensions since 1959 (37) and mesophases since 1980 (38), but liquid crystals based on a monomeric carbohydrate have existed since 1911 (39). In this case a

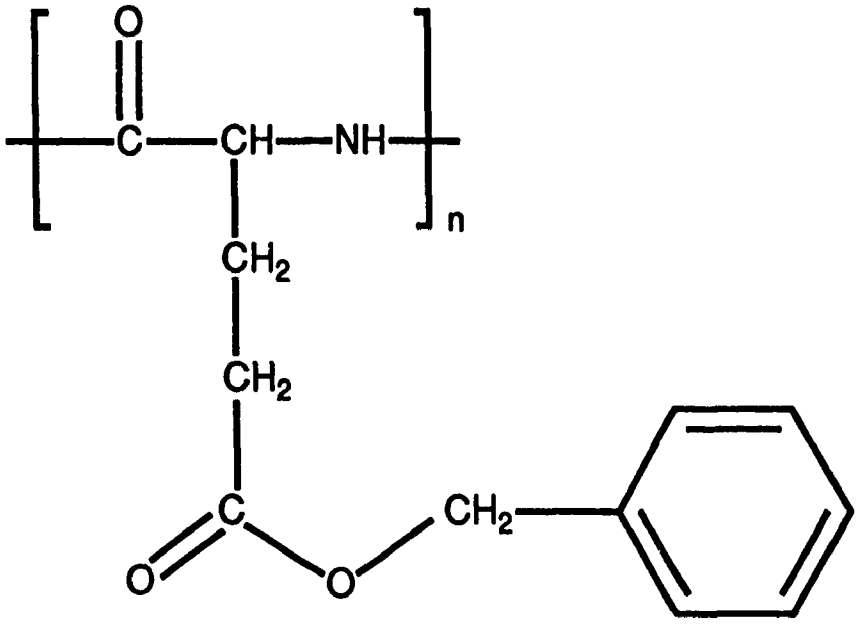

Figure 1.3 Polybenzyl-L-glutamate (PBLG). This molecule has an inherent stiffness due to an interaction between the amide and carbonyl groups in the polymer backbone. The result is a helical structure whose rigidity is sensitive to temperature and hydrogen bonding inhibitors.

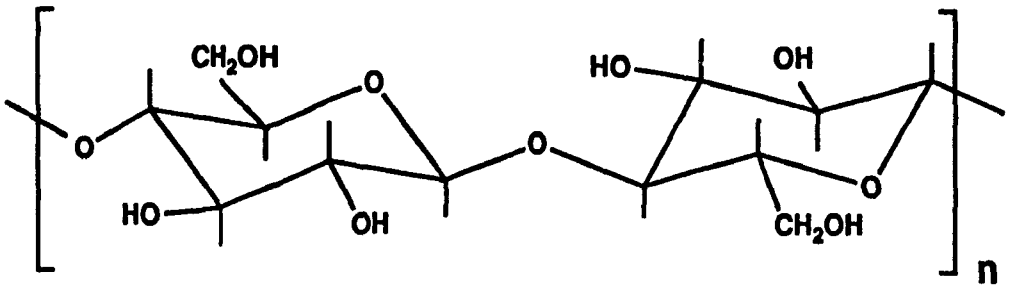

Figure 1.4 Two repeat units of a cellulose molecule. Cellulose is a 1,4 - β linked anhydroglucopyranose homopolymer.

long chain n-alkyl pyranoside was observed to have a double melting point, but it was not until 1938 that this was recognized as a thermotropic mesophase (40). Since this time several other n-alkyl carbohydrates have been found which exhibit liquid crystalline behaviour (41).

Cellulose derivatives are of interest as models for mesophase formation because they constitute the largest group of naturally occurring polymers that is considered to be semiflexible. The flexibility that is permitted is the result of individual monomer units rotating about the anhydroglucopyranose linkage oxygen bonds in the cellulose backbone (42). This flexibility is temperature dependent and affects the ability of the cellulosic compound to form a mesophase (43). The higher the axial ratio, the more the polymer is considered to be extended and rigid, but at elevated temperatures the axial ratio is reduced, the stiffness requirement for the formation of a mesophase is lost and the chain begins to behave as a random coil (44). While the semiflexible nature of cellulose and its derivatives is known to be temperature dependent, the role played by the solvent is less well defined. Most recent investigations that provide information on the axial ratio of cellulosics have concentrated primarily on solvents in which well ordered mesophases are produced. With the exceptions of cellulose acetate and nitrocellulose there is limited information on the rigidity of any individual cellulose derivative in several solvents.

The liquid crystalline properties of cellulose derivatives are also of interest because many cellulosics are capable of forming cholesteric mesophases with reflection colours. This property of visible reflection permits a great deal of information to be derived from classical optical methods that function in the visible region of the spectrum. The factors that influence the properties of the cellulosic mesophases, such as the solvent type, nature of the sidechain, concentration and temperature, can therefore be carefully examined and this allows a comparison with the behaviour of other cholesteric mesophases and the predictions of current theories.

1.3 POLARIZED LIGHT: DEFINITION AND APPLICATIONS

Many of the principal techniques used in the study of liquid crystalline structures are chiroptical methods. An understanding of how light interacts with these materials is important for the classification of a liquid crystal because this is done on the basis of its optical properties. A priority of this thesis is to study the factors that influence the cholesteric structure of cellulose derivative mesophases and these are examined by studying the associated optical properties. The principles upon which these optical properties are based are described below. The application of these principles to describe the interaction of light with a cholesteric liquid crystal is discussed in Chapters 4 and 5.

1.3.1 Polarization of Light

Light consists of oscillating electric and magnetic fields which are perpendicular to each other and propagate in a direction normal to that of the wave (Figure 1.5). For movement in the z-direction, the oscillating electric field, E, at any time, t, can be related to the wavelengt', λ, and the frequency, υ, of the electromagnetic wave by Equation [1.5].

$$E = E_0 \cos 2\pi (\upsilon t - z/\lambda) \qquad [1.5]$$

where E_0 = maximum amplitude of the field.

Equation [1.5] can be resolved into its component fields E_X and E_Y because the electric vector lies in the xy plane. These fields can be described by Equations [1.6] and [1.7].

$$E_X = E_{0X} \cos 2\pi (\upsilon t - z/\lambda + \delta_X) \qquad [1.6]$$

$$E_Y = E_{0Y} \cos 2\pi (\upsilon t - z/\lambda + \delta_Y) \qquad [1.7]$$

where δ_X and δ_Y are the phase angles of the two components.

The difference in the phase angle, $\Delta\delta$, of the two components can vary between zero and 2π. Figure 1.6 illustrates some of the possible wave shapes that the electric vector can trace as a function of various phase angle differences. The elliptical form is considered to

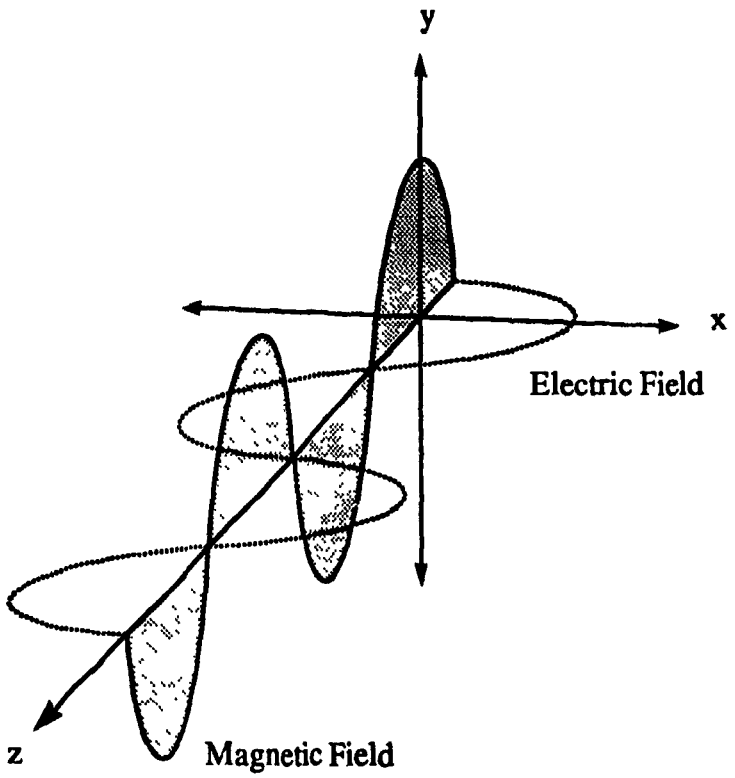

Figure 1.5 A plane polarized electromagnetic wave. The oscillating electric and magnetic fields are perpendicular to each other and propagate in a direction normal to that of the wave. In this diagram $E_x = 0$ and $E_y = 1$.

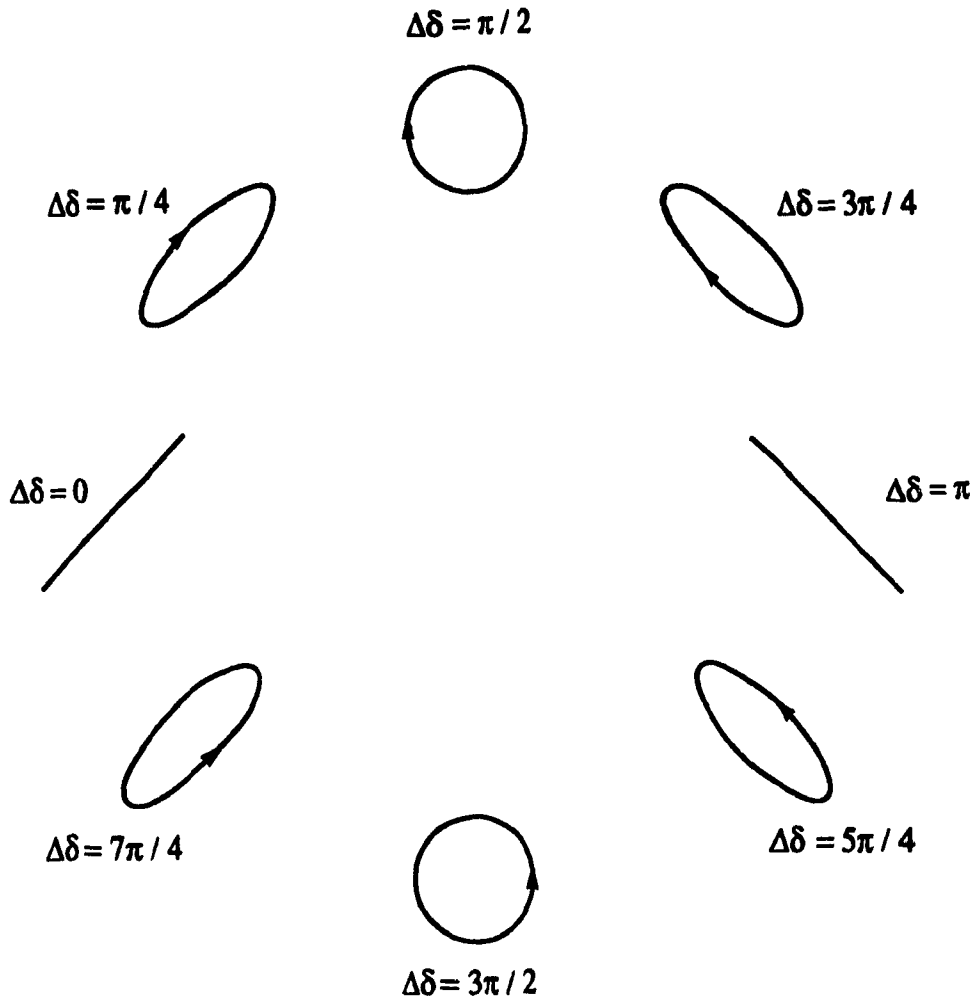

Figure 1.6 Possible wave shapes of the electric vector based on the phase differences of the E_X and E_y components of the field. Two special cases exist (i) when the phase angle difference between E_X and E_y, $\Delta\delta$, is zero or a multiple of π the electric vector is plane polarized and (ii) when $\Delta\delta = \pi / 2$ the electric vector is left-handed circularly polarized while at $\Delta\delta = 3\pi / 2$ it is right-handed circularly polarized.

be the norm but for instances where $\Delta\delta$ is zero or a multiple of π the ellipse flattens into a line and the light wave is called plane polarized. Another extreme exists when $\Delta\delta$ is $\pi / 2$ or an odd multiple of $\pi / 2$ and the electric vector trace becomes a perfect circle. Under these circumstances the wave is termed circularly polarized and can be either right-handed or left-handed, depending on the phase angle difference. An important feature of a plane polarized light wave is that it can be decomposed into coterminus beams of left-handed and right-handed circularly polarized light that have equal phase and amplitude and each of which contains 50% of the energy (Figure 1.7).

It is universally recognized that plane polarized and circularly polarized light are merely specialized forms of elliptically polarized light but historically the definitions of left-handed and right-handed circularly polarized light have often been contradictory or ambiguous. An unambiguous definition is that for a beam of circularly polarized light that is moving towards the observer, if the motion of the *approaching* electric vector is counter-clockwise then the light wave is right-handed while one that moves in a clockwise motion is left-handed. This definition has the advantage of keeping the handedness of light polarization consistent with other particles in nature that exhibit polarization (45).

1.3.2 Optical Activity

Optical activity is the result of the interaction of the electric vector of polarized light with the electrons of a molecule in an asymmetric environment. The electrons are acted upon by the polarized electric field of the light wave and are compelled to move. In a symmetric environment the electrons can simply move in the line of the electric vector with no resultant change in the polarization of the light wave, but in a chiral environment a nonsymmetrical motion is introduced to the electrons. The outcome of this motion is the generation of an electric vector that is not aligned with the electric vector of the light wave. Addition of the two vectors results in a rotation of the original electric vector from its initial polarization. Substances that rotate the plane of polarization of the approaching electric vector in a clockwise direction are called dextrorotatory while those that rotate the electric vector in a counter-clockwise direction are called laevorotatory; however, the sign

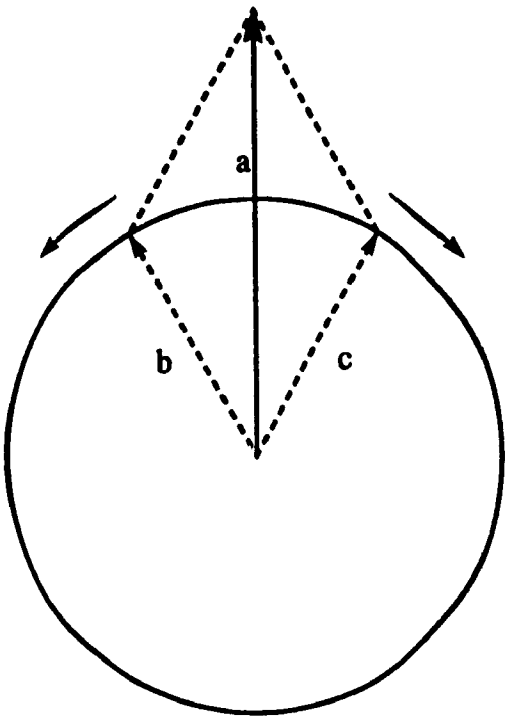

Figure 1.7 Decomposition of a plane polarized light wave into coterminus beams of left-handed and right-handed circularly polarized light. The plane polarized light wave, a, can be considered to be composed of a right-handed circularly polarized component, b, and a left-handed circularly polarized component, c, each of which contains 50% of the energy.

of the rotation is wavelength dependent (46). Despite the vectorial description used to illustrate its origin, optical activity is not a vectorial property; it has sign and magnitude but is not directionally dependent and so would be considered a scalar property. The optical activity of a sample is related not only to its thickness, but also to the wavelength of the incident light and the concentration of the optically active species.

The interaction of a plane polarized wave with an optically active medium can also be considered as the net effect of the interaction of left-handed and right-handed circularly polarized light. Section 1.4.1 has shown that linearly polarized light can be considered as coterminus beams of left-handed and right-handed circularly polarized light that have equal phase and amplitude, but when these two beams interact with an optically active medium the refractive indices for the left-handed and right-handed circularly polarized light waves, n_L and n_R respectively, will not be equal nor will the molar absorbances, ε_L and ε_R. In a region of no absorbance the net effect of the two components is a rotation of the plane of polarization (Figure 1.8a). However, if an absorption does occur over the wavelengths examined then the difference between ε_L and ε_R means that the vector lengths of the two circularly polarized beams are no longer equal and the plane polarized light wave becomes elliptically polarized (Figure 1.8b). The principal axis of the ellipse, equal to $|\varepsilon_L + \varepsilon_R|$, defines the pseudo plane of the rotated vector while the minor axis is equal to $|\varepsilon_L - \varepsilon_R|$. The quantities ε_L and ε_R are related to the ellipticity, ψ, through Equation [1.8].

$$\tan \psi = (\varepsilon_L - \varepsilon_R) / (\varepsilon_L + \varepsilon_R). \qquad [1.8]$$

Measurement of ψ with respect to wavelength is called circular dichroism (CD) spectroscopy while measurement of the angle of the principal axis, α in Figure 1.8, as a function of wavelength is called optical rotatory dispersion (ORD) spectroscopy. Figure 1.9 shows typical CD and ORD spectra. An important feature of these techniques is that they not only measure the wavelength of the maximum absorbance, λ_o, but they also measure the sign of the absorbance. The change in sign of the optical rotation in the ORD spectrum as it passes through λ_o is called a Cotton Effect. CD and ORD spectroscopy

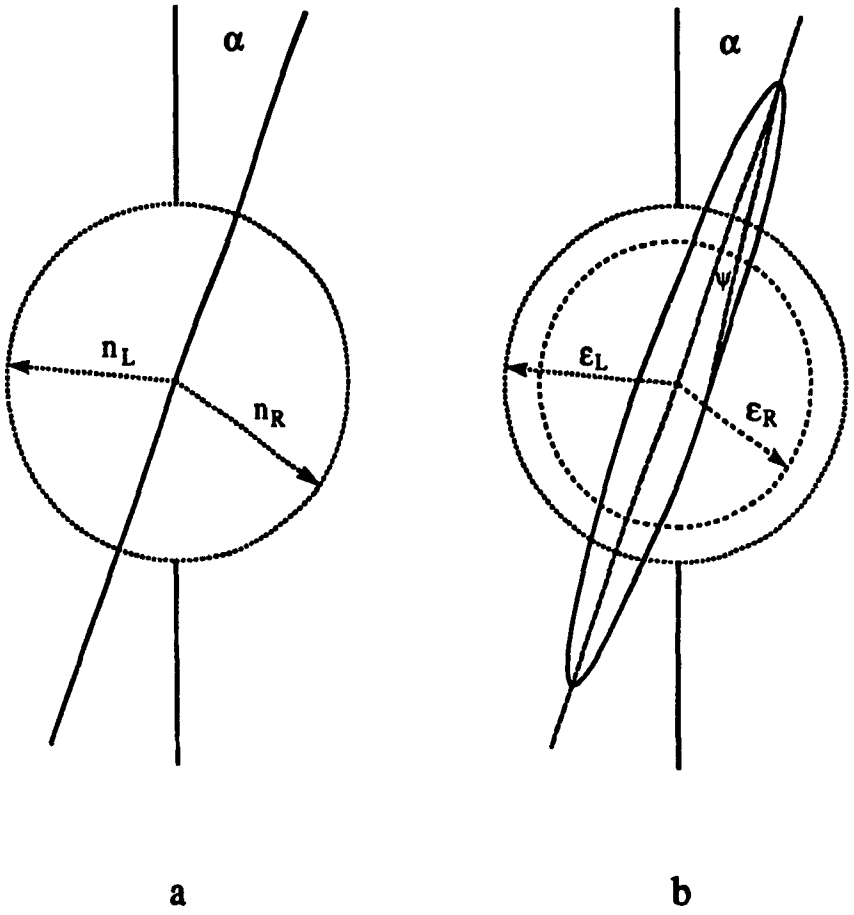

Figure 1.8 Possible interactions of the two circularly polarized components of light with optically active samples: (a) When n_L and n_R are equal and interact with an optically active medium the result is a rotation of the plane of polarization, α. (b) If measured in a region of an absorption then ε_L and ε_R will not be equal and the plane polarized electric vector becomes elliptically polarized. The principal axis of the ellipse defines the pseudo plane of polarization, α, and the ellipticity, ψ, is related to ε_L and ε_R through Equation [1.8].

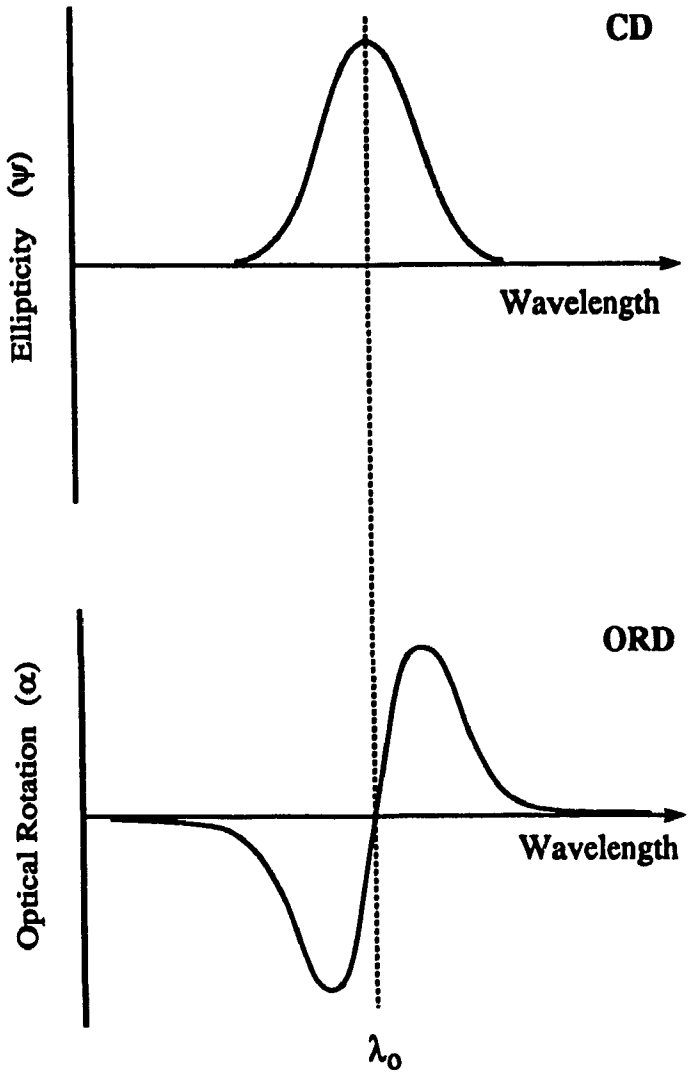

Figure 1.9 Typical ORD and CD spectra. ORD spectroscopy measures the rotation of the plane of polarization, α, as a function of wavelength while CD spectroscopy measures the variation of the ellipticity, ψ, as a function of wavelength. The cross-over wavelength of the ORD spectrum corresponds to the wavelength of maximum ellipticity in the CD spectrum.

have both proven to be extremely useful tools for investigating the solution conformations of biological macromolecules (47, 48).

1.3.3 Birefringence

The introduction of liquid crystalline order to a substance is accompanied by the development of anisotropic properties, particularly optical anisotropy. Optical anisotropy exists in any substance which responds differently to light linearly polarized in one direction and light linearly polarized in another. The source of this difference is molecular asymmetry. In a molecule possessing a much greater length than width the long axis can be considered the optic axis (49). Two extremes are possible as an oscillating electric field passes through the molecule: the polarized electric field is parallel or perpendicular to the optic axis. The movement of the electrons within the molecule due to the electric field is much easier in the former instance than in the latter. As the index of refraction is governed by the response of electrons to the electric field, the molecule described above will have two indices of refraction, depending on the direction of polarization within the molecule. Such a molecule is said to exhibit birefringence. For white light impinging on a birefringent material, two refractions occur. Snell's law, Equation [1.9],

$$n' / \sin \phi = n / \sin \phi' \qquad [1.9]$$

which relates the angle of light wave incidence, ϕ, and the angle of refraction, ϕ', to the refractive indices, n and n', of the incident and refracting media, respectively, is found to hold for one refracted beam of light but not the other. The beam that obeys Snell's law is called the ordinary or O-ray and the other is called the extraordinary or E-ray. The two emerging rays are linearly polarized at right angles to each other (49).

Although a single molecule can have intrinsic birefringence, in an isotropic medium with many other identical molecules whose molecular axes are randomly dispersed the observation of the birefringence is impossible. However, upon formation of the liquid crystalline phase an ordering of the molecular axes occurs. If such an ordered array is exposed to linearly polarized light then the form birefringence becomes

observable by the use of a polarizing microscope (50). The polarizing microscope at its simplest level contains a polarizer and an analyzer whose preferred directions are set perpendicular to each other. In the isotropic state, when the sample is between the polarizer and the analyzer, the light passes though the sample with no rotation of the plane polarized light and is not transmitted by the analyzer. In an anisotropic sample, the sample acts as a waveplate and introduces a phase shift. This results in a rotation of the plane of polarization and transmission through the analyzer is possible (Figure 1.10). The transmittance of the polarized light through the anisotropic medium also causes interference and may cause colours to be seen. The intensity and wavelength of the colours is a function of the sample thickness, composition of the light and the birefringence of the sample (51). The source of the interference effect is the different refractive indices of the anisotropic sample; the apparent velocity of light of one polarization is slower than light of the opposite polarization and thus produces a phase lag which in turn causes interference effects.

The onset of lyotropic liquid crystalline behaviour is a topic that is of interest to this thesis. The study of liquid crystals by polarizing microscopy has long been known to be an effective means of examining thermotropic mesophase properties and it has also been found to be capable of accurately determining the critical volume fraction in lyotropic samples (8, 43).

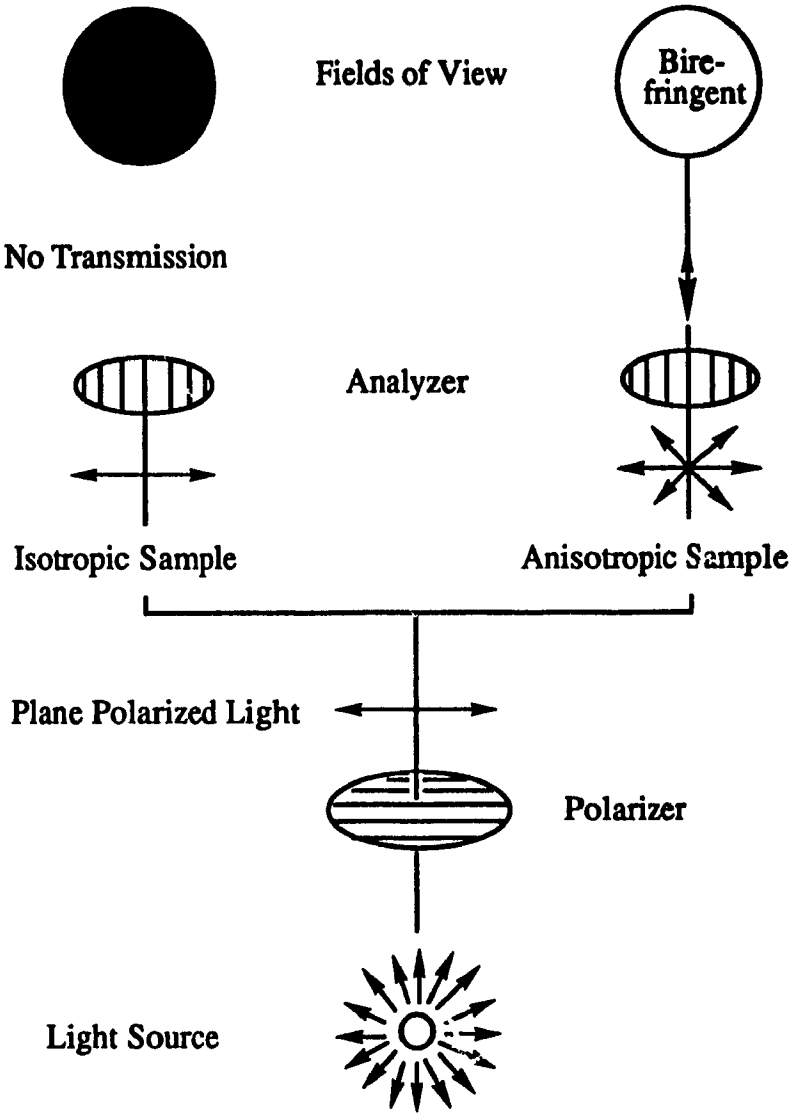

Figure 1.10 Possible fields of view in a polarizing microscope. Under crossed polars only a birefringent medium will allow the passage of light through the analyzer.

1.4 INTRODUCTION TO REMAINING CHAPTERS

The objective of this thesis is to provide insight into the factors that are responsible for governing the liquid crystalline behaviour of cellulose derivatives. The previous sections of this chapter have described the underlying principles of how liquid crystals are perceived and investigated. The following chapters discuss these ideas and techniques as they apply to cholesteric polymer liquid crystals in general and this study in particular.

Many cellulose derivatives have been investigated in the past but some fundamental questions about which factors are responsible for controlling the mesophase properties remain unanswered. In an attempt to resolve some of these questions this thesis presents the results of a study on the liquid crystalline properties of ethyl cellulose (EC) and some related polymers. Chapter 2 describes the preparation and characterization of EC of varying degrees of substitution and of two other alkyl derivatives of EC. Chapter 3 examines the chain stiffness and liquid crystalline phase separation behaviour of several cellulose derivatives, including EC. The physical dimensions of several cellulose derivatives are determined by the use of a recent hydrodynamic theory and the results compared with those of an older theory. The physical dimensions from the superior model are employed in three liquid crystalline phase separation theories and a comparison is made with experimental results to determine which theory best predicts the critical concentration for mesophase formation. The liquid crystalline phase separation behaviour of EC is examined in several solvents; potential errors in the technique are evaluated. Chapter 4 describes an investigation of the cholesteric structure of liquid crystalline EC and derivatives by measurement of the optical properties using a Circular Reflectance spectroscopy technique. The effects of solvent, concentration, temperature and degree of substitution on the cholesteric mesophase are explored. In addition, an investigation of thermal effects on the cholesteric film optical properties of EC and its derivatives is described. Chapter 5 reports on an ORD study of EC and its derivatives in the isotropic and anisotropic states. This includes the search for a pretransitional effect and the effects of solvent and degree of substitution on the ORD spectra. Finally, Chapter 6 presents the conclusions that can be drawn from the study as a whole, claims to original research and suggestions for future research based on the discoveries of this study.

1.5 REFERENCES

(1) V.P. Shibaev, S.G. Kostromin, N.A. Plate, S.A. Ivanov, V.Y. Vetrov and I.A. Yakolev, *Polym. Commun.*, **24**, 364 (1983).

(2) H.J. Coles and R. Simon, *Polymer*, **26**, 1801 (1985).

(3) M. Eich, J.H. Wendorff, B. Rech and H. Ringsdorf, *Die Makromol. Chem. (Rapid Commun.)*, **8**, 59 (1987).

(4) Y. Bouligand, P.E. Cladis, L. Liebert and L. Strzelelecki, *Mol. Cryst. Liq. Cryst.*, **25**, 233 (1974).

(5) P. Planer, *Ann. Chem.*, **118**, 25 (1861); as reported by G.S. Chilaya and L.N. Lisetski, *Mol. Cryst. Liq. Cryst.*, **140**, 243 (1986).

(6) F. Reinitzer, *Monatsh. Chem.*, **9**, 421 (1888); as reported by J.L. White and J.F. Fellers, *J. Appl. Polym. Sci.: Appl. Polym. Symp.*, **33**, 137 (1978).

(7) O. Lehmann, "Flussige Kristalle", Engelmann, Leipzig (1904); as reported by J.L. White and J.F. Fellers, *J. Appl. Polym. Sci.: Appl. Polym. Symp.*, **33**, 137 (1978).

(8) G. Friedel, *Ann. Phys.*, **18**, 273 (1922); as reported by J.L. White and J.F. Fellers, *J. Appl. Polym. Sci.: Appl. Polym. Symp.*, **33**, 137 (1978).

(9) E.M. Barrall II, "Liquid Crystals The Fourth State of Matter", (F. D. Saeva, ed.), Marcel Decker Inc., New York, 1979, pp. 335.

(10) S.E.B. Petrie, "Liquid Crystals The Fourth State of Matter", (F. D. Saeva, ed.), Marcel Decker Inc., New York, 1979, pp. 163.

(11) A. Saupe, *Angew. Chem. International Ed.*, **7**, 97 (1968).

(12) F.C. Bawden and N.W. Pirie, *Proc. R. Soc. (London) Ser. B*, **123**, 274 (1937).

(13) A. Elliot and E.J. Ambrose, *Discuss. Faraday Soc.*, **9**, 246 (1950).

(14) C. Robinson, *Trans. Faraday Soc.*, **52**, 571 (1956).

(15) D.G. Ballard, J.D. Griffiths and J. Watson, United States Patent No. 3,121,766 (1964); as reported by J. L. White and J.F. Fellers, *J. Appl. Polym. Sci.: Appl. Polym. Symp.*, **33**, 137 (1978).

(16) D.C. Prevorsek, "Polymer Liquid Crystals", (A. Ciferri, W.R. Krigbaum and R.B. Meyer, eds.), Academic Press, Inc., New York, 1982, pp. 329.

(17) F.W. Billmeyer, Jr., "Textbook of Polymer Science 3rd Ed.", Wiley - Interscience, New York, 1984, pp. 158.

(18) W. Kuhn, *Kolloid-Z.*, **76**, 258 (1936); as reported by E.F. Casassa and G.C. Berry, "Comprehensive Polymer Science", (G.A. Allen, ed.), Pergamon Press, Oxford, 1989, **2**, pp. 75.

(19) E.F. Casassa and G.C. Berry, "Comprehensive Polymer Science", (G.A. Allen, ed.), Pergamon Press, Oxford, 1989, **2**, pp. 74.

(20) O. Kratky and G. Porod, *Rec. Trav. Chem.*, **68**, 1106 (1949).

(21) H. Yamakawa and M. Fujii, *Macromolecules*, **7**, 128 (1974).

(22) M. Bohdanecky, *Macromolecules*, **16**, 1483 (1983).

(23) H. Toriumi, S. Minakuchi, Y. Uematsu and I. Uematsu, *Polym. J.*, **12**, 431 (1980).

(24) D.L. Patel and D.B. DuPré, *J. Chem. Phys.*, **72**, 2515 (1980).

(25) I. Uematsu and Y. Uematsu, *Advanc. Polym. Sci.*, **59**, 37 (1984).

(26) H. Kimura, M. Hosino and H. Nakano, *J. Phys. Soc. Jpn.*, **51**, 1584 (1982).

(27) T.V. Samulski and E.T. Samulski, *J. Chem. Phys.*, **67**, 824 (1977).

(28) H. Watanabe, K. Yoshioka, and A. Wada, *Biopolymers*, **2**, 91 (1964).

(29) D.B. DuPré and R.W. Duke, *J. Chem. Phys.*, **63**, 143 (1975).

(30) P. Pincus and P.G. de Gennes, *J. Polym. Sci.: Polym Symp.*, **65**, 85 (1978).

(31) R.R. Matheson, *Mol. Cryst. Liq. Cryst.*, **105**, 315 (1984).

(32) P.J. Flory, *Proc. R. Soc. (London) Ser. A*, **234**, 71 (1956).

(33) R.S. Werbowyj and D.G. Gray, *Mol. Cryst. Liq. Cryst. (Letters)*, **34**, 97 (1976).

(34) D.G. Gray, *J. Appl. Polym. Sci.: Appl. Polym. Symp.*, **37**, 179 (1983).

(35) M. Panar and O.B. Wilcox, Belgium Patent 656,359 (1976), German Federal Republic Patent 2,705,381(1977), France Patent 2,340,344 (1977).

(36) J. Maeno, United States Patent 4,132,464 (1979).

(37) R.H. Marchessault, F.F. Morehead and N.M. Walters, *Nature*, **184**, 632 (1959).

(38) H. Chanzy, A. Peguy, S. Chaunis and P. Monzie, *J. Polym. Sci., Polym. Phys. Ed.*, **18**, 1137 (1980).

(39) E. Fischer and B. Helferich, *Justus Liebigs Ann. Chem.*, **383**, 68 (1911) as reported by G.A. Jeffrey, *Acc. Chem. Res.*, **19**, 168 (1986).

(40) C.R. Noller and W.C. Rockwell, *J. Am. Chem. Soc.*, **60**, 2076 (1938).

(41) G.A. Jeffrey, *Acc. Chem. Res.*, **19**, 168 (1986).

(42) K.D. Goebel, C.E. Harvie and D.A. Brant, *Appl. Polym. Symp.*, **28**, 231 (1976).

(43) G.V. Laivins, Ph.D. Thesis, McGill University, 1984.

(44) L. Mandelkern and P.J. Flory, *J. Am. Chem. Soc.*, **74**, 2517 (1952).

(45) R.P. Feynman, R.B. Leighton and M. Sands, "The Feynman Lectures in Physics", Addison-Wesley Publishing Company, Reading, Massachusetts, **I**, 1963, pp. 33-2.

(46) E. Charney, "The Molecular Basis of Optical Activity", Robert E. Krieger Publishing Company, Malabar, Florida, 1985, pp. 30.

(47) S. Beychok, *Science*, **154**, 1288 (1966).

(48) J.T. Yang and P. Doty, *J. Am. Chem. Soc.*, **79**, 761 (1957).

(49) R.P. Feynman, R.B. Leighton and M. Sands, "The Feynman Lectures in Physics", Addison-Wesley Publishing Company, Reading, Massachusetts, **I**, 1963, pp. 33-9.

(50) C. Viney, *Polym. Sci. Engineer.*, **26**, 1021 (1986).

(51) A.L.E. Barron, "Using the Microscope", Chapman and Hall Ltd., London, 1965, pp. 133.

CHAPTER 2

SAMPLE PREPARATION AND CHARACTERIZATION

2.1 INTRODUCTION

Cellulose ethers have existed since the early 1900's. Since this time they have taken on an important commercial value in chemical industry with millions of kilograms being produced world-wide each year (1). The most widely utilized of the ether derivatives are (hydroxyethyl)cellulose (HEC), (hydroxypropyl)cellulose (HPC), (carboxymethyl)cellulose (CMC), (cyanoethyl)cellulose (CEC), methyl cellulose (MC) and ethyl cellulose (EC). Mixed ethers derivatives have also been developed. The applications of cellulose ethers are many and varied; thickening agents, pharmaceuticals, absorbents, sealants and films are traditional areas in which cellulose ethers have been employed.

The synthesis of any commercial cellulose ether first requires the preparation of alkali cellulose. High purity wood pulp or cotton linters are used as the sources of cellulose and these are converted to alkali cellulose using sodium hydroxide. The two possible reaction procedures used in the preparation of the ether derivatives are nucleophilic substitution and Michael addition. EC, MC and CMC are all produced by the former mechanism while CEC is a product of the latter. The syntheses of HPC and HEC are special cases of the substitution reaction because sidechain polymerization can also occur.

2.1.1 Ethyl Cellulose

Commercial EC is usually prepared from alkali cellulose by reaction with chloroethane (1). The typical commercial product is listed as having an ethoxyl content of 48% which corresponds to a degree of substitution (DS) of ~ 2.5, but in reality the DS can range anywhere between 2.3 and 2.6. Figure 2.1 shows two units of an idealized EC molecule with a DS of 2.5. The physical properties of EC, such as its softening point and solubility, have been found to be dependent on the DS (2).

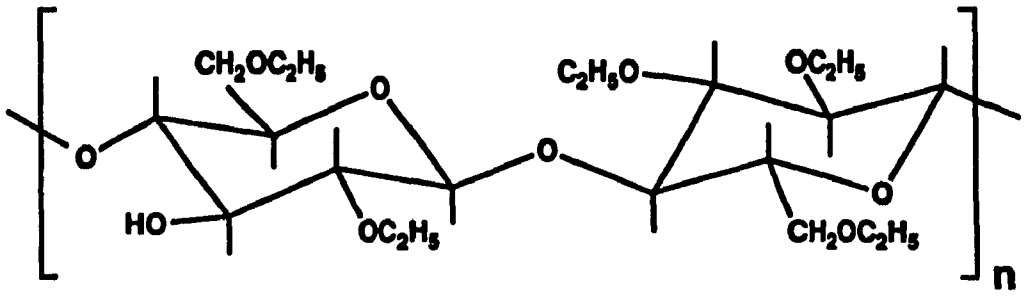

Figure 2.1 An idealized segment of an EC molecule with a DS of 2.5.

2.2 SAMPLE PREPARATION

Two modifications of an Aldrich Ltd. EC sample were required. The first involved the preparation of EC of varying DS up to tri-O-ethyl cellulose (TEC). The second involved the preparation of two mixed ether derivatives of EC: O-(ethyl)(methyl)cellulose (EMC) and O-(butyl)(ethyl)cellulose (BEC).

2.2.1 Preparation of EC of Varying DS

The reaction procedures employed for the preparation of EC of varying DS are described below. EMC and BEC were prepared by same general procedure as is described here except that the solvent, quantities of starting material, alkylating agent or number of alkylating reactions on the same sample are different. The general reaction scheme is shown in Figure 2.2.

The preparation of EC of varying DS (excluding sample EC-7; *vide infra*) was accomplished by dissolving 5.0 g of dry commercial grade EC in 60 mL of tetrahydrofuran (THF) in a two necked round bottom flask that was equipped with a nitrogen feed tube and a stirring bar. The flask was immersed in a temperature controlled oil bath to a depth that covered the solution mixture in the flask. Sodium hydride (NaH), 0.7 g, was added to the degassed solution and allowed to mix for one hour. The ethylating agent was iodoethane; this was added dropwise over a period of 1/2 hour. The temperature, reaction time and quantity of ethylating agent used are listed in Table 2.1. The reactions were terminated by removing the flask from the oil bath, allowing it to air cool and slowly adding 50 mL of methanol. After the methanol had reacted with any remaining NaH the solution was slowly poured into 200 mL of distilled water that contained 1 g of sodium thiosulphate (NaS_2O_3). Precipitation of the EC was immediate and after isolation by filtration and washing with large quantities of distilled water the sample was vacuum dried at 60 °C. The dried product was then redissolved in THF and precipitated in a distilled water / NaS_2O_3 solution, isolated by filtration, washed with large quantities of distilled water and vacuum dried at 60 °C. This last step, without the

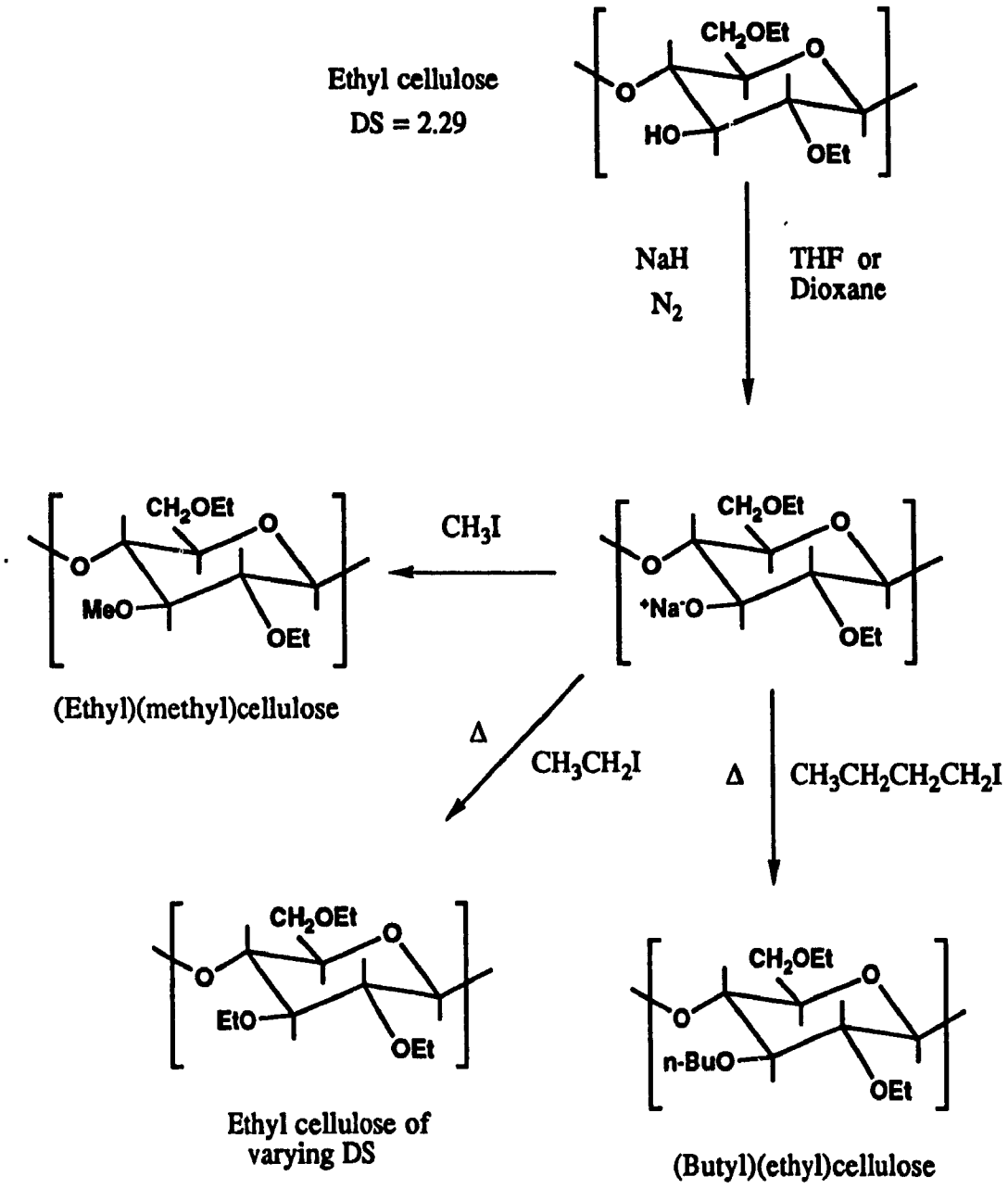

Figure 2.2 The general reaction scheme used for the syntheses of EC of varying DS, EMC and BEC.

NaS_2O_3, had to be repeated at least once before a clean sample was obtained. Yields for these reactions ranged from 3.5 - 4.5 g.

Table 2.1

Conditions for the Preparation of EC of Varying DS

	EC / g	iodoethane / mL	Temp / °C	Reaction Time / hrs
EC-1	5.0	1	40	3
EC-2	5.0	2	40	3
EC-3	5.0	5	40	3
EC-4	5.0	6.5	40	3
EC-5	5.0	8	40	3
EC-6	5.0	8	55	5

EC-7 was the first derivative of the commercial grade EC to be prepared and its reaction conditions were slightly different than those listed above. Using the apparatus described above dry commercial grade EC (20 g) was dissolved in 300 mL of THF, 3.2 g of NaH added and the solution stirred for two hours at 25 °C. Iodoethane (4 mL) was added and after stirring for two hours the temperature of the reaction mixture was raised to 40 °C where a second 4 mL addition of iodoethane was made. After two hours of stirring the temperature was raised to 55 °C, 10 mL of iodoethane were added and stirring continued two more hours. The temperature was increased to 60 °C and a second addition of 10 mL of iodoethane was made and the reaction mixture stirred for four hours. After cooling to room temperature, 50 mL of methanol was added and the solution was poured into 1500 mL of distilled water containing 3 g of NaS_2O_3. The product was isolated and cleaned in the usual manner except that dioxane was used to redissolve the polymer for cleaning purposes. The final yield of the white powder was 17 g.

2.2.2 Preparation of O-(Ethyl)(methyl)cellulose

To 150 mL of THF in a three necked roundbottomed flask that was equipped with a stirring bar, an air condenser, a nitrogen feed tube and a solvent delivery funnel, 10.0 g of EC was added. After dissolution the solution was degassed by bubbling nitrogen through the liquid. To this solution 1.6 g of NaH was added and the solution stirred for

two hours at 25 °C. Iodomethane (3 mL) was added dropwise and after stirring for two hours the temperature of the reaction mixture was raised to 35 °C. Iodomethane (3 mL) was added and the mixture stirred for two more hours. The temperature of the reaction mixture was raised to 40 °C, 4 mL of iodomethane were added and stirring continued for five more hours. After cooling to room temperature the product was isolated in the usual manner. The final yield was 8.2 g.

2.2.3 Preparation of O-(Butyl)(ethyl)cellulose

To 50 mL of THF in a three necked roundbottomed flask that was equipped with a stirring bar, an air condenser, a nitrogen feed tube and a solvent delivery funnel, 5.0 g of EC was added. After dissolution the solution was degassed by bubbling nitrogen through the liquid. NaH (0.8 g) was added and the mixture was stirred for an hour. The flask was then heated to 55 °C and 8 mL of 1-iodobutane was added dropwise. The reaction was allowed to proceed for 24 hours and after cooling to room temperature the sample isolated in the usual manner. A Fourier transform infrared (FTIR) spectrum showed the existence of an -OH stretching peak at 3,400 cm^{-1}. Half a gram of the polymer was set aside (BEC-1).

The remnant of BEC-1 (4.3 g) was dissolved in dioxane (50 mL) under nitrogen, 0.7 g of NaH added and the flask heated to 80 °C. 1-Iodobutane (14 mL) was added dropwise and the reaction allowed to proceed for 36 hours and after cooling to room temperature the product was isolated in the usual manner. Although smaller than the peak in BEC-1, an FTIR spectrum showed the continued existence of a small -OH stretching peak. Half a gram of the polymer was set aside (BEC-2).

The remnant of BEC-2 (2.5 g) was dissolved in dioxane (30 mL) under nitrogen, 0.5 g of NaH added and the flask heated to 80 °C. 1-Iodobutane (6 mL) was added and the reaction allowed to proceed for 24 hours. After cooling to room temperature the product was isolated in the usual manner. An FTIR spectrum showed no -OH stretching peak. The final yield was 2 g (BEC-3).

2.3 CHARACTERIZATION

Two EC samples (Aldrich) were used for the purposes of the thesis. One was used in the liquid crystal phase separation study of Chapter 3 while the other sample and derivatives prepared from it were used for all other investigations.

Characterization of EC and its products involves two objectives: (i) determination of the DS values of all the samples employed and (ii) a determination of the molar masses of the starting compound and final product of the reaction used to produce EC-7.

2.3.1 Determination of Degree of Substitution

The DS values were determined from the ^1H nuclear magnetic resonance (NMR) spectra obtained on Varian XL200 or XL300 spectrometers using $CDCl_3$ as the solvent and tetramethyl silane as the internal reference. Assignments of DS in EC were made on the basis of the ratio of the methyl component of the ethyl group peak area which appears at 1.18 ppm to the area of the peaks of all other protons which extend from 2.7 ppm to 5.0 ppm (Figure 2.3). Reproducibility was excellent between samples run on both the Varian XL200 and XL300 NMR spectrometers. The DS of the EC sample used in Chapter 3 was determined to be 2.52. The DS values for EC and its derivatives employed in Chapters 4 and 5 are listed in Tables 2.2 and 2.3. The effect of a change in DS of EC from 2.29 to 3.00 can also be shown by FTIR. The strong stretching peak at 3,400 cm^{-1} due to the unreacted hydroxyl groups in the starting compound completely vanishes in the trisubstituted derivative (Figure 2.4).

Table 2.2

DS of EC and its Synthesized Analogs

Sample	DS	Sample	DS
EC	2.29	EC-4	2.80
EC-1	2.55	EC-5	2.88
EC-2	2.65	EC-6	3.00
EC-3	2.70	EC-7	3.00

Figure 2.5 shows the NMR spectrum of EMC. The sharp peak at 3.55 ppm is due to the methoxyl group protons. The sample is trisubstituted. Figure 2.6 shows the

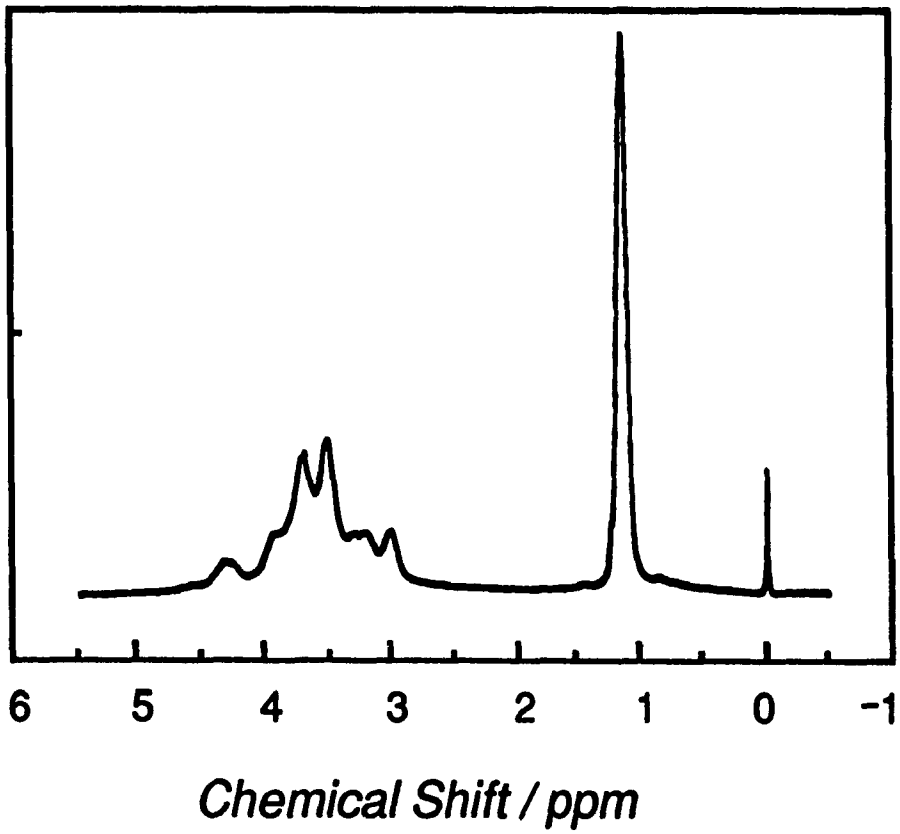

Figure 2.3 ^{1}H NMR of EC. The peak at 1.18 ppm is due to the methyl groups protons. All the other proton signals are contained in the region of 2.7 ppm to 5.0 ppm.

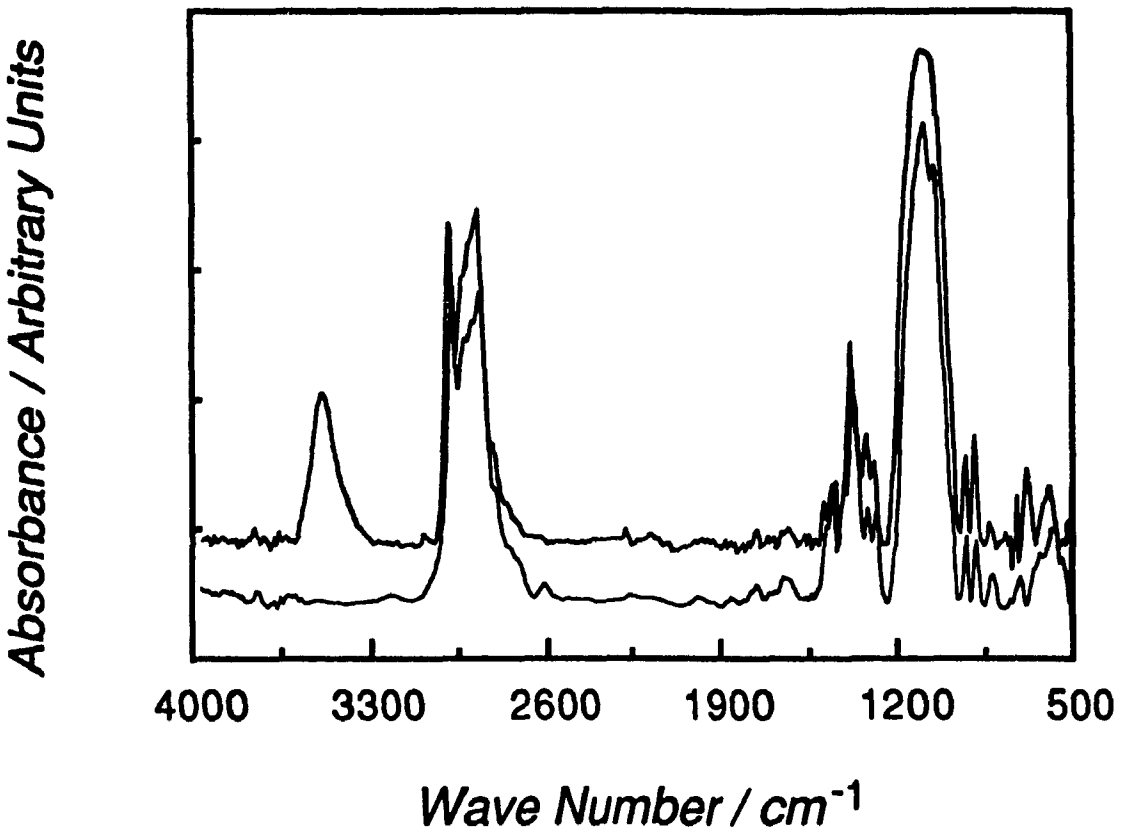

Figure 2.4 FTIR spectra of EC (upper trace) and EC-7 (lower trace). The -OH stretching band at 3400 cm^{-1} disappears when the sample is completely ethylated.

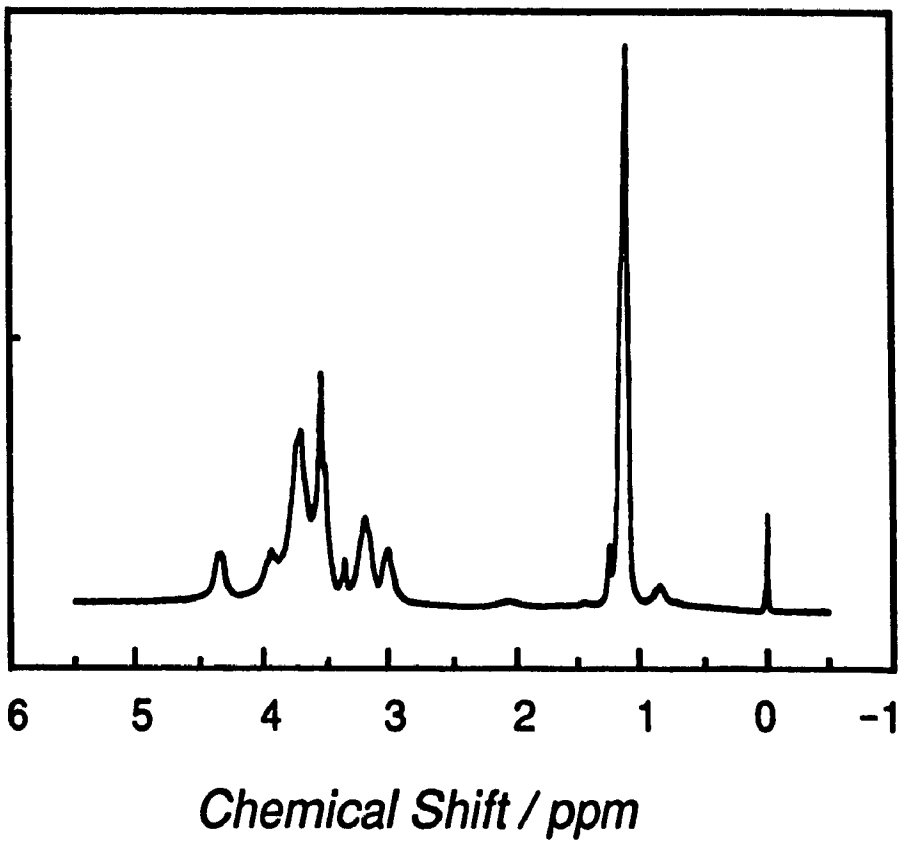

Figure 2.5 ^{1}H NMR spectrum of EMC. The sharp peak at 3.55 ppm is due to the methoxyl group protons.

NMR spectrum of BEC-3; the peaks at 0.85 ppm are due to the protons of the methyl component of the butyl group while the sharp peak at 1.28 ppm is due to the protons of the methylene groups at the 2 and 3 positions of the butyl group. As with TEC, the FTIR absorbance spectra of EMC and BEC-3 show no hydroxyl stretching peaks (Figure 2.7). The DS values of EMC and BEC are listed in Table 2.3.

Table 2.3

DS of EMC and BEC Samples

Sample	DS of Me	DS of n-Bu	Total DS
EMC	0.7	-	3.0
BEC-1	-	0.3	2.6
BEC-2	-	0.6	2.9
BEC-3	-	0.7	3.0

2.3.2 Determination of Molar Mass

Investigations of the liquid crystalline properties of cellulose tricarbanilate and (acetoxypropyl)cellulose have found significant variations in pitch with large changes in molar mass (3, 4). For the purposes of comparing the effect of DS on the liquid crystalline properties it is therefore necessary to ensure that there has been no significant change in molar mass due to the syntheses reactions. The method used to determine the molar mass was Low Angle Laser Light Scattering (LALLS). A Chromatix LALLS in the static mode was employed. The samples were prefiltered through a 1.0 μm filter and a 0.5 μm filter was used during sample injection into the LLAS. The dn/dc values of EC with DS = 2.52 and 3.00 in benzene were determined using a Brice-Pheonix Differential Refractometer and calculated to be -0.0278 and -0.0324, respectively, while the dn/dc value of EC with DS = 2.29 in 1,4-dioxane was found to be -0.0478. The molar mass of the sample used in Chapter 3 was found to be 168,000 g mol^{-1}. The molar masses of the EC-1 and EC-7 (DS = 2.29 and 3.00, respectively) samples used in Chapters 4 and 5 were found to be 65,000 and 62,000 g mol^{-1}, respectively. The degrees of polymerization based on the weight average molar masses of these samples are 280 and 252, respectively, which means that even the most rigorous synthesis procedure causes only minor chain degradation.

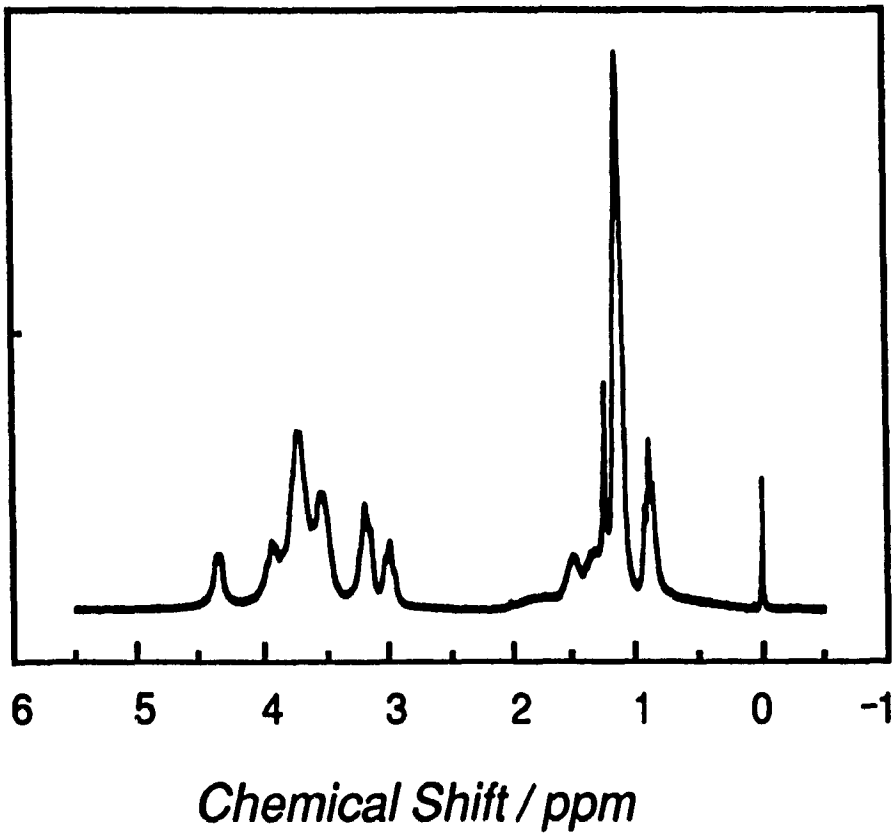

Figure 2.6 ^{1}H NMR spectrum of BEC-3. The peak at 0.85 ppm is due to the protons of the methyl component of the butyl group.

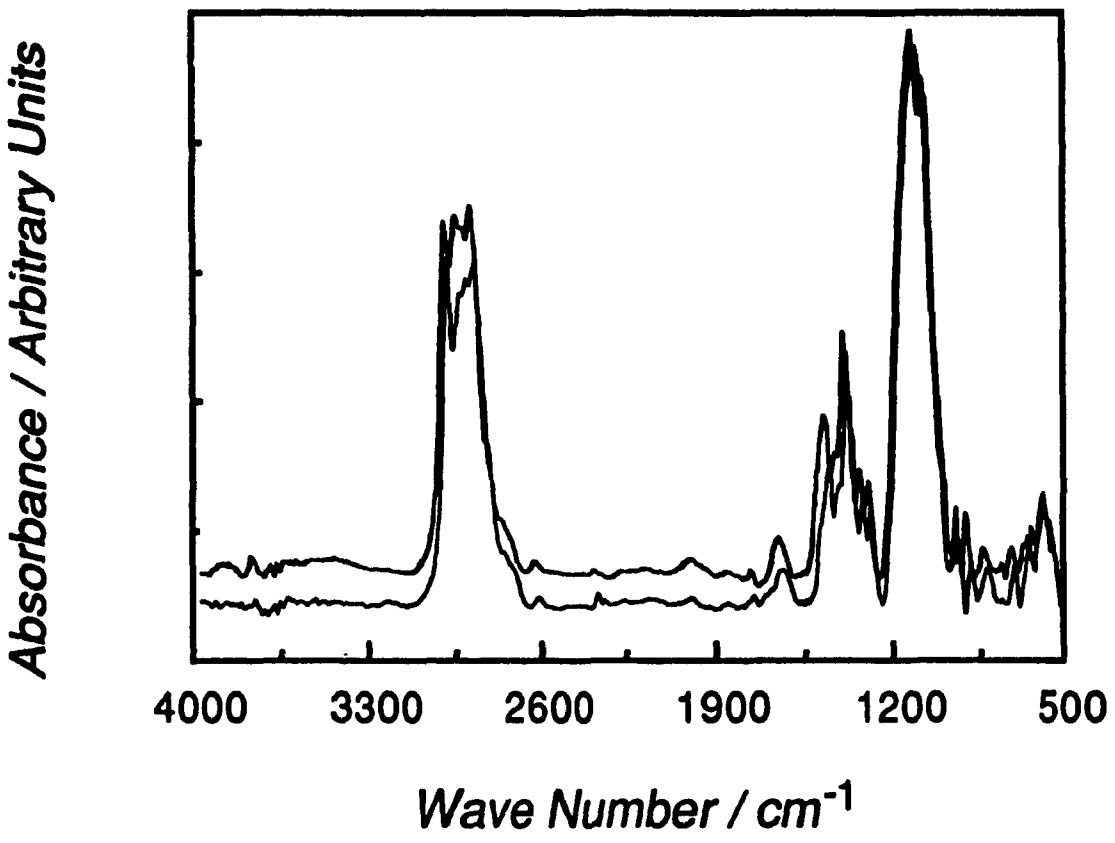

Figure 2.7 FTIR spectra of EMC (lower trace) and BEC-3 (upper trace). These trisubstituted cellulose derivatives lack the -OH stretching peak at 3,400 cm^{-1} which is characteristic of the starting compound (see Figure 2.4).

2.4 DISCUSSION

Although EC itself is a widely used commercial product there is little demand for its very highly substituted analogs. Thus, it was necessary to prepare the various EC derivatives. The reactions employed point out some interesting features of EC chemistry. NaH was employed as the base because sodium hydroxide proved ineffective even when multiple reactions of the same material were attempted. The size of the ether group that was to be introduced also appeared to played a role in the relative ease of the reactions. While the preparation of EMC was possible at a low temperature and the highly substituted ethyl derivatives required only moderately more rigorous conditions, the reaction conditions required to produce a fully substituted BEC sample involved high temperature, repetitive reactions and a very large excess of alkylating agent. This apparent selectivity can be ascribed to a possible steric effect. The most reactive positions of cellulose during a commercial etherification reaction are OH-2 > OH-6 >> OH-3 (5 - 8). Although not uniformly substituted, in commercial EC synthesis the OH-2 and OH-6 positions would therefore be expected to be the preferred sites of occupation. While it has been established that if the OH-2 position is substituted then the reactivity of the OH-3 position is substantially increased (7, 8), the fact remains that the remaining unreacted hydroxyls, located primarily at the 3 position, are even more hindered to potential nucleophilic attack. It would be expected that the approach of a large substituent would be more sterically hindered than the approach of a smaller one. This effect has been observed for reactions of alkyl halides and the OH-3 group of 1,2:5,6-di-O-isopropylidene-α-glucofuranose in dimethylformamide at 25 °C. The relative reactivities of the methyl, ethyl and n-propyl halides at this position were found to be ~15:~3:1 (9). It is therefore probable that the same steric effect slows or prevents the approach of the larger substituents in EC alkylation reactions.

A plot of the DS of the prepared EC analogs versus the molar ratio of iodoethane to hydroxyl groups that was added to the reaction mixture (Figure 2.8) under constant conditions shows that a large increase in the DS of EC can be achieved by the addition of a comparatively small quantity of ethylating agent. However, as larger quantities of iodoethane are added, the rate of the increase in the DS is lower than that observed for the

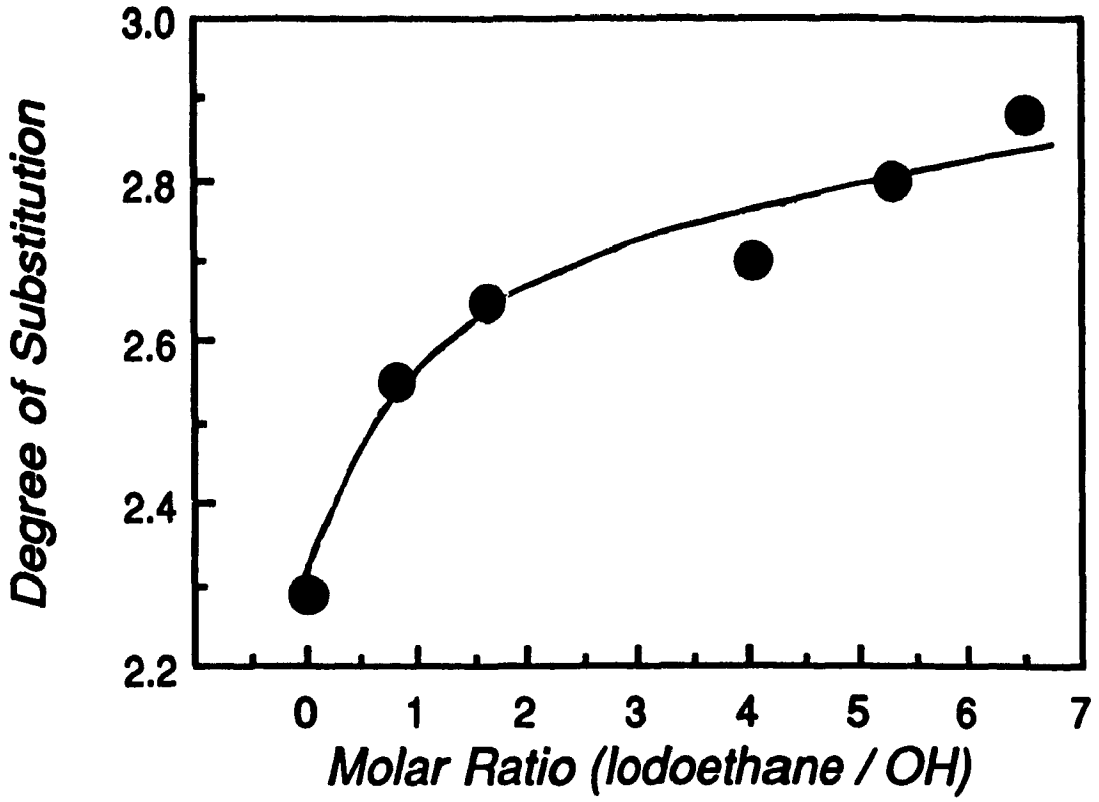

Figure 2.8 The DS of the EC analogs as a function of the molar ratio of iodoethane to hydroxyl groups added to the reaction mixtures under constant conditions.

reaction which produced EC-1. The probable reason for this lies in the relative reactivities of the hydroxyl groups at 2, 3 and 6 positions. It has been found that the heterogeneous reactions used to synthesize commercial EC and MC produce a heteropolymer containing eight different residues randomly substituted along the chain (7, 8). The reaction conditions used here are homogeneous and of the segments of the EC backbone that are only slightly substituted, the OH-2 and OH-6 positions should be the preferred sites of occupation for the ethylating agent. The rapid occupation of these reactive positions would account for the large increase observed for the initial ethylating reaction while the substitution of the remaining less reactive sites are responsible for the less rapid increases seen for samples of higher DS.

2.5 CONCLUSION

EC samples of several degrees of substitution have been prepared by the use of commercial grade EC as the starting material, sodium hydride as the base and iodoethane as the ethylating agent. By using iodomethane and n-iodobutane as the alkylating agent, mixed trisubstituted ether derivatives of EC were also prepared. The DS values of the samples were found to vary between 2.29 and 3.00 and molar mass measurements found that there was no major decrease in the degree of polymerization due to the reactions. The two commercial grade EC samples and the prepared derivatives are the samples employed in the remainder of the thesis.

2.6 REREERENCES

(1) "Kirk-Othmer Encyclopedia of Chemical Technology, Second Edition", (A. Stander, exec. ed.), Interscience Publishers, New York, 1964, Vol. 4, pp. 616.

(2) "Ethyl Cellulose - Properties and Uses", Hercules Powder Co., Wilmington, Del., 1962.

(3) M. Siekmeyer and P. Zugenmaier, *Die Makromol. Chem., Rapid Commun.*, **28**, 173 (1987).

(4) G.V. Laivins and D.G. Gray, *Polymer*, **26**, 1435 (1985).

(5) A. Parfondry and A.S. Perlin, *Carbohydr. Res.*, **57**, 39 (1977).

(6) K.-G. Rosell, *J. Carbohydr. Chem.*, **7**, 525 (1988).

(7) J. Reuben, *Carbohydr. Res.*, **157**, 201 (1986).

(8) J. Reuben, *Carbohydr. Res.*, **161**, 23 (1986).

(9) A.S. Perlin, private communication.

CHAPTER 3

CHAIN STIFFNESS AND MESOPHASE FORMATION

3.1 INTRODUCTION

The first half century of investigations on liquid crystals dealt exclusively with low molar mass organic compounds. Any of four general features can be present in these molecules: planar units such as benzene rings, a series of double bonds in the backbone, strong dipoles along the molecular axis and weak dipolar end groups are all typical (1). The result of any of these characteristics is a molecule with an anisotropic shape. It has been reported that an axial ratio of only three is required for a low molar mass organic compound to form a mesophase (2).

With the observation in 1937 that a polymer could form a liquid crystal (3) and the subsequent development of processes for the manufacture of high strength, low weight fibres from polymeric mesophases (4, 5), the interest in an understanding of the liquid crystalline phase separation phenomenon lead to a variety of theories. The application of these theories to cellulose and its derivatives has been fueled not only by an interest in the theoretical perspectives, but also by the practical and potentially practical ones. Patents have been awarded based on the production of fibres from anisotropic solutions of cellulose and its derivatives (6, 7) and the possibility of using liquid crystalline cellulosic solutions in the production of regenerated cellulose fibres has also been discussed (8).

3.1.1 Theories of Polymer Mesophase Formation

Two fundamentally different approaches have been used to describe the liquid crystalline phase separation behaviour of mainchain polymers in terms of the geometric features of the polymer. One approach is based on a virial expansion method while the other employs a lattice model. Both methods have been modified to account for several parameters not considered in the original theories. Among these modifications is the inclusion of attractive dispersive forces between segments of the polymer chains. Attractive dispersive forces alone were found to explain adequately low molar mass mesophase formation (9) and they have also been used to describe successfully polymer mesophase formation (10). However, as these theories ignore the role of the geometric

features of the polymer and lack an easily measurable physical parameter, they have not been as extensively employed as geometric theories in application to mainchain polymers.

3.1.1.1 Virial Expansion Theories

The first theory to predict the formation of an ordered solution for polymeric molecules was introduced in 1949 by Onsager (11). This theory modelled the polymer molecules as impenetrable rigid rods that possessed no intermolecular forces other than geometric ones. The free energy of the system, ΔF, was expressed as a function of the particle distribution by a virial expansion that was truncated at the second term (Equation [3.1]).

$$\Delta F / NkT = \text{Constant} + \ln c' + \sigma + bc'\rho' \qquad [3.1]$$

where
- N = number of rods in volume V
- k = Boltzmann constant
- T = temperature
- c' = rod concentration (N/V)
- σ = entropy loss due to orientation
- b = $(\pi/4) L^2 d$ (L = length, d = diameter of rod)
- ρ' = orientation dependent second virial term.

In the isotropic state the random distribution of the rods minimizes the orientational entropy whereas when in the anisotropic state, the translational entropy is minimized. The critical volume fraction, ϕ', is reached when the loss in orientational entropy due to the addition of a single molecule equals the gain in translational entropy. At this point the solution contains both isotropic and anisotropic regions and is called biphasic. As more of the solute is added, the solution eventually becomes fully anisotropic at some second concentration ϕ''. The theory gives the critical volume fractions as a function of the axial ratio, x, according to Equations [3.2] and [3.3].

$$\phi' = 3.34 / x \qquad [3.2]$$

$$\phi'' = 4.49 / x. \qquad [3.3]$$

The Onsager approach has been criticized as inappropriate for real polymer systems because truncating the virial expansion at the second term ignores higher order effects and requires that all parameters be dependent solely on the second virial term (12). For example, the solution is treated as a continuum in which the diameter of the polymer is considered to be the same as the diameter of the solvent molecules. The second virial coefficient is dependent on the ratio of the polymer / solvent diameter and is felt to be too large by a factor of at least two because of the truncation. For these reasons the Onsager theory has traditionally been considered to be applicable only for situations where the axial ratio of the polymer is much greater than one and the critical volume fraction is much less than unity. Despite these assertions, the Onsager model continues to elicit support. Odijk (13) has recently examined the effect of the third virial coefficient, both in terms of the truncation effect and the polymer / solvent diameter ratio, and stated that while the Onsager theory cannot always be considered quantitative in the normal range of polymer axial ratios, the influence of the third virial coefficient is much less severe than critics of the theory assume.

A difficulty with the Onsager theory, apart from objections to its theoretical validity, is that it was originally intended to describe the ordering of pure rigid rods. Real polymer systems tend to exhibit a number of features which deviate from this restriction, the foremost of which is that even the stiffest of polymers has some degree of flexibility. In Chapter 1.3 it was reported that a semiflexible polymer chain in solution can be represented by both a freely-jointed chain and a wormlike chain. Both models have been used in modified Onsager theories. When semiflexibility was introduced to the theory by modelling the polymer as a series of rigid segments connected by flexible joints (14, 15) the critical volume fractions were found to be given by Equations [3.4] and [3.5].

$$\phi' = 3.25 / x \qquad [3.4]$$

$$\phi'' = 4.86 / x. \qquad [3.5]$$

In modelling the semiflexible polymer as a wormlike chain Khokhlov and Semenov (16) found that in the elementary form of their theory the critical volume fractions for mesophase formation were

$$\phi' = 10.48 / x \qquad [3.6]$$

$$\phi'' = 11.39 / x \qquad [3.7]$$

for the case where the contour length, L, was much greater than the equivalent Kuhn segment length, k_w. They later modified this theory to include the effect of molar mass and found that the new critical volume fractions were as given in Equations [3.8] and [3.9] (17).

$$\phi' = d / k_w \left[(3.34 + 11.3N + 4.06N^2) / N (1 + 0.387N)\right] \qquad [3.8]$$

$$\phi'' = d / k_w \left[12 / (1 - (1 - \exp(-6N)) / 6N)\right]. \qquad [3.9]$$

where d = diameter

$N = L / k_w$ = number of equivalent Kuhn segments per molecule.

This theory in turn has recently been extended by Odijk (13) who considered not only the effect of semiflexibility, but also polydispersity and end effects. Odijk expressed his theory in terms of persistence length rather than equivalent Kuhn segment length, but for comparative purposes his equations for the critical volume fractions have been converted to the Kuhn standard and are given as Equations [3.10] and [3.11].

$$\phi' = d / k_w \left[(3.34 + 11.94N + 6.34N^2) / N (1 + 0.586N)\right] \qquad [3.10]$$

$$\phi'' = d / k_w \left[(4.486 + 22.48N + 70.16N^2) / N (1 + 5.66N)\right]. \qquad [3.11]$$

Khokhlov and Semenov (18, 19) have also introduced a model they term a universal approximate method and employed it to describe polymer mesophase ordering in both the solution and the melt. It was found that the properties of the liquid crystalline phase separation behaviour depend not only on the chain length and the axial ratio, but also on whether the chain is best represented by a freely-jointed Kuhn chain or a persistent wormlike chain. The method considers contributions from both steric repulsive and attractive forces and equates the free energy of the systems, F, according to Equation [3.12].

$$F = F_1 + F_2 + F_3 + F_4 \qquad [3.12]$$

where F_1 = translational entropy for the molecule

F_2 = orientational entropy

F_3 = free energy of the steric interaction of the segments in the second virial approximation

F_4 = energy of the forces of attraction.

According to this theory, the critical axial ratio for rigid rods is 3.5, for semiflexible freely-jointed chains is 7 and for persistent wormlike chains is 50.

3.1.1.2 Lattice Theories

A second description of the liquid crystal phase separation phenomenon was introduced by Flory (20) in 1956 and is based on a lattice model of a polymer in solution in which only geometric contributions to mesophase formation are considered. In this theory the rodlike molecule is allowed to adopt a continuously varying range of orientations by replacing each solute molecule by several submolecules that are laterally joined at their ends and are parallel to the orientation axis. The partition function that describes the free energy, ΔG, as a function of the composition, the disorientation index, y, and the axial ratio, x, is given as Equation [3.13].

$$\Delta G / kT = n_1 \ln v_1 + n_2 \ln v_2 - (n_1 + y n_2) \ln [1 - v_2(1 - y / x)] - n_2 [\ln (xy^2) - y + 1] + \chi_1 x n_2 v_1 \qquad [3.13]$$

where k = Boltzmann constant

T = temperature

n_1 = number fraction of solvent molecules

v_1 = volume fraction of solvent

n_2 = number fraction of solute molecules

v_2 = volume fraction of solute

χ_1 = free energy of interaction.

The disorientation index is expected to adopt a value which minimizes ΔG. The value of v_2 at the minimum ΔG is termed ϕ' and was defined in terms of the axial ratio and the disorientation index by Equation [3.14].

$$\phi' = [x / (x - y)] [1 - \exp(-2 / y)]. \qquad [3.14]$$

By equating $d\phi'/dy$ to zero and expressing the disorientation index in terms of a series expansion, it was found that for large values of the axial ratio the critical volume fraction for a stable oriented phase can be expressed solely as a function of the axial ratio. Equation [3.15] is generally considered to be valid for axial ratios greater than ten.

$$\phi' \equiv (8 / x) (1 - 2 / x). \qquad [3.15]$$

According to this theory a minimum value of 6.702 for the axial ratio is required for the coexistence of the two phases. As in the Onsager theory, the solution eventually becomes fully anisotropic at some higher concentration, ϕ''. In the Flory theory this volume fraction is equal to $12.5 / x$. Also like the Onsager theory, the validity of the Flory theory has been questioned at a fundamental level. Straley (21) has criticized the theory on the grounds that upon refinement it leads to inconsistencies and fails to predict phase separation even for long rods. Flory and Ronca (12) have acknowledged these criticisms but trace the source of the error to an incorrect description of the disorientation parameter, y, in the original theory. They determined that correction of the disorientation parameter model still leads to essentially the same final equations as the original lattice theory and consider Equation [3.15] to be acceptable for describing the critical volume fraction of most polymers. The refined model gives a value of 6.417 as the critical axial ratio for mesophase formation.

The lattice theory has been re-examined in terms of several factors, all of which attempt to give a more realistic description of the liquid crystalline phase separation phenomenon. Flory realized that even very rigid polymers such as helical polypeptides were subject to deviations from pure rigidity and that the cumulative effect of such deviations would be substantial in a long chain. In 1978 the lattice theory was re-examined in terms of semiflexible polymers in which the semiflexibility was imparted to

the chain by modelling it as a series of rigid rods connected by freely flexible joints (22). It was determined that the overall length of the molecule was not the primary factor determining the thermodynamic and phase separation behaviour but rather the axial ratio of the rigid segments along with their combined volume fractions. The concept of semiflexibility was also considered by Ronca and Yoon (23) in a lattice model, but they modelled the chain with wormlike character rather than as a freely-jointed Kuhn chain. In this theory the critical volume fraction for mesophase formation is a function of the molar mass, the axial ratio of the persistence length and the temperature. They state that there is a limiting cut-off length for the persistence length, which corresponds to a maximum curvature of the chain, below which the mesophase will not form.

Other features of real polymer systems have also been included in the lattice theory method. These include polydispersity (24), polymer systems composed of rigid rods separated by flexible spacers (25, 26, 27, 28), unoccupied sites in the lattice to account for possible free volume effects (29), and the influence of sidechains (30, 31).

Mean field theories have been used to successfully describe the formation of liquid crystals but they ignore the role of intermolecular repulsions and consider only the effects of attractive dispersion forces. Ten Bosch and Sixou (10) treated the formation of a nematic melt of polymer chains based on the Maier-Saupe approach, but the theory had to be extended to describe the formation of a lyotropic mesophase (32). The original geometric theories have been criticized because they ignore the possible role played by these intermolecular anisotropic attractive forces, but Flory and Ronca (33) have considered a lattice model in which factors other than geometric ones are present and concluded that the geometric shape of the molecule is the predominant factor in determining the phase separation behaviour. They also state that while polymers with axial ratios greater than 6.417 should form mesophases, those with lower axial ratios might be capable of forming ordered phases should the orientational anisotropic forces prove sufficiently strong. Warner and Flory (34) extended the previous theory to include the effects of diluent on the attractive dispersive forces and found that its presence diminishes the orientation dependent interactions between molecules. Ciferri and Marsano (35) have stated that the role played by anisotropic forces for poly(n-hexyl

isocyanate) (PHIC) and cellulose derivatives are probably of minor significance because the sidechains prevent any close proximity of the polarized bonds along the backbone of the chain. Krigbaum et al. (36, 37) used the approach of Warner and Flory, in addition to replacing the stiff rod with a Kuhn chain as suggested by Flory (22), but made the Kuhn segment length sensitive to temperature and measured the persistence length of PHIC in toluene and tetrahydrofuran over a range of temperatures and also calculated the Kuhn lengths of (hydroxypropyl)cellulose (HPC) in dimethylacetamide (DMAC) according to the data in the literature (38). It was found that by extrapolating the data for these systems to the isotropic temperature, the temperature where the mesophase is no longer thermally stable, produces axial ratios very near the value of the critical axial ratio predicted by Flory and Ronca. The inclusion of a temperature dependent segment length is an important adaptation of the original Flory theory which presumes the critical volume fraction is independent of temperature, because experiment has shown the critical volume fractions for both polybenzyl-L-glutamates and cellulose derivatives are temperature dependent (39, 40).

3.1.2 Hydrodynamic Theories

Implementation of any of the phase separation theories described above requires an estimate of a polymer's axial ratio in a given solvent. This means that measurements of both the persistence length, or the Kuhn length, and the diameter of the polymer must be made.

Measurement of the stiffness of a polymer in solution is possible by several methods: light scattering (41), sedimentation and diffusion (42), flow birefringence (43), dielectric measurement (44) and viscosity (45). Viscosity techniques for the measurement of the dimensions of cellulose and its derivatives have been frequently employed because their semiflexible nature and temperature sensitive conformations make them ideal candidates for testing the validity of frictional viscosity theories.

While the persistence length provides a reasonable estimate of a polymer's relative stiffness, a reliable estimate of the chain diameter is also needed to determine the axial

ratio. The length of the monomer unit of cellulose has been calculated by the use of x-ray data as 0.514 nm (46, 47) and 0.515 nm (48) while the width and thickness are reported as 0.9 nm and 0.5 nm, respectively (48). A potential problem exists however, in employing the dimensions of cellulose derivatives determined on the basis of their crystalline structure because in the crystalline form the conformations are rigid whereas in solution the possibility of sidechain flexibility exists. Direct measurement of a polymer's solution characteristics is therefore the preferred method for obtaining useful dimensional information, provided reliable theories exist to interpret the data. Hydrodynamic methods are attractive for reasons of relative simplicity of data measurement.

The relationship between viscosity and molar mass most widely recognized is the semi-empirical Mark-Houwink-Sakurada (MHS) equation which relates the molar mass, M, of a polymer to its intrinsic viscosity, $[\eta]_o$, through equation [3.16].

$$[\eta]_o = K M^a. \qquad [3.16]$$

K is a constant and the exponent, a, is frequently used as an approximate measure of the chain stiffness. The utilization of the MHS exponent as a measure of chain stiffness is theoretically possible because the exponent has four contributing factors (Equation [3.17]) (49).

$$a = 0.5 + a_\Phi + a_1 + 1.5\, a_2 \qquad [3.17]$$

where

$$a_\Phi = d \ln \Phi / d \ln M$$
$$a_1 = 3\, d \ln \alpha / d \ln M$$
$$a_2 = d \ln (<S^2>_o / M) / d \ln M.$$

It can be seen that the MHS exponent is related to the radius of gyration, $<S^2>_o$, the hydrodynamic character, Φ, and the linear expansion factor, α, and how they vary with changes in molar mass. For a polymer in a theta solvent the only contribution comes from the first term. The three additional parameters allow for deviations from the random coil configuration and are dependent on the specific polymer / solvent pair. The degree to which a polymer in any given solvent is perturbed from the idealized random coil towards

a rigid rod is reflected in the value of the MHS exponent. The value of the exponent thus provides some measure of information on the stiffness of the chain. In practice it is found that polymers behaving as random coils have MHS exponents of 0.5 while those behaving as rigid rods have a value of ~1.8 (8). Cellulose derivatives are considered to be semiflexible and typically have an MHS exponent value between 0.8 and 1 (50). The main source of flexibility in cellulose derivatives is the rotation of anhydroglucopyranose units at random positions along the chain (47, 51). While the MHS exponent can give an estimate of chain stiffness it does not provide any information on the molecular dimensions of the polymer and thus no information on the axial ratio.

3.1.2.1 Yamakawa - Fujii Hydrodynamic Transport Theory

As discussed in Chapter 1.3.1, the wormlike chain model, which adopts random-flight statistics at high molar masses, is considered to be an acceptable method for describing both flexible and rigid polymers in solution. However, a difficulty with the Kratky and Porod model of the wormlike chain is that while the model chain is characterized by L and k_w, the relationship between L and M is not known for many polymers unless the molecule has a rigid local conformation. Variations of the Kratky - Porod model have been developed which attempt to provide a more accurate description of a polymer in solution. These include the wormlike touched bead model (52), wormlike cylindrical model (53) and helical wormlike chain model (54). These theories are all based on the Kirkwood and Riseman (55, 56) theory of polymer hydrodynamics. Yamakawa and Tanaka (57) have developed a touched bead model that yields the same results as hydrodynamic models that have had the Oseen - Burgers procedure applied to cylindrical wormlike chains. The Oseen - Burgers procedure is a method used in hydrodynamics for calculating the friction properties when the mean relative velocity of a fluid over a cross section of the body is zero. Yamakawa and Fujii have stated that bead models and cylindrical models must yield the same final results (58).

Although Yamakawa has employed the bead model he later adopted the wormlike cylinder model. Yamakawa and Fujii's (58, 59) criticism of the wormlike cylindrical

hydrodynamic model introduced by Ullman (53) is that it includes an additional parameter beyond the physical dimensions of the polymer and the intrinsic viscosity and its inclusion makes it difficult to analyze experimental data to determine the shift factor, M_L, which is defined as the ratio of the molar mass to the contour length (Equation 3.18).

$$M_L = M / L. \qquad [3.18]$$

For cellulose derivatives M_L is taken here to be equal to the ratio of the molar mass of the substituted anhydroglucopyranose unit to the length of the unit.

The wormlike cylinder hydrodynamic model that Yamakawa and Fujii (58) developed relates the limiting viscosity number, $[\eta]_o$, of a wormlike chain to L, k_W and the diameter, d, by Equation [3.19].

$$[\eta]_o = \Phi (L_r, d_r) L_r^{3/2} k_W / M \qquad [3.19]$$

where $\Phi (L_r, d_r)$ is an approximate analytical expression dependent on L_r and d_r, the reduced chain parameters. $L_r = L / k_W$ and $d_r = d / k_W$. For infinitely long wormlike chains ($L \rightarrow \infty$) the polymer can be treated as a random-flight model where $< r_o^2 >$, the mean square end-to-end distance, is related to k_W by Equation [3.20].

$$k_W = (< r_o^2 > / L)_\infty = (< r_o^2 > / M)_\infty M_L. \qquad [3.20]$$

A difficulty with the Yamakawa - Fujii model is that it is an iterative method in which estimated values of k_W and d are used to produce computed intrinsic viscosity values which are then compared with the experimental results. The values of k_W and d that give the overall minimum in the average deviation are the values that best represent the Yamakawa - Fujii model. This theory has been used to compute the molecular dimensions of several cellulose derivatives (38, 60 - 66), but the method tends to gives values for the diameters of the polymers which are unrealistically small. The reason for the unrealistic dimensions is that the procedure used to compute k_W and d attempts to minimize two the parameters simultaneously. These two dimensions are interdependent and uncertainty in the value of one parameter creates uncertainty in the value assigned to

the other (40). The Yamakawa - Fujii model has also been criticized by Saito (60) and Kamide et al. (61) in two other respects. First, because Yamakawa and Fujii did not employ a draining term in the equation for fluid flow (which means that there is no solvent slip on the surface of the wormlike cylinder) the theory is considered to be oversimplified as it is claimed that there should be no distinct boundary between the solvent and the solvated polymer. Second, it is claimed that there is an error in one of the equations of the Yamakawa - Fujii theory that makes its application suspect at low axial ratios.

3.1.2.2 Bohdanecky Hydrodynamic Transport Theory

More recently, Bohdanecky (67) has presented a modification of the Yamakawa - Fujii theory. In this version, the assumption of Tsuji et al. (68), that the hydrodynamic volume occupied by 1 g of the cylindrical wormlike chain is equal to the partial specific volume, $\bar{v}$, of the polymer, is employed. The relationship among the intrinsic viscosity, reduced contour length and molar mass is

$$[\eta]_o = \left[\Phi L_r^{3/2} k_w^3 / M\right]. \qquad [3.21]$$

By combining Equation [3.21] with [3.19] and [3.20] the intrinsic viscosity can be related to the mean square end-to-end distance by Equation [3.22].

$$[\eta]_o = \left[\Phi_\infty (< r_o^2 >/M)_\infty^{3/2} M^{1/2}\right] F_1 \qquad [3.22]$$

where $$F_1 = \Phi / \Phi_\infty.$$

In the limit of very long chains ($L \rightarrow \infty$), Φ takes on the limiting value of 2.86×10^{23} (69), F_1 goes to unity and $(< r_o^2 >/M)_\infty$ can be determined. The value of F_1 can be approximated by Equation [3.23].

$$F_1 = (B_o + A_o / L_r^{1/2})^{-3} \qquad [3.23]$$

where $$B_o = 1.00 - 0.0367 \log d_r \qquad [3.24]$$

and $$A_O = 0.46 - 0.53 \log d_r. \qquad [3.25]$$

Combining Equations [3.22] through [3.25] gives Equation [3.26].

$$(M^2 / [\eta]_o)^{1/3} = A_\eta + B_\eta M^{1/2} \qquad [3.26]$$

where $$A_\eta = A_O M_L \Phi_\infty^{-1/3} \qquad [3.27]$$

and $$B_\eta = B_O \Phi_\infty^{-1/3} (< r_o^2 > / M)_\infty^{-1/2}. \qquad [3.28]$$

The assumption that the hydrodynamic volume is equal to $\bar{v}$ yields Equation [3.29] when B_O is assigned a value of 1.05. As a first approximation, the assignment of this value to B_O is possible because B_O is a very weak function of dr.

$$d_r^2 / A_O = (4\Phi_\infty / 1.215 \pi N_{AV})(\bar{v} / A_\eta) B_\eta^4 \qquad [3.29]$$

where N_{AV} is Avogadro's Number.

The quantity (d_r^2 / A_O) is related to d_r by the empirical Equations [3.30] and [3.31].

$$\log (d_r^2 / A_O) = 0.173 + 2.158 \log d_r \quad (d_r \leq 0.1). \qquad [3.30]$$

$$\log (d_r^2 / A_O) = 0.795 + 2.78 \log d_r \quad (0.1 \leq d_r \leq 0.4). \qquad [3.31]$$

Using the equations listed above, the molecular dimensions of a polymer can calculated from the values of the slope and intercept of a plot of $(M^2 / [\eta]_o)^{1/3}$ against $M^{1/2}$. These molecular dimensions provide the axial ratios that are required for the implementation of the theories describing polymer mesophase formation. This theory has been employed to determine the molecular dimensions of four cellulose derivatives (65, 67, 70, 71).

The primary polymer of interest in this study is ethyl cellulose (EC) and in this chapter estimates of the molecular dimensions of EC in several solvents are obtained by the combined use of the Bohdanecky hydrodynamic transport theory, a large body of existing EC intrinsic viscosity / molar mass information and measurement of the apparent partial specific volume of EC in several solvents. Confidence limits on the slopes and

intercepts of plots of log $[\eta]_o$ versus log M and plots of $(M^2 / [\eta]_o)^{1/3}$ versus $M^{1/2}$ are employed to gain an estimate of the possible variation in the values of the MHS constants, k_w and d. The data obtained are used in the previously described virial and lattice theories and the results compared with experimental values of the critical volume fraction for mesophase formation. Literature data for other cellulose derivatives that have been treated by the Yamakawa - Fujii theory are used to obtain the Bohdanecky molecular dimensions and the results are used for comparative purposes. The data for these other cellulose derivatives are compiled in Appendix A.

3.2 EXPERIMENTAL

The Bohdanecky method of determining the molecular parameters of a polymer requires a knowledge of the partial specific volume of the polymer in a solvent. Equation [3.32] relates $\bar{v}$ to the apparent volume, v_2, occupied by a mass, m_2, of the polymer in solution (72).

$$\bar{v} = v_2 / m_2. \qquad [3.32]$$

As v_2 can be defined by Equation [3.33]

$$v_2 = v - v_1 \qquad [3.33]$$

where v = solution volume

v_1 = solvent volume = m_1 / ρ_1

where ρ_1 = solvent density.

m_1 = solvent mass = $m - m_2$

where m = mass of the solution in volume v

m_2 = mass of the polymer in volume v,

the above equations can be recombined to form Equation [3.34].

$$\bar{v} = \frac{1}{m_2}\left(v - \frac{(m - m_2)}{\rho_1}\right). \qquad [3.34]$$

To determine $\bar{v}$ for a given polymer / solvent pair by Equation [3.34] requires a knowledge of the density of the solution. A convenient method for determining solution densities is by the use of a digital densitometer. The principle of this apparatus is based on the measurement of the variation of the vibration period, T, of a glass hollow U-tube filled with different samples. For a hollow body of mass M and volume V which is suspended on a spring with an elastic constant C and is filled with a sample of density ρ, then the vibration period of the system is

$$T = 2\pi ((\rho V + M) / C)^{0.5}. \qquad [3.35]$$

By taking the square of Equation [3.33] and inserting $A = 4\pi^2 V / C$ and $B = 4\pi^2 M / C$ Equation [3.36] is obtained.

$$T^2 = A\rho + B. \qquad [3.36]$$

For the difference of the densities of two samples Equation [3.37] holds.

$$\rho_1 - \rho_2 = (T_1^2 - T_2^2) / A. \qquad [3.37]$$

As the constant A contains both the volume and spring constants, it can be treated as an apparatus constant that may be determined by calibrating samples of known density. Once this is done the density of a polymer solution may be obtained by comparison with the density of the pure solvent. The solution density of each pure solvent and each EC / solvent pair was determined at 25.0 °C with a Paar Density Meter. The concentrations of the measured solutions were in the range of 1.2 - 2.3 % (w/v).

Confidence limits on the slope and intercept of plots of $(M^2 / [\eta]_0)^{1/3}$ versus $M^{1/2}$ and plots of log $[\eta]_0$ versus log M were computed using a Lionheart Press, Inc. statistics package. The best fit of the data was determined using a method of least squares and both the 95% and 68% confidence limits are calculated. Confidence limits are the assigned upper and lower values of a range of values where it is predicted with a 95% or 68% certainty that the true value actually falls within that range.

The concentration at which liquid crystalline phase separation occurs was found by detecting the onset of birefringence using a Reichert polarizing microscope. Samples were prepared by weighing known masses of EC into small vials and then adding known masses of solvent. The vials were capped and dissolution was aided by the use of a centrifuge. For highly concentrated samples, $\phi > 0.50$, the sample vials were prepared by weighing a known mass of EC into a vial, weighing the vial, adding a large volume of solvent and, after complete dissolution, allowing the solvent to evaporate. Measurement of the mass of the vial allowed to concentration to be calculated and solution homogeniety was then achieved by centrifugation. Each sample was smeared onto a microscope slide and a glass coverslip was pressed on top of the sample. The samples were immediately examined for the appearance of birefringence between crossed polars. The EC used in this portion of the thesis had a DS of 2.52 and a weight average molar mass of 168,000 (73).

3.3 RESULTS AND DISCUSSION

A survey of the literature reveals that the relationship between intrinsic viscosity and molar mass for EC in several solvents has been extensively studied at 25.0 °C. The data obtained in these studies are reproduced in Tables 3.1 - 3.3. All intrinsic viscosity data are reported in units of $cm^3\ g^{-1}$.

Table 3.1

Intrinsic Viscosity, $[\eta]_o$, of Ethyl Cellulose (DS = 2.52) [a]

Solvent	Number Average Molar Mass of the EC Fractions [b]					
	140,000	119,000	87,000	64,000	57,000	40,000
Benzene	421	374	307	237	197	-
n-Butyl Acetate	418	356	287	216	193	138
Chloroform	438	386	308	226	201	143
Ethyl Acetate	406	339	280	-	187	129
Ethyl Methyl Ketone	379	323	260	205	180	129

[a] Measured by Moore and Brown (74).
[b] Uncertainties are reported as ± 3% for the molar mass and ± 2% for the intrinsic viscosity.

Table 3.2

Intrinsic Viscosity, $[\eta]_o$, of Ethyl Cellulose (DS = 2.54) [a]

Solvent	Weight Average Molar Mass of the EC Fractions					
	410,000	329,000	201,000	181,000	130,000	98,000
Methanol	223	206	143	135	110	93

[a] Measured by Scherer et al. (75).

Table 3.3

Intrinsic Viscosity, $[\eta]_o$, of Ethyl Cellulose (DS = 2.56) [a]

Solvent	Viscosity Average Molar Mass of the EC Fractions [b]						
	93,000	90,000	84,000	72,000	59,000	30,000	22,000
Acetic Acid	278	-	-	220	191	-	77.0
n-Butyl Acetate	283	-	-	229	192	-	76.0
Chloroform	324	302	284	254	220	113	90.0
m-Cresol	288	261	248	223	192	107	83.6
Dioxane	289	-	-	220	200	-	77.0
Ethyl Acetate	273	-	-	218	179	-	78.5
Pyridine	239	-	-	193	162	-	66.5

[a] Measured by Staudinger and Reinecke (76).
[b] Molar masses recalculated from re-evaluated MHS equations of Moore and Brown (74).

In the case of the study by Staudinger and Reinecke (Table 3.3), their assignments of molar mass to each EC fraction have been ignored and the molar masses used here have been made on the basis of the intrinsic viscosity - molar mass study of Moore and Brown (Table 3.1). The reason for ignoring the molar masses of Staudinger and Reinecke is that their molar mass assignments were made on the basis of osmotic pressure, π, experiments which yielded plots of π / concentration versus concentration that were nonlinear. This suggests that their apparatus may have been deficient; the most probable source of error in their study is leakage of polymer through the membrane used in the osmometer. Assignments of molar mass to the fractions of EC studied by Staudinger and Reinecke are made here on the basis of the work by Moore and Brown because both studies used EC of nearly identical degree of substitution (DS) and had three common solvents. Molar mass assignments of the EC fractions studied by Moore and Brown were also made on the basis of osmotic pressure measurements, but in this case all plots of π / concentration versus concentration were linear and no leakage of EC through the membrane was detected. The molar masses of the EC fractions in the Staudinger and Reinecke study are calculated here by substituting the EC / n-butyl acetate, chloroform and ethyl acetate viscosity values of Staudinger and Reinecke into the re-evaluated MHS

equations of Moore and Brown for these EC / solvent systems (*vide infra* Section 3.3.1) and taking the average value of the computed molar masses.

3.3.1 The Mark-Houwink-Sakurada Constants

The Mark-Houwink-Sakurada (MHS) parameters for the listed EC / solvent systems in Tables 3.1, 3.2 and 3.3 have all been re-evaluated by plotting the logarithm of the intrinsic viscosity against the logarithm of the molar mass (Figure 3.1) and using a best fit to evaluate the MHS constant K and exponent a for each system. The constant K is obtained from the anti-log of the y-axis intercept while the MHS exponent is equal to the slope of the double logarithmic plot. The re-evaluated parameters are listed in Table 3.4. The values of K and a at the 68% and 95% confidence limits are given in Table 3.5.

Table 3.4

Mark-Houwink-Sakurada Constants (Best Fit)

Solvent	K	a	correlation coefficient
Benzene [a]	0.030	0.806	0.9908
n-Butyl Acetate [a]	0.014	0.870	0.9985
Chloroform [a]	0.011	0.896	0.9979
Ethyl Acetate [a]	0.010	0.893	0.9968
Ethyl Methyl Ketone [a]	0.019	0.838	0.9977
Methanol [b]	0.0647	0.632	0.9980
Acetic Acid [c]	0.010	0.892	0.9996
m-Cresol [c]	0.020	0.831	0.9988
Dioxane [c]	0.0084	0.913	0.9981
Pyridine [c]	0.0090	0.891	0.9999

[a] Based on data from ref. (74); [b] Based on data from ref. (75); [c] Based on modified data from ref. (76).

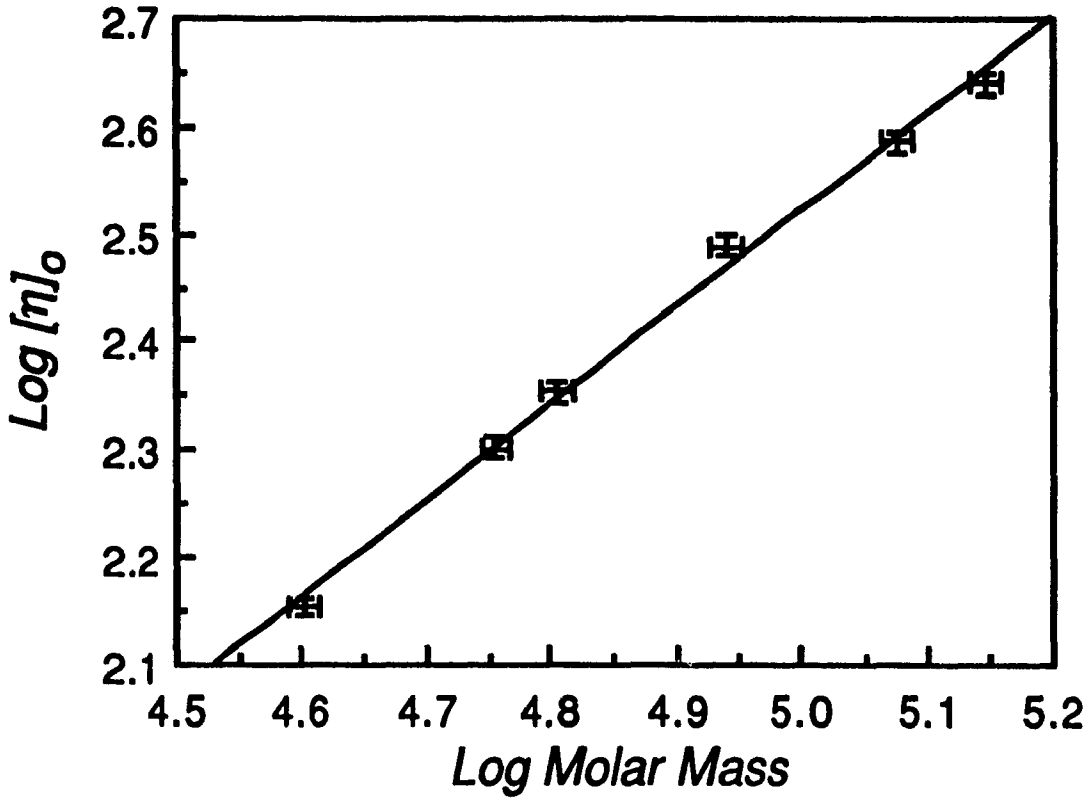

Figure 3.1 Mark-Houwink-Sakurada plot for EC in chloroform. (Based on data from ref. (74))

Table 3.5

Upper and Lower Limits of the Mark-Houwink-Sakurada Constants

	95% Limits		68% Limits	
Solvent	K	a	K	a
Benzene [a]	0.24	0.624	0.086	0.715
	0.0038	0.989	0.011	0.897
n-Butyl Acetate [a]	0.028	0.810	0.020	0.840
	0.0071	0.931	0.010	0.900
Chloroform [a]	0.026	0.821	0.017	0.859
	0.0048	0.971	0.0072	0.934
Ethyl Acetate [a]	0.039	0.775	0.020	0.834
	0.0027	1.01	0.0053	0.952
Ethyl Methyl Ketone [a]	0.042	0.766	0.028	0.802
	0.0082	0.910	0.012	0.874
Methanol [b]	0.121	0.580	0.0886	0.606
	0.0345	0.683	0.0473	0.678
Acetic Acid [c]	0.022	0.823	0.015	0.858
	0.0049	0.960	0.0071	0.926
m-Cresol [c]	0.033	0.788	0.026	0.810
	0.013	0.876	0.016	0.854
Dioxane [c]	0.045	0.760	0.019	0.836
	0.0016	1.06	0.0037	0.992
Pyridine [c]	0.013	0.856	0.011	0.874
	0.0062	0.926	0.0075	0.909

[a] Based on data from ref. (74).
[b] Based on data from ref. (75).
[c] Based on modified data from ref. (76).

As reported in Section 3.1.2, the exponent of the MHS equation is commonly associated with the rigidity of a polymer in solution. Other factors have also been listed as having some impact on the value the exponent (77) but in reality their effect on the calculated value for a freely-draining coil is minor compared to the potential impact of the

scatter of the experimental data. Tables 3.4 and 3.5 listed the values of the constants K and a as determined by a best fit of the experimental data to a straight line and the upper and lower values obtained at the 68% and 95% confidence limits. These data show that within the 95% confidence interval a large variation in the calculated value of the exponent a of the MHS equation is possible and that even at the 68% confidence limits a considerable range of values exists. For example, EC in benzene has the lowest correlation coefficient associated with the best fit data in Table 3.4 (0.9908) and the possible range of values at the 95% confidence limits extends from 0.624 to 0.989. Based on these values EC in benzene could be described as a near random coil or as an extended polymer. This re-enforces the idea that while the MHS exponent can be used as a rough estimate of chain stiffness, it cannot be considered an absolute method unless a large number of data are employed and the MHS plot has an extremely high correlation coefficient. The large potential variation in the constant K is the result of the necessity to extrapolate the data back to zero molar mass and as the data are contained in a comparatively narrow range, a small degree of scatter in the data results in a wide range of possible K values; this potential variation is inherent to the viscosity / molar mass technique. Despite its restricted applicability to statements about chain rigidity, the technique is completely valid for molar mass determinations because both the constant K and the exponent a change simultaneously when determining confidence limits. The molar mass obtained for a given intrinsic viscosity by an equation using the constants at the 95% confidence limits will therefore be very close to the value obtained by the best fit equation. A common practice in the literature is to assign a small uncertainty value (typically $\pm$ 0.02 - 0.05) to the exponent a in the MHS equation and assume that this adequately describes the uncertainty; this assumption is invalid.

3.3.2 A Comparison of the Molecular Dimensions Determined by the Yamakawa - Fujii and Bohdanecky Methods

The differences between the dimensions that are produced by the models of Yamakawa and Fujii (58) and Bohdanecky (67) are best revealed by a comparison of the

results produced by the two methods using the same data sets. Bohdanecky and co-workers (67, 71) have calculated the dimensions of nitrocellulose (NC) in acetone and cellulose tricarbanilate (CTC) in dioxane, pyridine and acetone, but only the data for CTC in pyridine are reported here*. Therefore, the intrinsic viscosity / molar mass data for several cellulose derivative / solvent systems that have been treated by the Yamakawa - Fujii model are plotted as $(M^2 / [\eta]_o)^{1/3}$ versus $M^{1/2}$ (Figure 3.2) to determine the Bohdanecky constants A_η and B_η. The cellulose derivative / solvent systems thus treated are NC in acetone (64, 78); cellulose triacetate (CTA) in acetone, DMAC, tetrachloroethane (TCE), trifluoroacetic acid (TFA), dichloromethane (DCM) and trichloromethane (TCM) (64, 79); CTC in dioxane and acetone (64, 80); (acetoxypropyl)cellulose (APC) in dimethylphthalate (DMP) (65); HPC in DMAC, ethanol and dichloroacetic acid (DCA) (35, 38, 60); and the benzoic acid ester of HPC (BzPC) in benzene and acetone (62). With the exception of BzPC, the partial specific volume for each of these polymers in at least one solvent is available in the literature; for those polymer / solvent pairs that are not specifically listed the partial specific volume is assumed to be the same as that of the listed polymer / solvent pair. The partial specific volume of BzPC in acetone and benzene is taken to be the same as that of APC in acetone (65). The dimensions of these cellulose derivatives as calculated by the method of Bohdanecky and the reported Yamakawa - Fujii results are given in Table 3.6.

---

* In the paper by Bohdanecky and co-workers (71) on CTC in acetone, dioxane and pyridine, the calculated dimensions of CTC in acetone are based on their own data while for CTC in dioxane the data employed is from the paper by Sutter and Burchard (42). The paper by Bohdanecky (71) on the NC / acetone system employs the data of Meyerhoff (78), but it is apparent from Figure 10 of the Bohdanecky paper that a linear regression fit was not used to calculate the slope and intercept. To compare the results of the Bohdanecky method with those of the Yamakawa - Fujii model it is necessary to utilize the same data for both calculations, so the data for CTC in acetone and dioxane have been calculated according to the data of ref. (80) while the data for NC in acetone has been recalculated using a linear regression fit.

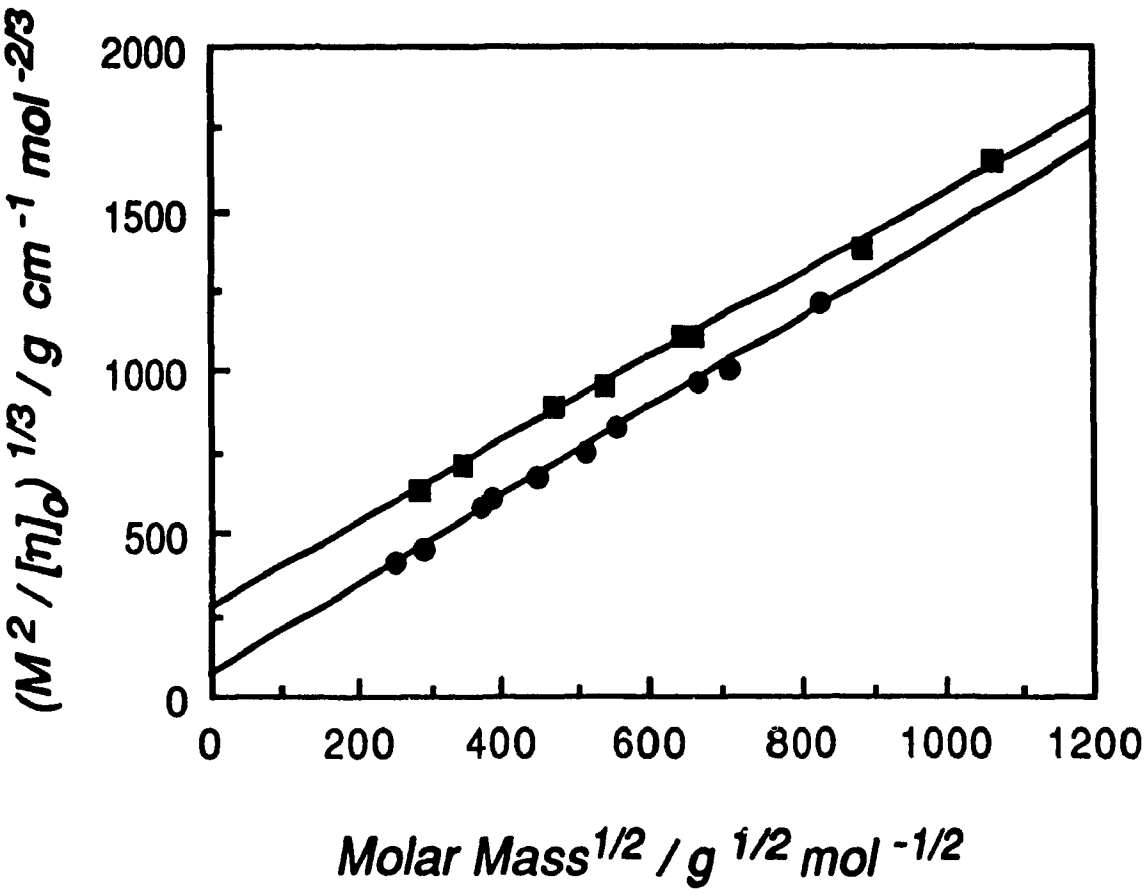

Figure 3.2 Examples of Bohdanecky plots for BzPC in acetone (squares; based on data from ref (62)) and CTA in tetrachloroethane (circles; based on data from ref.(79)).

Table 3.6

Comparison of the Equivalent Kuhn Segment Length and Diameter of Cellulose Derivatives as Calculated by Bohdanecky and Yamakawa - Fujii Theories

		Bohdanecky		Yamakawa - Fujii	
Polymer	Solvent	k_w / nm	d / nm	k_w / nm	d / nm
NC	Acetone	40.6	0.78	33.0 [a]	0.40 [a]
NC	Acetone	40.6	0.78	31.2 [b]	1.1 [b]
CTA	Acetone	12.3	0.88	11.4	0.6
CTA	DMAC	13.7	0.89	13.2	0.8
CTA	DCM	9.2	0.93	7.8	0.6
CTA	TCE	6.6	0.80	7.0	0.8
CTA	TCM	6.4	0.79	7.0	0.8
CTA	TFA	10.7	0.85	11.0	1.0
HPC	DMAC	16.3	1.12	14	1.04 [c]
HPC	Ethanol	16.2	1.09	-	-
HPC	DCA	10.6	0.89	20.0	1.04 [c]
APC [d]	DMP	11.4	1.14	11.8	1.2 [c]
APC [d]	DMP	11.4	1.14	14.3	0.5
CTC	Acetone	17.8	1.16	17.2	1.4
CTC	Dioxane	23.4	1.09	29.2	1.5
CTC	Pyridine	20.3	1.2	19.2	1.0
BzPC	Benzene	24.6	1.61	17.5	1.0
BzPC	Acetone	21.4	1.69	13.5	1.1

[a] Results of ref. (58)
[b] Results of ref. (64)
[c] Y.- F. k_w determined using a d value estimated from x-ray or density data.
[d] Corrected Bohdanecky results are shown.

Table 3.6 reveals that when the Yamakawa-Fujii method is employed considerable variation in the diameter of a single polymer can exist depending on the solvent employed. For example, for CTA the calculated diameter ranges from 0.6 to 1.0 nm. An extreme case that illustrates the uncertainty of the method can be found in the treatment of the data for NC in acetone; while the calculated k_w values are approximately the same, the diameter of NC is radically different from one report to the next, yet both studies

employed the same data to calculate the dimensions. Due to the large possible variations in the diameter values provided by the method, the Yamakawa - Fujii diameters are sometimes ignored completely and the diameter utilized is the value provided by x-ray data; such is the case for HPC.

The Bohdanecky method tends to supply diameter values that are more consistent both in terms of the diameter of a single cellulosic in differing solvents and the relative diameters of the various derivatives. For example, the calculated diameter of CTA in the solvents examined falls in the comparatively narrow range of 0.79 - 0.93 nm. The relative size of the cellulose sidechain substituent increases from top to bottom in Table 3.6 and this is also reflected in the diameters provided by the Bohdanecky method. The diameter values provided by the Bohdanecky theory for CTA and HPC agree closely with the values computed by a method of Flory (2) which relates the diameter of a polymer, d, to its shift factor, M_L, Avogadro's number, N_A, and bulk density, ρ, through Equation [3.38].

$$d = (M_L / N_A \rho)^{1/2}. \qquad [3.38]$$

The diameters of CTA and HPC calculated from Equation [3.38] are 0.85 and 1.06 nm, respectively. The Bohdanecky method can therefore be considered as a viable adaptation of the Yamakawa and Fujii model.

3.3.3 Chain Stiffness and Critical Volume Fraction for Mesophase Formation of Cellulose Derivatives by the Bohdanecky Theory

By applying the axial ratios (k_w/d) for the cellulose derivative / solvent pairs listed in Table 3.6 to the lattice theory of Flory (22) and virial expansion theories of Grosberg and Khokhlov (G.-K.) (15) and Odijk (13) and comparing the predicted liquid crystal phase separation behaviour with the experimental values, ϕ' (exp), it is possible to determine which of the theories is best suited to predicting the mesophase formation of these cellulose derivatives. The Bohdanecky model has recently been used to obtain the molecular dimensions of another cellulose derivative, (cyanoethoxylpropyl)cellulose

(CEPC) in tetrahydrofuran (70). Based on a constant M_L of 533 g mol^{-1} nm^{-1}, k_w and d were determined to be 26.8 nm and 1.38 nm, respectively. The data for these cellulose derivatives are listed in Table 3.7.

Table 3.7

Axial Ratios of Several Cellulose Derivatives Calculated by the Bohdanecky Theory, the Predicted Critical Volume Fractions by Lattice and Virial Expansion Theories and the Experimental Critical Volume Fractions

			φ' (Freely-jointed)		φ' (Wormlike) [a]		
Polymer	Solvent	Axial Ratio	Flory	G.-K.	Odijk	φ'(exp)	Ref.
NC	Acetone	52.0	0.15	0.06	0.22	0.12	81
CTA	Acetone	14.0	0.49	0.23	0.78	0.24	81
CTA	DMAC	15.4	0.45	0.21	0.71	0.22	81
CTA	TFA	12.6	0.53	0.26	0.87	0.21	82, 83
CTA	TCE	8.3	0.73	0.39	Isotropic	0.22	81
HPC [b]	Ethanol	25.6	0.29	0.13	0.38	0.37	70, 84
HPC [c]	Ethanol	14.9	0.46	0.22	0.74	0.37	84
HPC	DMAC	14.6	0.47	0.22	0.76	0.35	35
HPC	DCA	11.9	0.56	0.27	0.92	0.15	35
APC	DMP	10.0	0.64	0.32	Isotropic	0.53	65
BzPC	Benzene	15.3	0.45	0.21	0.77	0.35	62
BzPC	Acetone	12.7	0.53	0.26	0.90	0.35	62
CEPC	THF	20.7	0.35	0.16	0.55	0.34	70

[a] Calculated using M = 100,000.
[b] DS = 2.75, Degree of Molar Substitution = 3.9.
[c] DS is not listed, Degree of Molar Substitution = 4.

The virial expansion theories of Khokhlov and Semenov (17) and Odijk (13) have been found to give almost quantitative predictions for mesophase formation for polymers with extremely extended backbones (85), but it is obvious from Table 3.7 that the freely-jointed theories appear to provide the overall best estimates of the critical volume fractions for mesophase formation for the cellulosics examined here. Based on Table 3.7 there is no reason to favour either the lattice theory or the freely-jointed virial expansion theory; the experimental results usually fall between the predictions of these theories. However,

these data would appear to bear out the assertion that the validity of wormlike virial expansion theories are best suited to extremely extended polymers in which liquid crystals form at low volume fractions. It is of interest to note that one of the cellulose derivatives listed in Table 3.7 has a very high axial ratio; NC in acetone has an axial ratio that is nearly twice as large as next highest in Table 3.7 and the predicted critical volume fraction given by the wormlike chain virial expansion theory of Odijk is reasonably close to the experimentally observed value. The axial ratio of this polymer / solvent pair is marginally higher than the predicted critical axial ratio for persistent wormlike chains in the universal approximate method of Khokhlov and Semenov (18, 19). The high extension of NC is perhaps not an unusual feature given the polarity of the nitro groups. As opposed to a cellulose derivative like CTC where intramolecular interactions between the carbonyl and amine groups of the carbanilate sidechains are predicted to help stabilize the extended structure (42), in NC it is possible that the backbone of the chain is extended in an attempt to minimize the interactions among the nitro groups.

3.3.4 Molecular Dimensions and Mesophase Formation of EC

There are several papers in the literature on the viscosity of EC in a number of solvents. It is of interest to re-interpret these data in terms of the Bohdanecky hydrodynamic theory by using the data in Tables 3.1 - 3.3, measuring the apparent partial specific volume of EC in these solvents and estimating the molecular dimensions.

The apparent partial specific volumes in $cm^3\ g^{-1}$ of EC were found to be: acetic acid (0.87), benzene (0.88), n-butyl acetate (0.87), chloroform (0.86), m-cresol (0.84), dioxane (0.87), ethyl acetate (0.88), ethyl methyl ketone (EMK) (0.87), methanol (0.86) and pyridine (0.90). To obtain an estimate of the potential variation of the calculated molecular dimensions due to the scatter of the data, the dimensions at the 95% confidence limits have also been calculated. The slopes and intercepts that are determined for the best fit and confidence limits in the plots of $(M^2 / [\eta]_o)^{1/3}$ versus $M^{1/2}$ are shown in Figure 3.3. The dimensions have also been calculated using a constant M_L of 453 g mol^{-1} nm^{-1}. The calculated EC dimensions and axial ratios are given in Table 3.8.

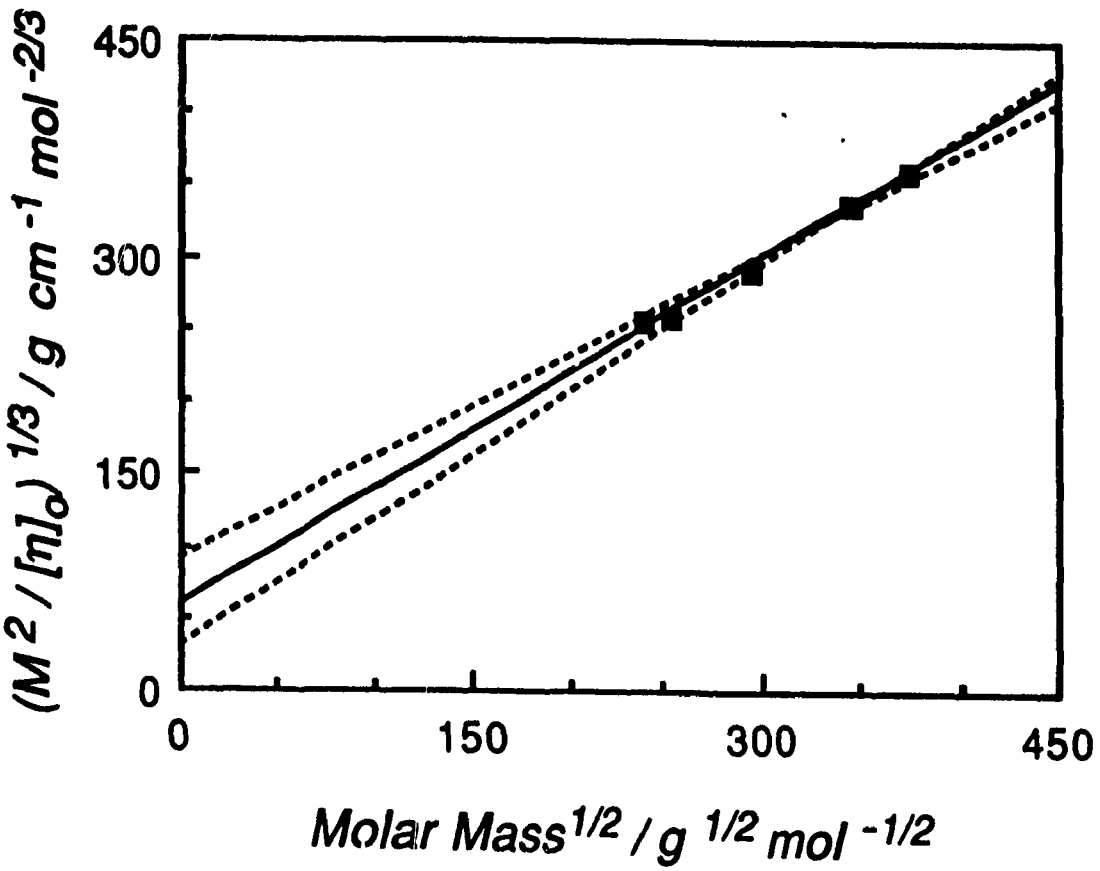

Figure 3.3 Bohdanecky plot for EC in benzene. The solid line represents the best fit line for the data. The dashed lines represent the plots at the 95% confidence limits. (Based on the data from ref.(74))

Table 3.8

EC Dimensions as Determined by the Bohdanecky Theory: Best Fit and 95% Confidence Limits

	Bohdanecky [a]		Constant M_L [b]			
Solvent	k_w / nm	d / nm	k_w / nm	d / nm	Axial Ratio	c.c.[c]
Benzene	5.82	0.58	14.0	1.39	10.1	0.9973
	13.6	0.78	17.9	1.02	17.5	
	24.6	0.91	23.3	0.86	27.0	
n-Butyl Acetate	13.9	0.79	17.5	1.00	17.6	0.9995
	16.7	0.83	18.9	0.94	20.1	
	19.9	0.87	20.5	0.90	22.9	
Chloroform	14.9	0.79	18.7	0.99	18.9	0.9994
	18.4	0.84	20.4	0.92	21.9	
	22.2	0.87	22.3	0.87	25.5	
Ethyl Acetate	11.2	0.74	15.7	1.04	15.1	0.9985
	17.6	0.85	19.0	0.92	20.6	
	25.9	0.94	22.9	0.83	27.5	
EMK	11.1	0.75	15.2	1.02	14.9	0.9994
	14.2	0.81	16.9	0.96	17.5	
	17.7	0.83	18.5	0.90	20.5	
Acetic Acid	9.70	0.71	14.5	1.06	13.7	0.9998
	13.2	0.78	16.5	0.98	16.9	
	17.1	0.83	18.6	0.83	20.6	
m-Cresol	8.00	0.66	13.7	1.13	12.1	0.9988
	10.8	0.72	15.2	1.02	15.0	
	14.4	0.80	17.3	0.96	18.0	
Dioxane	6.28	0.62	12.8	1.27	10.1	0.9984
	14.4	0.81	17.3	0.97	17.8	
	26.8	0.93	24.1	0.84	28.8	
Pyridine	10.8	0.79	13.8	1.01	13.7	0.9999
	12.6	0.82	14.7	0.96	15.4	
	15.0	0.88	16.0	0.93	17.0	
Methanol	2.97	0.53	5.80	1.03	5.61	0.9994
	5.77	0.76	6.34	0.84	7.60	
	9.13	0.98	7.07	0.76	9.29	

[a] All numbers reported were determined using the values provided by the Bohdanecky theory.

[b] All numbers reported were determined using $M_L = 453$ g mol^{-1} nm^{-1}.

[c] Correlation coefficient for best fit data.

Based on Equation [3.38], which relates the diameter of the polymer to its density, EC has a diameter of 0.81 nm. This value is in close agreement with the diameters calculated by the Bohdanecky theory for the best fit lines, but like the MHS constants it is apparent from Table 3.8 that only a minor degree of scatter in the data of the plots used to calculate the Bohdanecky constants A_η and B_η causes a significant variation in the calculated molecular dimensions. For example, in the EC / benzene system, which has the lowest correlation coefficient associated with the best fit line, d and k_W are 0.78 and 13.6 nm, respectively; however, based on the parameters determined at the 95% confidence limits d can vary between 0.58 and 0.91 nm while k_W ranges between 5.8 and 24.6 nm. These possible variations in the molecular dimensions in turn affect the calculated axial ratio; the axial ratio calculated from the slope and intercept of the best fit line is 17.5 but at the 95% confidence limits the axial ratios are 10.1 and 27.0. Even at the 68% confidence limits the axial ratios for this system range from 13.7 to 21.9. For systems that have higher correlation coefficients associated with the best fit line, nontrivial variations in the calculated axial ratios also exist. For example, the data for EC in n-butyl acetate has the highest correlation coefficient (0.9995) calculated from the information of Moore and Brown (74), yet the axial ratio range based on the 95% confidence limits is from 17.6 to 22.9. These potential variations in the axial ratio will in turn affect the predicted values of the critical volume fractions which are computed from the liquid crystal phase separation theories. To determine the extent to which these possible variations affect the predicted critical volume fractions, the data from Table 3.8 are used to calculate the predicted critical volume fractions according to the freely-jointed theories of Flory (22) and Grosberg and Khokhlov (15). These predicted critical volume fractions are then compared with the experimentally observed values. The data are compiled in Table 3.9.

Table 3.9

Axial Ratios of EC, the Predicted Critical Volume Fractions Based on the Freely-Jointed Theories of Flory (22) and Grosberg and Khokhlov (15) and the Experimental Critical Volume Fractions

Solvent	Axial Ratios [a]	ϕ' (Flory)	ϕ' (G.-K)	ϕ' (Exp.)[b]
Benzene	10.1	0.64	0.32	No LC
	17.5	0.40	0.19	
	27.0	0.27	0.12	
n-Butyl Acetate	17.6	0.40	0.18	No LC
	20.1	0.36	0.16	
	22.9	0.32	0.14	
Chloroform	18.9	0.38	0.17	0.36
	21.9	0.33	0.15	
	25.5	0.29	0.13	
Ethyl Acetate	15.1	0.46	0.22	No LC
	20.6	0.35	0.16	
	27.5	0.27	0.12	
EMK	14.9	0.46	0.22	No LC
	17.5	0.40	0.19	
	20.5	0.35	0.16	
Acetic Acid	13.7	0.50	0.24	0.45
	16.9	0.42	0.19	
	20.6	0.35	0.16	
m-Cresol	12.1	0.55	0.27	0.40
	15.0	0.46	0.22	
	18.0	0.40	0.18	
Dioxane	10.1	0.64	0.32	0.48
	17.8	0.40	0.18	
	28.8	0.26	0.11	
Pyridine	13.7	0.50	0.24	0.46
	15.4	0.45	0.21	
	17.0	0.42	0.19	
Methanol	5.61	0.92	0.58	No LC [c]
	7.60	0.78	0.43	
	9.29	0.68	0.35	

[a] The data are from Table 3.8 and represent the axial ratios calculated from the best fit line and values at the 95% confidence limits.

[b] No LC means that no mesophase was found up to $\phi = 0.55$.

[c] EC exhibits limited solubility in the concentration range predicted for mesophase formation.

For systems that form liquid crystals the experimentally determined critical volume fractions are all within the 95% confidence intervals of the values predicted by the lattice theory of Flory. None of the mesophases are formed in the volume fraction range predicted by the freely-jointed virial expansion theory of Grosberg and Khokhlov. It is of interest to note that according to the hydrodynamic theory used, the axial ratio of EC in solvents where no mesophase was observed is far above the predicted critical axial ratio of 6.417 given by Flory and Ronca (12). In benzene, n-butyl acetate, ethyl acetate and EMK the predicted phase separation does not occur even at concentrations corresponding to the upper 95% confidence limit of the Flory theory. In fact, the axial ratios of these solvents are, even at the lower 95% confidence limit, above those of many of the mesophase forming cellulosic / solvent systems listed in Table 3.7. To speculate on why some of the EC / solvent systems do not form mesophases despite having apparently extended backbones, it is necessary to examine both the individual EC / solvent systems and the viscosity theory used to calculate the dimensions.

The polymer / solvent interaction parameter of EC in several solvents has been reported as: benzene (0.33), n-butyl acetate (0.33), chloroform (0.29), ethyl acetate (0.34) and ethyl methyl ketone (0.42) (76). These values would suggest that chloroform, in which EC forms a mesophase, is a marginally better solvent than the others in which mesophases do not form. This suggestion is also supported by the results of an approximate experimental procedure in which heptane, a nonsolvent for EC, was added to EC solutions of the solvents listed above (86). The volumes of heptane required to initiate non-liquid crystalline phase separation for chloroform, benzene, n-butyl acetate, ethyl acetate and EMK were in the ratio of 19.3 : 2.3 : 7.3 : 8.8 : 9.4, respectively. Several other solvents in which EC does not form mesophases were also listed and in all cases only minor additions of heptane were required to initiate phase separation. It is therefore possible that even in poor solvents cellulose derivatives can have extended backbones but that to form a mesophase requires a "good" solvent.

The possibility also exists that EC is not as extended as the Bohdanecky calculations would suggest. While EC possesses large negative d ln $[\eta]$ / dT values in the solvents that do not permit mesophase formation (87, 88), this cannot be taken as

evidence of an extended chain structure. The temperature dependence of $[\eta]$ can be written as Equation [3.38] (49).

$$d \ln[\eta] / dT = d \ln \Phi / dT + 1.5\, d \ln \langle S^2 \rangle_0 / dT + 3\, d \ln \alpha / dT \quad [3.38]$$

Although the intrinsic viscosity / temperature dependence behaviour of a cellulose derivative has been shown to be primarily due to the $d \ln \langle S^2 \rangle_0 / dT$ term (89), the fact that some cellulose derivatives in theta solvents also show large negative $d \ln [\eta] / dT$ values (90, 91) means that this quantity is not necessarily indicative of an extended structure at lower temperatures. If EC does not, in fact, have as highly extended a structure in the solvents which do not form mesophases as the Bohdanecky theory suggests, the reason for the high calculated values might be due to the possibility of a draining effect. Two extremes of hydrodynamic behaviour exist: freely-draining and non-freely draining. A polymer / solvent system is considered to be freely-draining if the solvent molecules flow freely past each segment of the chain and nonfreely-draining if the solvent molecules within the coils of the polymer chain move with the chain. Polymers which exhibit a behaviour intermediate between the two extremes are called partially free-draining. The Bohdanecky theory is based on the Yamakawa - Fujii formulation which treats the chain as freely-draining. Kamide and Saito (49) have stated that a draining effect can affect both the value of $[\eta]_0$ and the calculated Yamakawa - Fujii persistence length. As they have also stated that some cellulose derivatives exhibit a draining effect, the possibility exists that EC in the non-mesophase forming solvents does not drain freely and therefore gives intrinsic viscosity values that do not accurately reflect the geometry of the EC chain in solution. These compensated intrinsic viscosity values would in turn affect the calculated molecular dimensions. A comparison between polymer / solvent systems which exhibit large and small draining effects would therefore be invalid.

3.4 CONCLUSION

The equivalent Kuhn segment length and diameter of several cellulose derivatives that have already been estimated using the Yamakawa - Fujii theory have been re-calculated using the Bohdanecky theory. The Bohdanecky theory is found to be a viable adaptation of the Yamakawa - Fujii method as it provides reasonable estimates of the chain diameter and comparable equivalent Kuhn segments lengths. These dimensions were used to determine the critical volume fractions for liquid crystalline phase separation according to virial expansion theories and a lattice theory. Based on a comparison with experimental data for a variety of cellulose derivatives, the freely-jointed lattice theory of Flory and the freely-jointed virial expansion theory of Grosberg and Khokhlov were found to provide the best estimates of the critical volume fraction for mesophase formation.

Few cellulose derivatives have had their liquid crystalline phase separation behaviour examined in more than a limited number of solvents. The dimensions of ethyl cellulose (EC) in several solvents were calculated using the Bohdanecky theory and were found to be extended even in solvents which do not allow EC to form a mesophase. A statistical routine was used to calculate the MHS constants, physical dimensions and critical volume fractions according to the freely-jointed theories at the 95% confidence limits for EC in each solvent. It was demonstrated that considerable variation could exist in the calculated MHS constants, molecular dimensions and predicted critical volume fractions unless extremely high correlation coefficients exist for plots of log $[\eta]_o$ versus log M and plots of $(M^2/[\eta]_o)^{1/3}$ versus $M^{1/2}$, respectively. For those EC / solvent systems which did form liquid crystals, the freely-jointed lattice theory of Flory was found to be superior to the freely-jointed virial expansion theory of Grosberg and Khokhlov for predicting the critical volume fractions for mesophase formation.

3.5 REFERENCES

(1) J.L. White, *J. Appl. Polym. Sci.: Appl. Polym. Symp.*, **41**, 3 (1985).

(2) P.J. Flory, *Advanc. Polym. Sci.*, **59**, 1 (1984).

(3) F.C. Bawden and N.W. Pirie, *Proc. R. Soc. (London) Ser. B*, **123**, 274 (1937).

(4) D.G. Ballard, J.D. Griffiths and J. Watson, United States Patent No. 3,121,766 (1964); as reported by J. L. White and J.F. Fellers, *J. Appl. Polym. Sci.: Appl. Polym. Symp.*, **33**, 137 (1978).

(5) D.C. Prevorsek, "Polymer Liquid Crystals", (A. Ciferri, W.R. Krigbaum and R.B. Meyer, eds.), Academic Press, Inc., New York, 1982, pp. 329.

(6) M. Panar and O.B. Willcox, Dem. Brevet. Français 7,703,473 (1977).

(7) C. McCorsley and J. Varga, United States Patents 4,142,913 and 4,144,080 (1979).

(8) R.D. Gilbert and P.A. Patton, *Prog. Polym Sci.*, **9**, 115 (1983).

(9) W. Maier and A. Saupe, *Z. Naturforschg.*, **14A**, 882 (1959); as reported by S. Chandrasekhar, "Liquid Crystals", Cambridge University Press, Cambridge, 1977, pp. 41.

(10) A. ten Bosch, P. Maissa and P. Sixou, *J. Chem. Phys.*, **79**, 3462 (1983).

(11) L. Onsager, *Ann. N.Y. Acad. Sci.*, **51**, 627 (1949).

(12) P.J. Flory and G. Ronca, *Mol. Cryst. Liq. Cryst.*, **54**, 289 (1979).

(13) T. Odijk, *Macromolecules*, **19**, 2313 (1986).

(14) A.R. Khokhlov, *Phys. Lett. A*, **68**, 135 (1978).

(15) A. Yu. Grosberg and A.R. Khokhlov, *Advanc. Polym. Sci.*, **41**, 53 (1981).

(16) A.R. Khokhlov and A.N. Semenov, *Physica (The Hague)*, **108A**, 546 (1981).

(17) A.R. Khokhlov and A.N. Semenov, *Physica (The Hague)*, **112A**, 605 (1982).

(18) A.R. Khokhlov and A.N. Semenov, *J. Stat. Phys.*, **38**, 161 (1985).

(19) A.R. Khokhlov and A.N. Semenov, *Macromolecules*, **19**, 373 (1986).

(20) P.J. Flory, *Proc. R. Soc. (London) Ser. A*, **234**, 71 (1956).

(21) J.P. Straley, *Mol. Cryst. Liq. Cryst.*, **22**, 333 (1973).

(22) P.J. Flory, *Macromolecules*, **11**, 1141 (1978).

(23) G. Ronca and D.Y. Yoon, *J. Chem. Phys.*, **76**, 3295 (1982).

(24) P.J. Flory and A. Abe, *Macromolecules*, **11**, 1119 (1978).

(25) R.R. Matheson, Jr. and P.J. Flory, *Macromolecules*, **14**, 954 (1981).

(26) S.V. Vasilenko, A.R. Khokhlov and V.P. Shibaev, *Macromolecules*, **17**, 2270 (1984).

(27) S.V. Vasilenko, A.R. Khokhlov and V.P. Shibaev, *Macromolecules*, **17**, 2275 (1984).

(28) R.E. Boehm, D.E. Martire and N.V. Madhusudana, *Macromolecules*, **19**, 2329 (1986).

(29) P.J. Flory and P.A. Irvine, *J. Chem. Soc.: Faraday Trans.*, **80**, 1807 (1984).

(30) E.L. Wee and W.G. Miller, "Liquid Crystals and Ordered Fluids, Vol III", (J.F. Johnson and R.S. Porter, eds.), Plenum Press, New York, 1978, pp. 371.

(31) M. Ballauf, *Macromolecules*, **19**, 1366 (1986).

(32) F. Fried and P.Sixou, *J. Polym. Sci.: Polym. Chem. Ed.*, **22**, 239 (1984).

(33) P.J. Flory and G. Ronca, *Mol. Cryst. Liq. Cryst.*, **54**, 311 (1979).

(34) M. Warner and P.J. Flory, *J. Chem. Phys.*, **73**, 6327 (1980).

(35) A. Ciferri and E. Marsano, *Gazz. Chima. Ital.*, 565 (1987).

(36) W.R. Krigbaum, *Faraday Discuss. Chem. Soc.*, **79 / 8**, (1985).

(37) W.R Krigbaum, H. Hakemi, A. Ciferri and G. Conio, *Macromolecules*, **16**, 1264 (1983).

(38) M.A. Aden, E. Bianchi, A. Ciferri, A. Conio and A. Tealdi, *Macromolecules*, **17**, 2010 (1984).

(39) W.G. Miller, C.C. Wu, G.L. Santec, J.H. Rai and K.D. Goebel, *Pure and Appl. Chem.*, **38**, 37 (1974).

(40) G.V. Laivins, Ph.D. Thesis, McGill University, 1984.

(41) L.J. Fetters and H. Yu, *Macromolecules*, **4**, 385 (1971).

(42) W. Sutter and W. Burchard, *Die Makromol. Chem.*, **179**, 1961 (1978).

(43) J.W.M. Noordermeer, R. Daryanani and H. Janeschitz-Kriegl, *Polymer*, **16**, 359 (1975).

(44) A.K. Gupta, E. Marchal and W. Burchard, *Macromolecules*, **8**, 843 (1975).

(45) P.J. Flory, O.K. Spurr, Jr. and D.K. Carpenter, *J. Polym. Sci.*, **27**, 231 (1958).

(46) R.H. Marchessault and A. Sarko, *Adv. Carbohydr. Chem.*, **22**, 445 (1967).

(47) D.A. Brant and K.D. Goebel, *Macromolecules*, **5**, 536 (1972).

(48) B.A. Tonneson and O. Ellefsen, "Cellulose and Cellulose Derivatives, Vol V, Part IV", Interscience, New York, 1971, pp. 282.

(49) K. Kamide and M. Saito, *Advanc. Polym. Sci.*, **83**, 1 (1987).

(50) M. Kurata, M. Iwama and K. Kamada, "Polymer Handbook", (J. Brandrup and E.H. Immergut, eds.), Interscience Publishers, New York, 1966, Ch. IV.

(51) K.D. Goebel, C.E. Harvie and D.A. Brant, *J. Appl. Polym. Sci.: Appl. Polym. Symp.*, **28**, 671 (1976).

(52) J.E. Hearst, *J. Chem. Phys.*, **40**, 1506 (1964).

(53) R. Ullman, *J. Chem. Phys.*, **53**, 1734 (1970).

(54) H. Yamakawa, *Macromolecules*, **10**, 692 (1977).

(55) J.G. Kirkwood and J. Riseman, *J. Chem. Phys.*, **16**, 565 (1948).

(56) J.G. Kirkwood, *J. Polym. Sci.*, **12**, 1 (1954).

(57) H. Yamakawa and G. Tanaka, *J. Chem. Phys.*, **57**, 1537 (1972).

(58) H. Yamakawa and M. Fujii, *Macromolecules*, **7**, 128 (1974).

(59) H. Yamakawa and M. Fujii, *Macromolecules*, **6**, 407 (1973).

(60) M. Saito, *Polym. J.*, **15**, 213 (1983).

(61) K. Kamide, M. Saito and H. Suzuki, *Die Makromol. Chem.: Rapid Commun.*, **4**, 33 (1983).

(62) S.N. Bhadani, S.-L. Tseng and D.G. Gray, *Die Makromol. Chem.*, **184**, 1727 (1983).

(63) C. Conio, E. Bianchi, A. Ciferri, A. Tealdi and A. Aden, *Macromolecules*, **16**, 1264 (1983).

(64) S. Dayan, P. Maissa, M.J. Vellutini and P. Sixou, *Polymer*, **23**, 800 (1982).

(65) G.V. Laivins and D.G. Gray, *Macromolecules*, **18**, 1746 (1985).

(66) P. Maissa, M.J. Seurin and P. Sixou, *Polym. Bull.*, **15**, 257 (1986).

(67) M. Bohdanecky, *Macromolecules*, **16**, 1483 (1983).

(68) T. Tsuji, T. Norisuye and H. Fujita, *Polym. J.*, **7**, 558 (1975).

(69) P.L. Auer and C.S. Gardener, *J. Chem. Phys.*, **23**, 1546 (1955).

(70) J.W. Mays, *Macromolecules*, **21**, 3179 (1988).

(71) J. Danhelka, M. Netopilik and M. Bohdanecky, *J. Polym. Sci. B*, **25**, 1801 (1987).

(72) J.F. Rabek, "Experimental Methods in Polymer Chemistry", J. Wiley and Sons, Ltd., New York, 1980, pp. 524.

(73) Chapter 2, this thesis.

(74) W.R. Moore and A.M. Brown, *J. appl. Chem.*, **8**, 363 (1958).

(75) P.C. Scherer, A. Tanenbaum and D.W. Levi, *J. Polym. Sci.*, **43**, 531 (1960).

(76) H. Staudinger and F. Reinecke, *Liebigs Ann.*, **535**, 47 (1938).

(77) S.M. Aharoni, *J. Macromol. Sci.: Phys.*, **21**, 105 (1982).

(78) G. Meyerhoff, *J. Polym. Sci.*, **29**, 399 (1958).

(79) K. Kamide, Y. Miyazaki and T. Abe, *Polym. J.*, **11**, 523 (1987).

(80) W. Burchard and E. Husemann, *Die Makromol. Chem.*, **44-46**, 358 (1961).

(81) S.M. Aharoni, *Polym. Prepr.*, **22**, 116 (1981).

(82) D.L. Patel and R.D. Gilbert, *J. Polym. Sci. B.*, **19**, 1449 (1981).

(83) G.H. Meeten and P. Navard, *Polymer*, **23**, 483 (1987).

(84) R.S. Werbowyj and D.G. Gray, *Macromolecules*, **13**, 69 (1980).

(85) A. Teramoto, *Pure Appl. Chem.*, in press.

(86) W.R. Moore, J.A. Epstein, A.M. Brown and B.M. Tidswell, *J. Polym. Sci.*, **23**, 23 (1957).

(87) W.R. Moore and A.M. Brown, *J. Coll.Sci.*, **14**, 1 (1959).

(88) W.R. Moore and A.M. Brown, *J. Coll.Sci.*, **14**, 343 (1959).

(89) H. Suzuki, Y. Miyazaki and K. Kamide, *Eur. Polym. J.*, **16**, 703 (1980).

(90) W.R. Krigbaum and L.H. Sperling, *J. Phys. Chem.*, **64**, 99 (1960).

(91) L. Mandelkern and P.J. Flory, *J. Am. Chem. Soc.*, **74**, 2517 (1952).

CHAPTER 4

CIRCULAR REFLECTANCE SPECTROSCOPY STUDIES

4.1 INTRODUCTION

A special form of the nematic mesophase exists when each "layer" of the structure is twisted relative to its neighbour such that the preferred direction of the molecules in each layer trace out a helix for the supramolecular structure. This twisted nematic ordering is called cholesteric structure and depending on the rotation direction of the layers a liquid crystal with a left-handed or right-handed cholesteric structure may be obtained (Figure 1.2). The distance between any two layers separated by a 360° rotation of the layer directors is called the pitch so the two features characterizing a cholesteric liquid crystal are the twist sense and pitch. The reasons for the development of the twist in a cholesteric liquid crystal have been the subject of much debate. Any successful theory must account not only for the development of the twist, but also correctly predict the response of the pitch to changes of concentration and temperature. Factors typically investigated in an attempt to determine which features influence the pitch and cholesteric twist sense of cellulose derivatives have included temperature, concentration, solvent type, molar mass and nature of the sidechain substituent. Theories describing the formation of a nematic mesophase were presented in Chapter 3; mean field, geometric and combined mean field - geometric approaches have been used to explain the formation of the liquid crystal. By including a chiral component these approaches have also been employed to explain the origin of the twist in cholesteric mesophases.

4.1.1 Formation of a Cholesteric Mesophase

Keating (1) and Böttcher (2) proposed a model for a cholesteric liquid crystal in which elongated chiral molecules made anharmonic rotational vibrations in each layer of the cholesteric structure. The inclusion of an anharmonic term meant that the mean field described by the potential function is asymmetric and, unlike a symmetric field in which a nematic ordering of the molecular layers occurs, a twist develops. The theory states that the decrease in the pitch which occurs with increasing temperature is the result of an increase in the amplitude of the anharmonic rotational oscillations of the asymmetric molecules. The pitch, P, is related to the temperature, T, by Equation [4.1]

$$P = \frac{2\pi}{\theta} = \frac{4\pi d I \omega_0^4}{A' k T} \qquad [4.1]$$

where
- θ = twist angle between successive layers
- d = interlayer distance
- I = molecule's moment of inertia
- A' = constant in the anharmonicity term
- k = Boltzmann constant.

While the predicted inverse relationship between the pitch and temperature is the behaviour almost uniformly observed for pure low molar mass cholesteric liquid crystals (3) this relationship is frequently not exhibited by cholesteric polymer liquid crystals.

At the same time as the Keating-Böttcher theory was being developed another approach was being formulated by Goossens (4) and Wulf (5). In these theories the mean field approach of Maier and Saupe (6), which predicts nematic ordering, was extended to include dipole - quadrupole interactions. The angular dependence of the interaction energy between two chiral molecules in adjacent layers of the cholesteric was found to be minimized if a twist existed between the two molecules; however, the potential function describing the mean field is symmetric so the pitch according to this model is independent of temperature. Stegemeyer and Finkelmann (7, 8) developed a variation of the Goossens - Wulf model which included the temperature dependence of the hindrance to rotation about the molecules' long axes. For a symmetrically smooth cylinder this rotation would be free and produces nematic structure, but in the case of asymmetric molecules, one of the two mutually perpendicular directions of the short axis is preferred orientation which introduces a short range rotational order. The result of this rotational order is a twist of the layers which is temperature dependent. An increase in temperature produces a less restricted rotation which in turn produces a decreased twist angle between adjacent molecules which is accompanied by an increase in pitch.

Lin-Liu et al. (9, 10) combined features of the Keating-Böttcher and Goossens-Wulf theories to model the cholesteric phase. In this theory the potential function that describes the mean field is asymmetric as in the Keating-Böttcher model and displaced

from the origin as in the Goossens-Wulf theory. As a result of the combination of these features, the theory predicts several notable possibilities that depend on the initial condition of the potential function describing the mean field: the ability of the pitch to increase or decrease as a function of increasing temperature; the possibility that a pure cholesteric mesophase can increase its pitch, change twist sense and then decrease in pitch with increasing temperature; and the possibility that a chiral molecule could produce a nematic structure. This theory preceded the experimental work of Mori (11) on lyotropic poly(L-glutamic acid) samples and Watanabe and Nagase (12) on thermotropic poly[(γ-benzyl-L-glutamate)-*co*-(γ-dodecyl-L-glutamate)] which demonstrated that the cholesteric polymer liquid crystals could increase their pitch as a function of temperature, change twist sense and then decrease in pitch.

The geometric factors that govern the helicoidal twist sense of polymer mesophases have been examined by Kim (13) who theorized that in a polybenzyl-L-glutamate (PBLG) liquid crystal the twist sense of the cholesteric mesophase would be governed by the chirality of its constituent molecules. Right-handed molecules cause the formation of a left-handed cholesteric mesophase while molecules with left-handed chirality produce a right-handed one. This is at variance with a combined statistical-geometric theory of Kimura et al. (14) who state that the conversion from one cholesteric twist sense to the other occurs thermally with no transformation in the PBLG molecular configuration. Equation [4.2] shows the relationship of Kimura et al. among the pitch, P, the geometric features and the temperature.

$$\frac{2\pi}{P} = \frac{24\,\tilde{\lambda}\,\Delta}{\pi L D}\, c\,f(c) \left[\frac{T_N}{T} - 1\right] \qquad [4.2]$$

where

$\tilde{\lambda}$ = a scaling factor

Δ = the height of the groove in the twisted rod

L = the length of the rod

D = the diameter of the rod

c f(c) = a concentration term

T_N = the temperature where the pitch is infinite (nematic)

T = the temperature.

Although this theory has been found to adequately describe the temperature dependence of the pitch of polypeptides and some cellulose derivative mesophases, its applicability to statements about geometric features has been questioned by Sikora et al. (15) who state that the calculated geometric features are affected by factors such as molar mass and molecular flexibility.

Samulski and Samulski (16) have examined the role of dispersion forces on chiral dielectric molecules embedded in an isotropic dielectric medium and determined that an asymmetric term in the pair potential is sufficient to describe the origin of the cholesteric twist of PBLG. The theory predicts that a critical dielectric constant, ε^*, exists which equals the product of the principal values of the dielectric constant perpendicular to the molecular axis. The dielectric constant of the solvent medium plays a role in determining the cholesteric twist sense because the twist sense can be reversed by the addition of another solvent which causes the dielectric constant of the medium to pass through ε^*. This approach was later extended by Osipov (17) who found that the chiral interaction potential is a function not only of the solvent, but also of temperature.

4.1.2 Interaction of Polarized Light with Cholesteric Structures

When viewed under a microscope equipped with crossed polars all classes of mesophase possessing an effective molecular optic axis exhibit birefringence. However, the most dramatic optical effects in the liquid crystal field can be seen with the unaided eye and are found in cholesteric liquid crystals. At appropriate temperatures or concentrations, cholesteric liquid crystals, including mesophases of many cellulose derivatives, display colours which are dependent on the viewing angle. An understanding of how light interacts with cholesteric liquid crystals to produce this effect is important to investigations in the field. An unambiguous description of light and the twist sense of cholesteric liquid crystals is often complicated by contradictory conventions for the handedness of circularly polarized light and the twist sense of cholesteric liquid crystals. The interaction of light with a mesophase as described below and throughout the thesis employs the definition of right-handed and left-handed circularly polarized light given in

Chapter 1.3.1 and the cholesteric twist senses are as shown in Figure 1.2.

The interaction of a light wave with a cholesteric liquid crystal depends on the texture of the mesophase. The texture of a mesophase is determined by the orientations of the cholesteric domains. Two major classes of texture exist: planar and homeotropic.

4.1.2.1 Light Interaction with Planar Liquid Crystals

Planar texture is observed when the optic axes of the supramolecular structures (see Figure 1.2) are oriented normal to the surface of the mesophase. If the helicoidal structure has its optic axis normal to the surface then the texture is called monodomain whereas if several axes exist then the mesophase is said to have a polydomain cholesteric structure (Figure 4.1).

De Vries (18) presented the first successful description of the optical properties of a cholesteric liquid crystal. The mesophase was modelled as a series of birefringent plates each of which was rotated at a constant angle θ relative to its neighbour. The conditions for constructive interference of the reflected light wave were found to be met when

$$\frac{2\pi}{2\theta}\ 2\bar{n}d\ = \lambda \qquad [4.3]$$

where $\bar{n}$ = mean refractive index of a layer
d = layer thickness
λ = wavelength of light.

All other wavelengths of light that are reflected interfere destructively. As the pitch, P, equals $2\pi d / \theta$, the wavelength of maximum reflection, λ_0, is related to the mean refractive index and the pitch by Equation [4.4]

$$\lambda_0 = \bar{n}\, P. \qquad [4.4]$$

The general case of white light, or a scan of all wavelengths of light, interacting with a planar cholesteric structure can be understood by treating white light as a composition of an infinite number of plane polarized light waves each of which is rotated

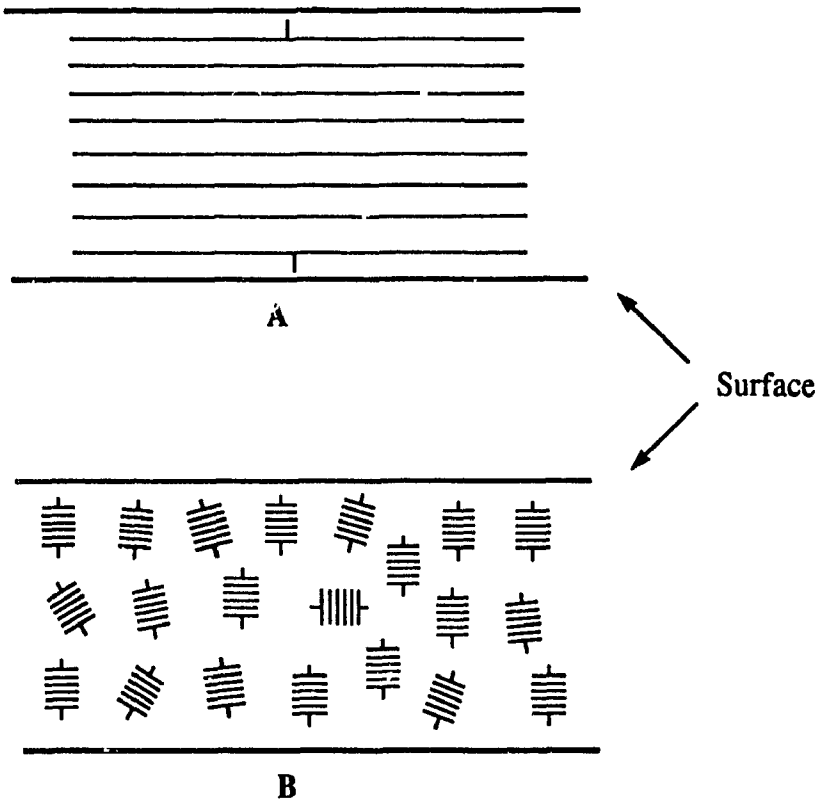

Figure 4.1 Possible planar textures for cholesteric liquid crystals. (A) represents monodomain planar texture where a single optic axis is aligned normal to the surface. (B) represents polydomain texture where the optic axes are perferentially, but not exclusively, oriented normal to the surface.

at a different angle. If absorbance is ignored and only the reflection and transmittance of light is considered then two extremes are possible for the interaction of a plane polarized light wave with a cholesteric liquid crystal: the first where the light wave meets a layer in which the director of the layer is aligned parallel with the plane of the wave and the index of refraction in this direction is n_x, the second where the director of the layer is aligned perpendicular to the plane of the wave and the index of refraction is n_y (Figure 4.2). A plane polarized wave can be decomposed into a left-handed circularly polarized component and a right-handed circularly polarized component, each of which contains 50% of the energy (Figure 1.6). When a plane polarized light wave whose wavelength equals the pitch of the mesophase meets the first layer of a right-handed (left-handed) cholesteric structure whose director is parallel to the incoming wave, and proceeds into the sample, the right-handed (left-handed) component rotates by the same angle as the directors of the successive nematic layers. The lack of interaction of the right-handed (left-handed) wave means that while each successive layer is seen as possessing the same refractive index, the slight rotation of the next layer relative to the layer it is currently passing through causes the light wave to encounter a slightly different index of refraction at the interface (18). Fresnell's law dictates that for a light wave with intensity I_0 moving from one material with refractive index n_1 into a second material with refractive index n_2, that part of the light wave will be reflected with an intensity of I_R according to Equation [4.5].

$$I_R = I_0 [(n - 1) / (n + 1)]^2 \qquad [4.5]$$

where $n = n_2 / n_1$.

The result is a small part of the light wave reflects back at the interface of each layer of the cholesteric structure which interferes constructively if its wavelength is given by

$$\lambda_x = n_x P. \qquad [4.6]$$

Destructive interference occurs for light wave reflections with wavelength not equal to $\bar{n}P$.

When a plane polarized wave with wavelength equal to the pitch of the right-

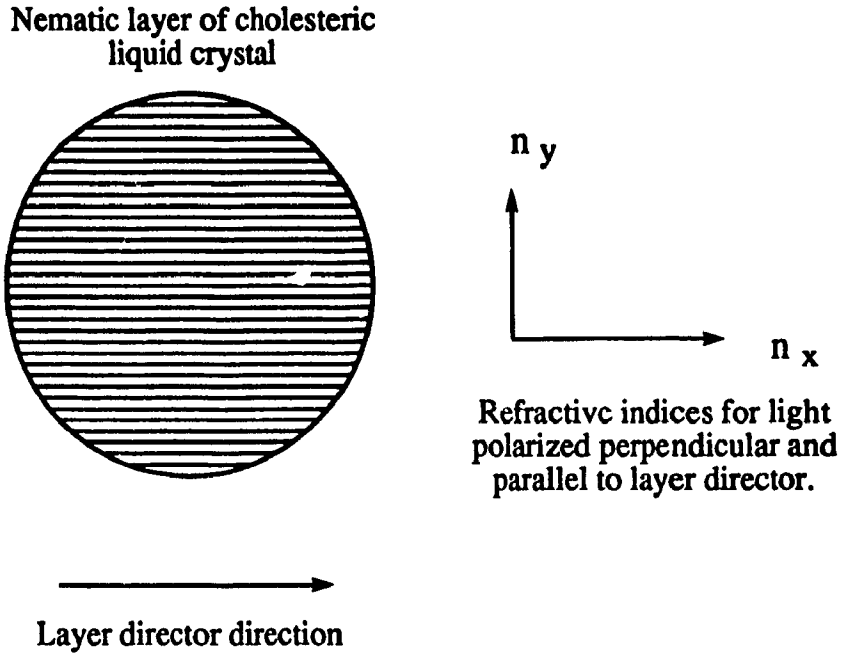

Figure 4.2 A nematic layer of a cholesteric liquid crystal. Two refractive indices for a polarized light wave may be observed: the first, n_x, where the light wave falls parallel to the layer director of the nematic layer; the second, n_y, where the lightwave falls perpendicular to the layer director of the nematic layer. These refractive indices govern the width of the spectral region selectively reflected by the cholesteric liquid crystal.

handed (left-handed) cholesteric structure intersects a layer of the structure at an angle perpendicular to the director of the layer, the variation of the layer refractive indices the right-handed (left-handed) circularly polarized light encounters in each layer is again zero but in this instance the variation in the refractive index at the interface is related to n_y rather than n_x. In this case the wavelengths constructively reflected are

$$\lambda_y = n_y P. \qquad [4.7]$$

For cases where the light waves intersect with the director somewhere between the two extreme cases, the light wave sees values of the refractive index intermediate between n_x and n_y. The width of the spectral region selectively reflected, $\Delta\lambda$, is

$$\Delta\lambda = (n_x - n_y) P. \qquad [4.8]$$

For the case of the left-handed (right-handed) circularly polarized wave component intersecting with a right-handed (left-handed) cholesteric structure the light wave makes contact with each layer at a different angle and sees only an average index of refraction as it traverses the sample so only a single wavelength of light is reflected. Thus, only circularly polarized light in a narrow spectral region is constructively reflected whereas all other wavelengths of light, regardless of polarization, are transmitted or destructively reflected (Figure 4.3).

If the optical properties of the selective reflection are monitored as a function of the intensity of transmitted left-handed and right-handed circularly polarized components then the technique of measuring the *apparent* circular dichroism is called Circular Reflectance (CR) spectroscopy. In theory the reflection peak should have a flattened plateau corresponding to $\Delta\lambda$ as a peak maximum, but the fact that pure monodomain structure is very rare means that the reflection peak takes on a nonideal shape that possesses a wavelength of maximum reflection corresponding to λ_0 in the de Vries equation. This nonideal peak shape is the result of polydomain structure because while the de Vries equation is valid for a planar monodomain sample, for polydomain samples the incoming light will not be collinear with all optic axes. In this case the relationship developed by

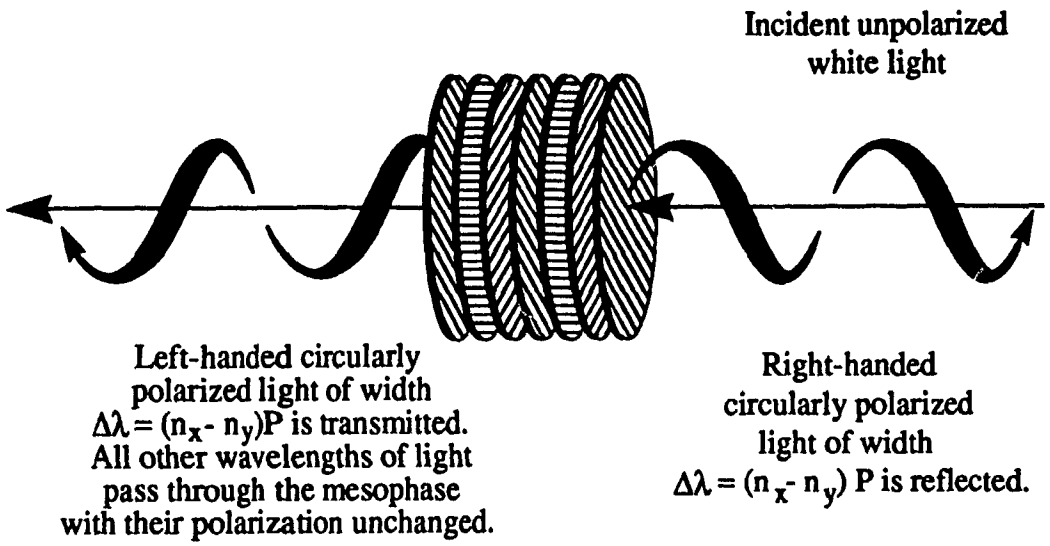

Figure 4.3 The interaction of unpolarized white light with a right-handed cholesteric liquid crystal. The width of the spectral region selectively reflected, $\Delta\lambda$, is directly related to the difference in the two refractive indices of the nematic layers (see Figure 4.2).

Fergason (20) (Equation [4.9]) must be used to provide the value of λ_0 of an individual domain.

$$\lambda_0 = \bar{n} P \cos 1/2[\sin^{-1} ((\sin \varphi_i) / 1.5) + \sin^{-1} ((\sin \varphi_r) / 1.5)] \qquad [4.9]$$

where φ_i = angle of incidence
φ_r = angle of reflected light

Equation [4.9] reduces to Equation [4.4] when the light wave is collinear with the optic axis. The fact that polydomain texture exists in real samples does not affect the value of λ_0 but does explain the source of the experimentally observed diffuse peak shape and tailing at wavelengths lower than the absorption maximum.

The two primary optical methods for studying cholesteric liquid crystals that utilize the light wave behaviour described above are optical rotatory dispersion (ORD) (*vide infra* Chapter 5) and CR. CR measures the differential transmission of left-handed and right-handed circularly polarized light as a function of wavelength where the maximum differential of the transmitted polarized components corresponds to λ_0 which also equals the wavelength maximum in an absorbance spectrum and the cross-over wavelength of the pseudo Cotton Effect in an ORD spectrum. The circular polarized dichroic ratio, D, is defined by Equation [4.10].

$$D = (I_R - I_L) / (I_R + I_L) \qquad [4.10]$$

where I_R = intensity of the transmitted right-handed component
I_L = intensity of the transmitted left-handed component.

A negative D value corresponds to a negative CR signal and indicates the existence of a right-handed cholesteric structure while a positive D value corresponds to a positive CR signal and is characteristic of the left-handed cholesteric structure. This technique therefore provides information on both the reflection wavelength and twist sense of the cholesteric structure. The mean refractive index of the mesophase can be determined by the use of a refractometer equipped with a polarizer and this allows the value of the pitch

to be calculated. Values of both the pitch and wavelength of maximum reflection can be used to describe the optical properties of liquid crystals.

4.1.2.2 Light Interaction with Homeotropic Liquid Crystals

The major type of cholesteric homeotropic texture which exists is fingerprint texture. A fingerprint texture is observed when the optic axis of the cholesteric structure adopts an alignment parallel to the surface of the liquid crystal (Figure 4.4).

When a homeotropic liquid crystal with a sufficiently long pitch is examined under a polarizing microscope equally spaced parallel lines similar to a fingerprint are observed. The source of these lines is the variation in the observed layer birefringence. Layers parallel to the direction of observation have a minimum of birefringence while those aligned normal to the direction of observation exhibit maximum birefringence. The difference in the observed birefringence of the layers causes a series of dark and bright lines to be seen and the period of the stripped pattern is equal to the half-pitch. This technique is often used to determine the pitch of long pitch samples but its application to samples of short pitch is limited. Colours may also be observed for these types of mesophases but are the result of the diffraction properties of the grating-like spacings of the nematic layers.

A special case of periodic spacing can occur if the binding energy of the mesophase to the surface of its container is greater than the energy responsible for the helical twist (21). A fingerprint texture occurs but the periodicity is much greater than the true pitch of the sample.

4.1.3 Liquid Crystals of Cellulose Derivatives

The first paper detailing the formation of a cellulose derivative liquid crystal, (hydroxypropyl)cellulose (HPC) in water, was published in 1976 by Werbowyj and Gray (22). Many subsequent investigations of liquid crystalline cellulose derivatives have been made on ether and acetate derivatives of HPC in the thermotropic state or using organic

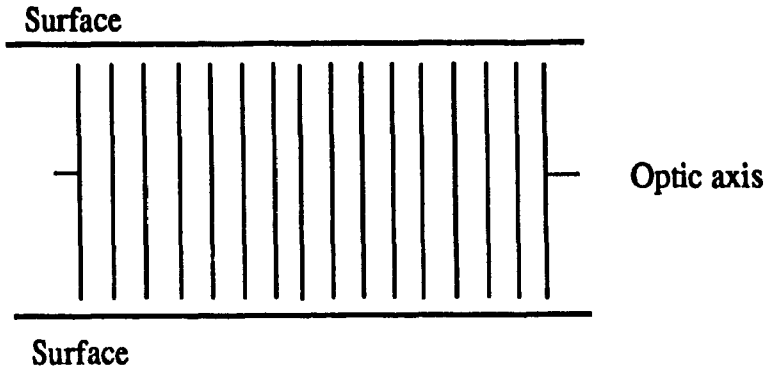

Figure 4.4 Homeotropic texture in a cholesteric liquid crystal where the optic axis is oriented parallel to the surface. If the spacing between the nematic layers is sufficiently large then a fingerprint pattern may be observed under a polarizing microscope.

solvents in the lyotropic state (23 - 28). Cellulose derivatives possessing sidechains smaller than those of commercial grade HPC tend to form mesophases with reflection colours in more limited selections of solvents. For example, cellulose triacetate or commercially produced methyl cellulose require very strong solvents such as dichloroacetic acid (DCA) or trifluoroacetic acid (TFA) (29 - 31). It has been hypothesized that the role the sidechains play in the formation of the mesophase is to inhibit crystallization and thereby permit the polymer chains to move into an ordered arrangement (32). Should sufficiently large sidechains be incorporated onto the cellulose backbone then thermotropic in addition to lyotropic behaviour may be observed in the bulk polymer. In the absence of large sidechains, solvents capable of preventing backbone interaction must be used. Although cellulose normally forms a liquid crystal only in various uncommon solvent mixtures, a report has been made of liquid crystalline order in the cellulose cell structure of a plant (33). Solvents employed for the production of cellulose mesophases include water / N-morpholine-N-oxide (34), TFA / chlorinated alkanes (35), lithium chloride / N,N-dimethylacetamide (36) and ammonia / ammonium thiocyanate (37); however, reflection colours in a cellulose mesophase have yet to be reported.

Liquid crystals composed of both high and low molar mass molecules are sensitive to their composition and environment. It is these factors which are investigated in the attempt to understand and control the liquid crystalline properties. Low molar mass liquid crystals are known to be very sensitive to their composition. For example, even minor changes such as the addition of a small quantity of a chiral species to a nematic mesophase can convert the mesophase to a cholesteric structure (38, 39). Polymer liquid crystals have also been shown to be sensitive to their composition in terms of their enantiomeric composition (40). While each enantiomer alone forms a cholesteric liquid crystal, equal proportion mixtures of the enantiomers induces the formation of a nematic liquid crystal. Cellulose derivatives lack enantiomers, but a study on the effect of the relative isomer composition of a chiral solvent, 2-amino-1-butanol, on HPC mesophases determined that there is no discernable effect on the mesophase properties (41).

While many cellulose derivatives have been found to form mesophases (42, 43,

44), only a few have been investigated in any detail. The presence of reflection colours in mesophases makes them attractive for the purposes of structural investigations through their optical properties. However, even for cellulose derivatives that form mesophases with reflection colours, not all reports include information on both the cholesteric twist sense and temperature dependence of λ_0 or the pitch. Information on the cholesteric twist sense and the temperature dependence of the pitch of several cellulose derivatives is presented in Table 4.1.

Table 4.1

Cholesteric Twist Sense and / or Pitch Temperature Dependence of Several Cellulose Derivative Mesophases

HPC

Solvent	Twist Sense	P(T)	Reference
Water	Right	Increases / Decreases [a]	(22, 44)
Methanol	Right	NR [b]	(45)
Acetic acid	Right	NR	(45)
Water-cast film	Right	Increases	(46)
2-Amino-1-butanol	Right	NR	(47)

(Acetoxypropyl)cellulose

Thermotropic	Right	Increases	(23, 24)
Acetone	Right	NR	(23)
Dibutyl phthalate	Right	Increases	(24)

Thermotropic Esters of HPC

Ester	Twist Sense	P(T)	Reference
Propionic acid	Right	Increases	(25, 26)
n-Butyric acid	Right	Increases	(26)
Isobutyric acid	Right	Increases	(26)
Phthalic acid	Right	Increases	(26)
Acrylic acid	NR	Increases	(27)

(Ethoxypropyl)cellulose

Thermotropic	Right	Increases	(28)

(Hydroxyethyl)cellulose

Solvent	Twist Sense	P(T)	Reference
Thermotropic	NR	Increases	(48)
Ethylene Glycol	NR	Increases	(48)

(Hydroxybutyl)cellulose

Thermotropic	NR	Increases	(48)
Dimethylacetamide	NR	Increases	(48)

Table 4.1 (continued)

Solvent	Twist Sense	P(T)	Reference
Cellulose acetate			
TFA	Left	NR	(29)
TFA	Left	Increases	(30)
Cellulose acetate-trifluoroacetate			
TFA	Right	NR	(29)
Cellulose triacetate			
TFA	Left	NR	(29)
Ethyl cellulose (nominal DS = 2.5)			
Acetic acid	Left	Decreases	(49, 50)
DCA	Right	NR	(49)
Methyl cellulose			
DCA	Left	Increases	(31)
TFA	Left	Increases	(31)
(Acetyl)(ethyl)cellulose			
Chloroform	Right / Left [d]	Increases / Decreases	(51, 52)
Dichloromethane	Right / Left [d]	NR	(51)
m-Cresol	Right / Left [d]	NR	(51)
Aqueous phenol	Right / Left [d]	NR	(51)
Acetic acid	Right / Left [d]	NR	(51)
DCA	Right	NR	(51)
Cellulose tricarbanilate			
Ethyl methyl ketone	Right	Increases	(50)
2-Pentanone	Right	Increases	(50)
DEME [c]	Left	Increases	(53)
Cellulose dicarbanilate			
Pyridine	Right / Left [e]	NR	(50)
3-Chlorophenylurethane ester of HPC			
DEME	Right	Increases	(54)

Table 4.1 (continued)

Solvent	Twist Sense	P(T)	Reference
(Acetoacetoxypropyl)cellulose			
Acetic acid	Left	NR	(55)
Tri-O-2-(2-methoxyethoxy)ethyl cellulose			
Thermotropic	Right	Increases	(56)
Thermotropic oligomer	Right / Left [f]	Increases / Decreases	(56)
Tri-O-(butoxyethyl)cellulose			
Thermotropic	Left	Increases	(56)
Thermotropic oligomer	Left / Right [f]	Increases / Decreases	(56)
Tri-O-heptyl cellulose			
Thermotropic	Left	Decreases	(56)
6-O-Trityl-2,3-di-O-benzyl cellulose			
Chloroform	Right	NR	(57)
Bromoform	Right	Increases	(57)
Tetrahydrofuran	Right	NR	(57)
6-O-Trityl-2,3-O-butyl cellulose			
Chloroform	Right	Increases	(58)
6-O-Trityl-2,3-O-pentyl cellulose			
Chloroform	Right	Increases	(58)
Tetrahydrofuran	Right	Increases	
6-O-Trityl-2,3-di-O-hexyl cellulose			
Chloroform	Right	NR	(58)
Terahydrofuran	Left	Increases	(58)

[a] The decrease in pitch that is seen with increasing temperature is artificial. The concentration is affected by a temperature dependent phase separation.
[b] NR = not reported.
[c] DEME = diethylene glycol monoethyl ether.
[d] The twist sense and temperature dependence of the pitch depend on the acetyl content.
[e] The twist sense is concentration sensitive.
[f] The twist sense depends on temperature.

It is obvious from Table 4.1 that while the majority of cellulosic mesophases studied to date form right-handed cholesteric structures it is also possible for left-handed systems to exist. The variation in the liquid crystalline properties for cellulose derivatives is perhaps unexpected because all these polymers share the same chiral backbone. The fact that cellulose derivatives can form both right-handed and left-handed cholesteric liquid crystals means that the sidechains play a more significant role than just aiding in the formation of the mesophase. Given the limited number of solvents in which most cellulose derivatives mesophases have been studied, no general conclusions are possible concerning a preferred twist sense or temperature dependence of the pitch. The question therefore becomes: to what extent do the solvents and sidechains play a role in determining the liquid crystalline properties of cellulose derivatives?

The cellulose derivative employed in this thesis to address this question is ethyl cellulose (EC). EC was the first and is still one of the few cellulosic mesophases found to have a solvent dependent cholesteric twist sense (49). Other studies on EC mesophases have focused on phase separation with a second polymer (59, 60), dielectric behaviour (61), birefringence (50, 62, 63), phase and rheological behaviour (49, 64 - 67), morphology (68), pitch as a function of concentration and temperature (50, 68), the effect of inorganic acids (69), and the introduction of acetyl groups (51, 52, 70). In this chapter the effects of solvent, temperature, concentration and degree of substitution (DS) on the mesophase properties of EC are examined by CR. The solvents employed include those successfully utilized in the EC liquid crystalline phase separation study of Chapter 3. Other factors examined include the effects of substituting methyl and butyl groups onto the previously unreacted hydroxyl groups, the effect of temperature on cholesteric films which are prepared by casting the cholesteric films from chloroform solutions of EC and its derivatives, and the search for induced optical activity in mesophases containing achiral dyes.

4.2 EXPERIMENTAL

With the exception of the EC (DS = 2.29) / chloroform and tri-O-ethyl cellulose / chloroform samples, all mesophase samples were prepared by weighing measured quantities of polymer and solvent into a small vial that was then tightly capped. Mixing was aided by centrifugation. After mesophase formation the samples were stored in the dark. This was especially important for EC / m-cresol samples as these mesophases rapidly discoloured if left exposed to light. Samples of EC in chloroform and DCA also degraded visibly with time. Chain degradation of EC is known to occur in several solvents over prolonged periods of time (71).

Thin samples of each mesophase were prepared for optical measurements by sandwiching the mesophase between a glass slide and coverplate. The glass coverplate was sealed to the slide with Devcon epoxy in an attempt to slow evaporative loss of solvent. Samples of EC and tri-O-ethyl cellulose in spectral grade chloroform were prepared by flame-sealing one end of a 0.4 mm thick glass microslide (Vitro Dynamics Inc., Rockaway, NJ, 07866, USA), packing the slide with a known mass of polymer and injecting a known mass of solvent with a microsyringe. The samples were cooled in dry ice and the open end of the microslides were then also flame sealed. Mixing in the microslides was aided by low speed centrifugation. Mesophases of EC in monochloroacetic acid (MCA) and phenol were prepared by mixing EC and the solid "solvents" in a small vial and heating to ~ 60 °C.

Cholesteric films of the samples were prepared by making anisotropic solutions of the cellulose derivatives in chloroform, placing the mesophase between two glass slides and then slowly shearing the slides apart. The two slides were then placed in a small enclosed container containing a saturated chloroform atmosphere. The slides had a single drop of chloroform placed in the centre of the sample and after several hours the slides were removed and dried completely. The region of the slide that had had the chloroform drop placed on it offered the best texture for CR measurement. All samples were checked for linear birefringence effects. Cellulose derivative films exhibiting linear birefringence have been shown to exhibit circular reflection peaks whose signs vary as a function of

their orientation in the beam path of the spectropolarimeter (72).

CR spectra were recorded with a Jasco J-500C Spectropolarimeter. All mesophase samples were placed directly in the beam path with the surfaces of the sample oriented perpendicular to the beam. When temperature control was required the spectropolarimeter was equipped with a Mettler FP2 Hot Stage. The temperature was varied at the rate of 1 ^{o}C min.$^{-1}$ when scans at intervals of 2.5 ^{o}C or greater were required and at a rate of 0.2 ^{o}C min.$^{-1}$ when scans at intervals of less than 2.5 ^{o}C were required. Refractive index measurements were made with an Abbé refractometer whose temperature was controlled by a water recirculation bath. The refractometer was equipped with a polarizing filter whose direction of polarization was established by the use of laser equipped with a polarizer of known orientation. After the method of Suto et al. (62, 63), all samples examined in the refractometer were allowed to relax for 30 min. before measurement. The cellulose derivatives employed in this section of the thesis are those listed in Tables 2.2 and 2.3

4.3 RESULTS AND DISCUSSION

4.3.1 The Effect of Concentration on the Cholesteric Structure of Ethyl Cellulose Mesophases

The composition feature most easily examined for lyotropic cellulose derivative mesophases is the concentration dependence of the reflection wavelength. Figure 4.5 shows the effect of concentration on the reflection wavelength of some EC (DS = 2.29) mesophases. The concentration dependence can be construed as "normal" in that an increase in the EC concentration decreases the reflection wavelength of the mesophases. While the vast majority of cellulose derivatives have been found to possess cholesteric structures whose pitches or reflection wavelengths decrease with increasing concentration this behaviour is not unequivocal; it has been reported that mesophases of cellulose tricarbanilate in ethyl methyl ketone and 2-pentanone (50) increase in pitch with increasing concentration. A more extreme case is reported for cellulose dicarbanilate in pyridine where an increase in the polymer concentration causes a reversal of the cholesteric twist sense (50).

Samples prepared with volatile solvents such as chloroform usually have their optical properties reported as reflection wavelength rather than pitch because measurement of the mean refractive index is difficult. For mesophases prepared with less volatile solvents the pitch can also be reported if the refractive indices of the E-ray and O-ray are measured. In an unsheared cholesteric liquid crystal the light wave polarized parallel to the longitudinal direction of the plate of the Abbé refractometer has refractive index $n_{\parallel}$ which corresponds to the E-ray while the light wave polarized perpendicular to the plate has refractive index $n_{\perp}$ and corresponds to the O-ray. The birefringence of the sample, Δn, is described by Equation [4.11] while the mean refractive index, $\bar{n}$, of a cholesteric is described by Equation [4.12].

$$\Delta n = n_{\parallel} - n_{\perp} \qquad [4.11]$$

$$\bar{n} = (2n_{\parallel} + n_{\perp}) / 3. \qquad [4.12]$$

Figure 4.6 shows that an EC mesophase can be adequately described by the

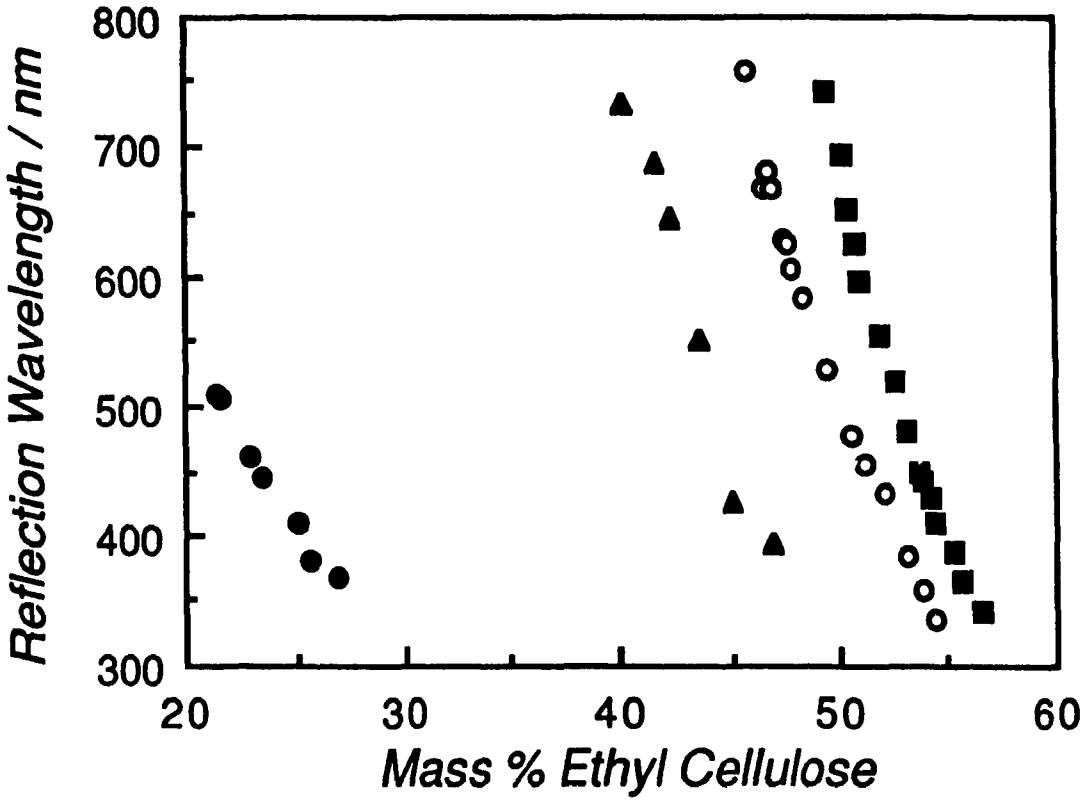

Figure 4.5 Variation of reflection wavelength with concentration for EC (DS = 2.29) mesophases. EC in bromoform (filled circles), chloroform (filled triangles), aqueous phenol (open circles) and m-cresol (filled squares).

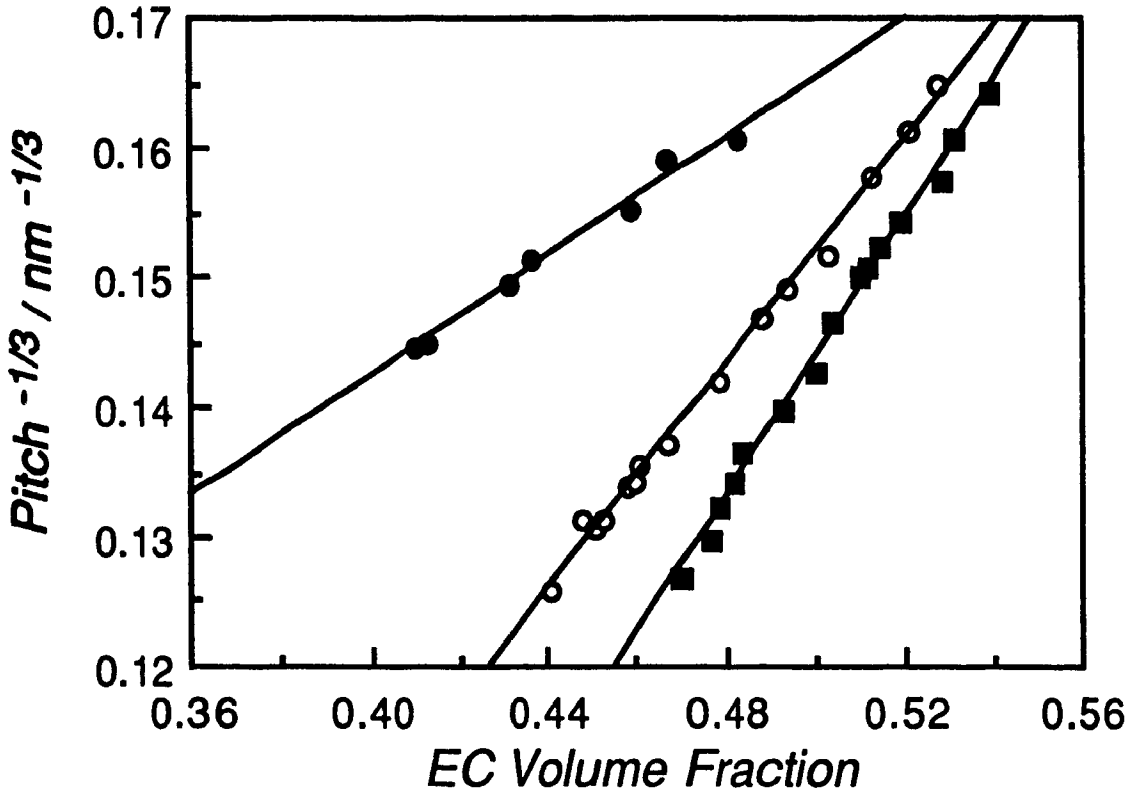

Figure 4.6 Variation of helicoidal pitch with volume fraction for EC (DS = 2.29) mesophases. EC in bromoform (filled circles), aqueous phenol (open circles) and m-cresol (filled squares).

inverse cube relationship between pitch and volume fraction which is commonly observed for several cellulose derivative / solvent systems (23, 24, 45). While the concentration dependence of the pitch is a useful feature in examining the behaviour of cellulosic liquid crystals, it is the effects of solvent, temperature and sidechains on the mesophase properties which are the factors of greatest interest.

4.3.2 Cholesteric Twist Sense of Ethyl Cellulose Mesophases

Using the CR technique to directly identify the cholesteric twist senses, this study has investigated mesophases of EC in several solvents. Table 4.2 lists the cholesteric twist senses of the various EC mesophases and the dielectric constants of the solvents employed.

Table 4.2

Solvent Dielectric Constants and
Cholesteric Twist Senses of EC (DS = 2.29) Mesophases

Solvent	Dielectric Constant (73)	Cholesteric Twist Sense
MCA	12.3 [a]	Left
Pyridine	12.3 [b]	Left
m-Cresol	11.8 [b]	Left
Phenol	9.78 [a]	Left
Dichloromethane	9.08 [c]	Left
DCA	8.2 [d]	Right
Acetic Acid	6.15 [c]	Left
Chloroform	4.806 [c]	Left
Bromoform	4.39 [c]	Left

[a] at 60 °C, [b] at 25 °C, [c] at 20 °C, [d] at 22 °C

It is apparent from Table 4.2 that the left-handed twist sense appears to be the most common cholesteric structure for EC with DS of 2.29 as all its mesophases are left-handed except when DCA is employed as the solvent. EC in DCA is assigned a right-handed cholesteric structure based on a negative CR reflection peak (Figure 4.7). EC in

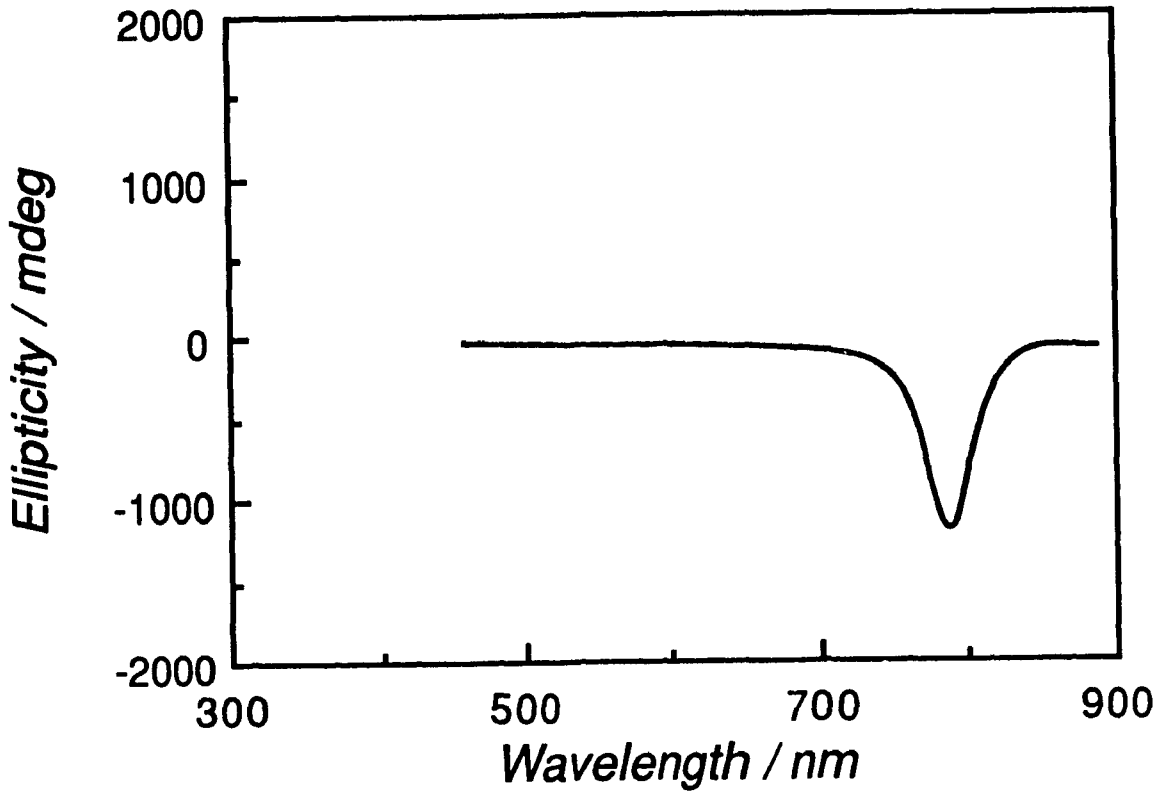

Figure 4.7 CRS spectrum of EC (DS = 2.29) in dichloroacetic acid (24.0 % w/w). The negative reflection peak indicates that right-handed circularly polarized light is reflected and that this mesophase has a right-handed helicoidal twist sense.

DCA has previously been examined and, based on ORD spectra, is one of the few cellulose derivatives reported to have a solvent dependent cholesteric twist sense (49, 50): the ORD spectrum of EC in acetic acid showing a full pseudo Cotton Effect conclusively proves that the system has a left-handed cholesteric structure; however, the assignment of a right-handed cholesteric structure to EC in DCA was made on the basis of an ORD spectrum of a long pitch sample possessing only a positive low wavelength tail of a pseudo Cotton Effect that occurs above the operational range of the instrument. This method of assigning cholesteric twist sense on the basis of low wavelength ORD curve tailing is potentially prone to error if the wavelength of maximum reflection is far above the operating limits of the spectrometer and the polymer has electronic transitions whose absorption band signs are sensitive to its environment. In such a case the electronic absorption bands of a strong transition, such as those associated with aromatic chromophores, could easily dominate the optical properties that accompany long pitch mesophase ordering in the visible region of the spectrum. The fact that the sign of CD absorption bands for cellulosics can be solvent dependent (41) means that it would be possible, in theory, to see long pitch mesophase samples of the same polymer in different solvents that have the same cholesteric twist sense yet exhibit low wavelength ORD curve tails of opposite sign. Further evidence favouring exercising caution when using ORD curve tailing for cholesteric twist sense assignment can be found in studies of a long pitch mesophase of methylol cellulose in dimethylsulphoxide where different regions of the same sample produced ORD curve tailings of variable sign (74, 75). For these reasons direct identification of the twist sense is the preferred method of assignment.

PBLG mesophases have been studied extensively and their cholesteric twist sense is known to be solvent dependent (76, 77, 78). The results of the original studies of cellulose derivatives tentatively suggested that this solvent dependence might not exist in cellulosic mesophases as all samples studied were found to have right-handed cholesteric structure. However, subsequent studies (29, 49, 50, 53, 55, 56, 58) have demonstrated that the twist sense of several cellulosic mesophases are left-handed and that the twist senses of a limited number of cellulosics (49, 50, 53, 58) are even solvent dependent. Table 4.1 illustrated that although the majority of studied cellulosic mesophases have

right-handed cholesteric structures and a few are left-handed, no cellulose derivative has had its mesophase properties examined in more than a few solvents. It is therefore significant that EC with DS of 2.29 has been examined in a variety of solvents including one that produces an opposite twist sense as this permits an examination of a theory that attempts to predict the twist sense.

Theories that have attempted to describe the relationship between the cholesteric twist sense of lyotropic polymer mesophases and the solvent employed have frequently used PBLG as their model. The theory of Samulski and Samulski (16) that relates the twist sense of the mesophase to the dielectric constant of PBLG and solvents finds that the critical dielectric constant, ε^*, for determining the twist sense is related to the dielectric constant of the polymer. Non-interacting solvents with a dielectric constant higher than ε^* form cholesteric mesophases with one twist sense while solvents with a dielectric constant that is lower than the critical value form mesophases of opposite twist sense. However, assuming that the solvents employed in this study are non-interactive, the dielectric theory does not describe successfully the formation of a right-handed or left-handed cholesteric structure for EC mesophases as solvents with dielectric constants both higher and lower than that of DCA cause the formation of left-handed mesophases whereas EC in DCA forms a right-handed structure. For PBLG mesophases the correlation between the dielectric constant and the twist sense was highest in chlorinated solvents but for EC no trend exists even in this class of solvents.

The assumption of non-interaction between polymer and solvent is an important feature of the dielectric theory. For example, according to this theory PBLG in m-cresol should have an opposite twist sense than in dioxane, yet at room temperature it does not. Infrared studies of the PBLG / m-cresol system suggest that temperature sensitive hydrogen bonding exists between the hydroxyl group of m-cresol and the carbonyl groups of PBLG (77, 78). Such interactions have been found to change the orientation of the permanent dipole moments of the sidechains (79) which in turn would affect the critical dielectric constant of the polymer. While the validity of the dielectric theory does not necessarily come into question under such circumstances, the PBLG / m-cresol system illustrates the difficulty of accurately assigning true dielectric behaviour. A similar

polymer / solvent effect can also be postulated for the mesophase systems examined here. Many of the solvents employed here possess the capability of strongly interacting with EC. Like PBLG, these interactions could affect the value of the polymer's critical dielectric constant. Strong interactions between the solvent and polymer can provide a possible explanation for the reversal of twist sense seen for EC in DCA. Low molar mass derivatives of cholesterol have been shown to change their mesophase twist sense when different types of achiral groups are substituted onto the parent molecule (3). Similar behaviour has also been recently observed for cellulose derivatives when unreacted hydroxyl groups are replaced by achiral substituents such as acetyl groups or acetyl derivatives. The cholesteric twist sense of cellulose acetate (CA) in TFA changes from left-handed to right-handed when trifluoracetylation of the hydroxyl groups occurs (29) and the introduction of acetyl groups onto the EC chain produces the same effect in chloroform (51, 52). However, the introduction of acetyl halide groups onto a cellulose ether by reaction with solvents such as TFA or DCA does not always ensure a change in twist sense as methyl cellulose retains its left-handed twist sense in both DCA and TFA despite reacting with these solvents (30). Zugenmaier and Haraud (44) have found that by mixing acetic acid and DCA in varying ratios, EC liquid crystals can be prepared with variable pitch and cholesteric twist sense.

The variation of cholesteric twist sense with changes in temperature is a widely studied area of both small molecule and polymer liquid crystals. As with the solvent dependence of the twist sense, PBLG has often been cited as the model system for theories attempting to interpret the twist sense temperature dependence of polymeric systems. DuPré and Duke (80) postulated that sidechain orientation in PBLG molecules may play a role in determining the cholesteric twist sense and based on a nuclear magnetic resonance study Samulski and Czarniecki (81) concluded that this assessment was correct; changes in the pitch and cholesteric twist sense of PBLG mesophases with variations in temperature and / or solvent were ascribed to subtle changes in the sidechain structure of the PBLG molecules that results in a change in the apparent molecular helicity. These observations agree with a theory by Kim (13) which states that the chiral sense of the molecule determines the cholesteric twist sense of the liquid crystal.

However, the theory of Kimura et al. (14) does not require any change in the molecular chirality and states that it is possible for a molecule with a single chiral sense to form either a right-handed or left-handed liquid crystal. An infrared study of a thermotropic PBLG derivative by Watanabe and Nagase (12) found that as the mesophase changes its twist sense with increasing temperature there is no sudden drastic change the infrared spectra which suggests that the helical backbone at least does not undergo any radical transformation during the transition from one twist sense to the other. Recent work on thermotropic cellulosic oligomers has shown that it is also possible for these compounds to increase in pitch, change twist sense and then decrease in pitch with increasing temperature (56), but no studies have yet been made to determine if there is an equivalent change in the orientation of the sidechains as the cholesteric structure changes its twist sense. While a possible variation in the orientation of the sidechains due to temperature or solvent effects which thereby introduces variable apparent chirality to a polymer with a backbone of a single chiral sense may be an attractive theory for polymers with large sidechains, it is difficult to see how such an effect could come into play for polymers such as EC or CA which have comparatively small sidechains. Even allowing for solvent reactions with hydroxyl groups, the substituents introduced are small and should have little effect on the observed chirality of the polymer chains.

4.3.3 Temperature Dependence of the Reflection Wavelength of Ethyl Cellulose Mesophases as a Function of Solvent

As shown in Table 4.1, measurement of the temperature dependence of the pitch or reflection wavelength of cellulose derivative mesophases as a function of solvent is largely an unexplored area. It therefore is of interest to examine the thermal properties of EC mesophases in several solvents. Measurement of the reflection wavelengths as a function of temperature for liquid crystals of EC with DS of 2.29 in several solvents reveals that this polymer exhibits an unique range of behaviour. Three types of behaviour are observed depending on the solvent employed: (i) the mesophase is left-handed and the reflection wavelength decreases with increasing temperature, (ii) the mesophase is left-

handed and the reflection wavelength increases with increasing temperature, and (iii) the mesophase is right-handed and the reflection wavelength increases with increasing temperature. Table 4.3 lists the cholesteric twist sense and the temperature behaviour of the EC / solvent systems investigated. Figure 4.8 shows the temperature behaviour of the reflection wavelength of EC in four solvents that all produce left-handed mesophases yet two of which decrease in reflection wavelength with increasing temperature while the other two increase in reflection wavelength. These effects are all reversible when the temperature is reduced.

Table 4.3

Cholesteric Twist Sense and Reflection Wavelength as a Function of Temperature for EC (DS = 2.29)

Solvent	Twist Sense	λ_0 (T)
Acetic acid	Left (49 [a])	Decreases (49 [a])
Bromoform	Left	Decreases
MCA	Left	Increases
Chloroform	Left	Decreases
m-Cresol	Left	Increases
DCA	Right (49 [a])	Increases
Aqueous Phenol	Left	Increases
Phenol	Left	Increases
Pyridine	Left	Decreases
1,1',2,2'-Tetrachloroethane	Left	Decreases

[a] nominal DS = 2.5

All mesophase samples of PBLG and its derivatives examined exhibit the same pitch temperature dependence; the sign of the slope of a plot of reciprocal pitch or reflection wavelength versus temperature is always negative regardless of the cholesteric twist sense or solvent employed (12, 78, 82). Investigations of cellulose derivative mesophases prior to this study have shown only a little more variation in this relationship: all right-handed mesophases examined to date increase their reflection wavelength with an increase in temperature; however, cellulose tricarbanilate can form, depending on the

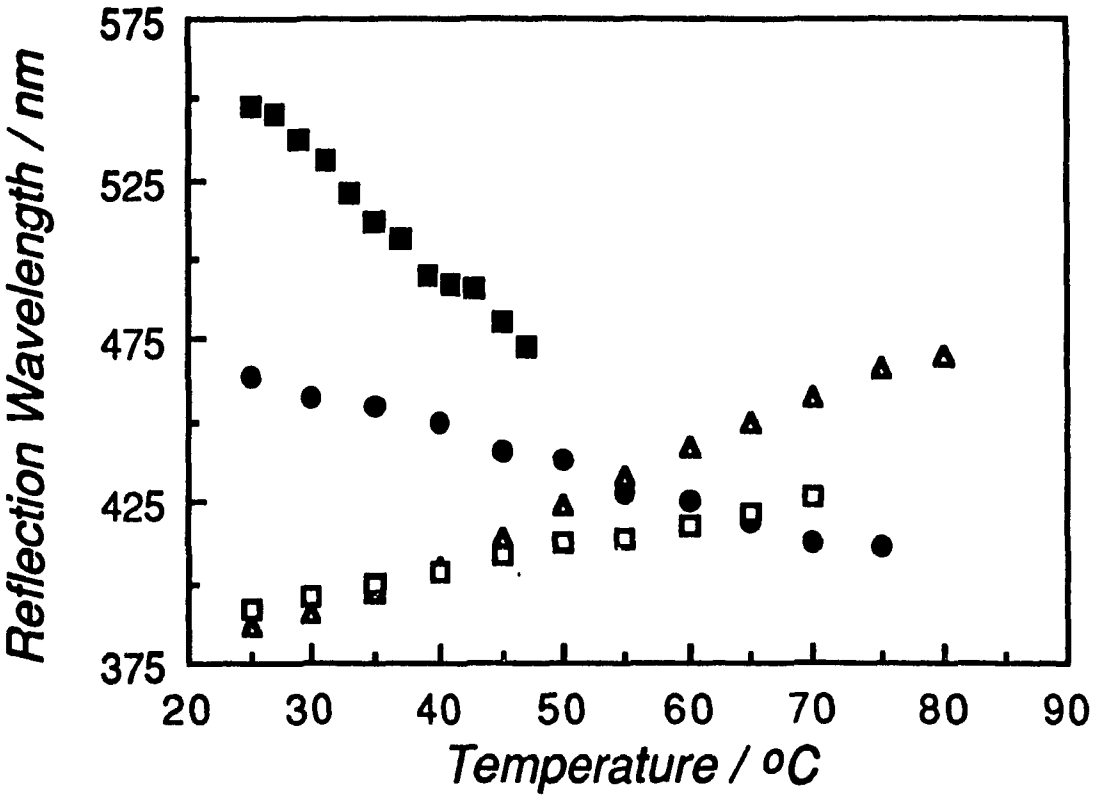

Figure 4.8 Variation of reflection wavelength with temperature for left-handed EC (DS = 2.29) mesophases in various solvents. EC in chloroform (43.7 % w/w, filled square), in bromoform (23.0 % w/w, filled circle), in m-cresol (54.4 % w/w, open square) and in aqueous phenol (50.9 % w/w, open triangle).

solvent employed, a left-handed or a right-handed mesophase which both increase in reflection wavelength with increasing temperature (49, 53). The finding here that plots of reflection wavelength versus temperature for left-handed mesophases of EC in bromoform, chloroform, pyridine, acetic acid and 1,1',2,2'-tetrachloroethane all have slopes of one sign while left-handed mesophases of EC in phenol, m-cresol, aqueous phenol and MCA samples have slopes of opposite sign is important because it demonstrates that the liquid crystalline behaviour of a cellulosic mesophase is much more sensitive to its environment than previously realized. These results also permit an evaluation of the theories that relate the pitch of the mesophase to the temperature.

Converting the plots of reflection wavelength versus temperature to pitch versus temperature requires measurement of the refractive indices of the mesophase as a function of temperature (Figure 4.9). The birefringence and mean refractive indices of EC mesophases in m-cresol and acetic acid have also been measured as a function of temperature by Suto et al. (62, 63) and are found to exhibit essentially the same behaviour. By calculating the mean refractive index of samples that have the same twist sense but opposite reflection wavelength / temperature relationships and plotting the pitch versus temperature relationship (Figure 4.10) it is found that the change in reflection wavelength for both EC samples is due primarily to changes in the pitch rather than large differences in the rate of change of the mean refractive index.

While the discovery that the signs of dP / dT and $d\lambda_0 / dT$ are solvent dependent is unique, such behaviour has been predicted for mesophases by the mean field theory of Lin-Liu et al. (9, 10) which states that although a preferred pitch / temperature relationship exists, an opposite behaviour is possible. The conditions for this opposite behaviour would require that the potential curves describing the mean field interaction potentials be of opposite symmetry. The theory of Kimura et al. (14) which has been used to describe the thermal features of PBLG and some cellulose derivatives would require that the geometric features of EC in each class of solvent be of opposite molecular helicity for this behaviour to occur. However, to fully use the Kimura theory requires a knowledge of the temperature at which the cholesteric structure moves to infinite pitch, T_N, i.e. nematic ordering, but for all EC mesophases the clearing temperature, the temperature where the

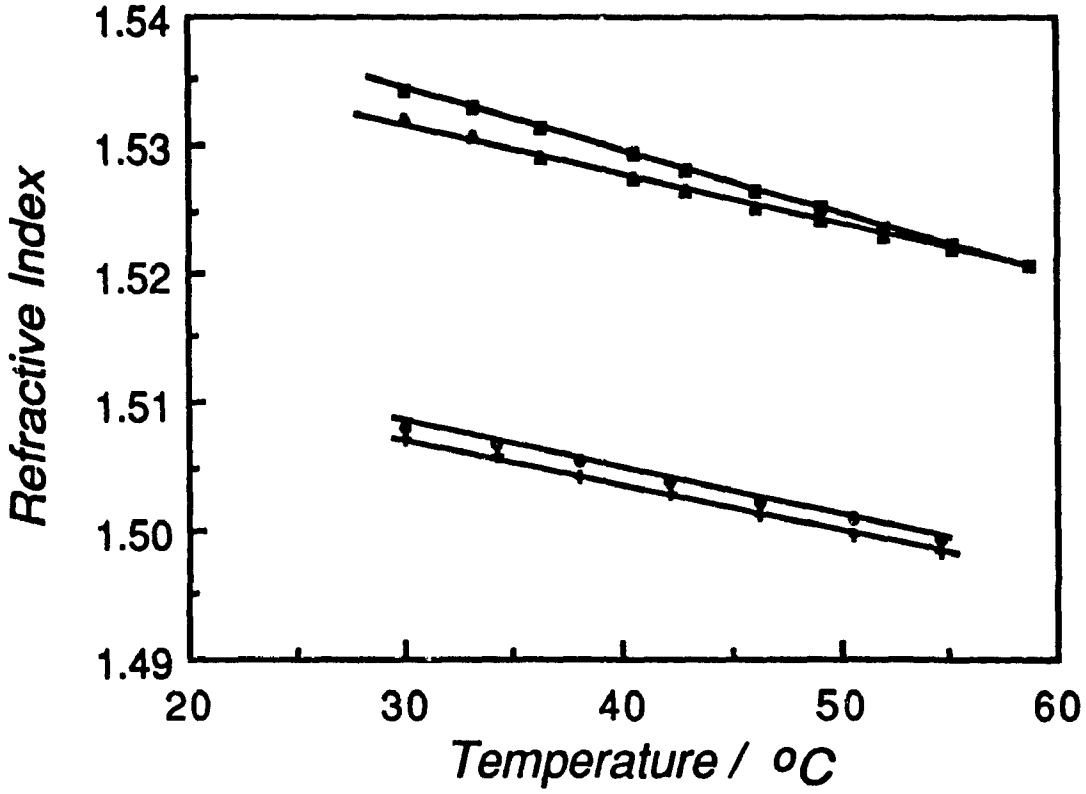

Figure 4.9 Variation of refractive index with temperature. EC (DS = 2.29) in bromoform, 26.9 % w/w ($n_{\parallel}$, filled squares, $n_{\perp}$, filled triangles). EC (DS=2.29) in m-cresol, 54.4 % w/w ($n_{\parallel}$, open circles, $n_{\perp}$, crosses). The birefringence is the difference between the two lines and is also temperature dependent.

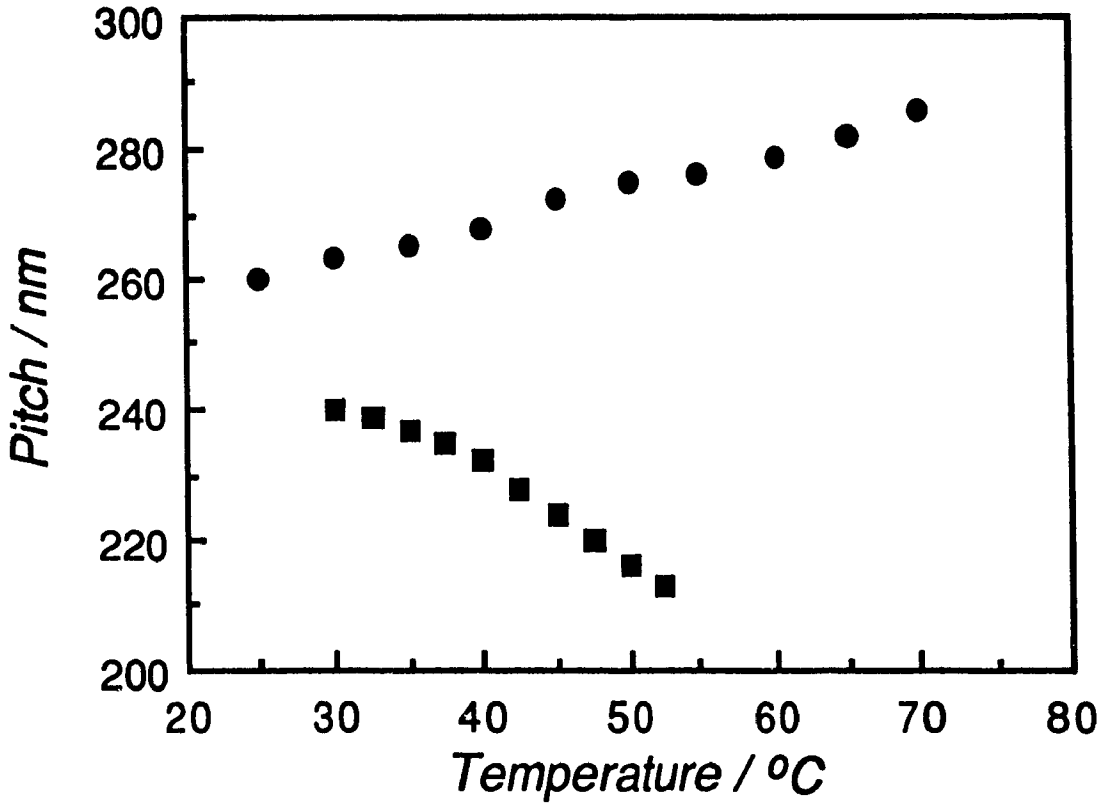

Figure 4.10 Variation of helicoidal pitch with temperature for EC (DS = 2.29) in bromoform (26.9 % w/w, squares) and m-cresol (54.4% w/w, circles). Both mesophases have a left-handed cholesteric twist sense.

solution converts to the isotropic phase, is reached before T_N.

4.3.4 Effect of Degree of Substitution on the Cholesteric Structure of Ethyl Cellulose Mesophases

It is evident from Table 4.1 and the results of the preceding sections that numerous types of sidechains have been incorporated onto the cellulose backbone and that different types of behaviour can be observed depending on the sidechain structure and the solvent employed. How sensitive are the liquid crystalline properties of cellulosics to minor variations in the number sidechains? A change in the DS is one of the subtlest variation of a cellulosic homopolymer that is possible. While x-ray diffraction studies of EC fibres have established that a change in DS from 2.5 to 3.0 has no effect on the molecular conformations (49) (both are left-handed threefold (3/2) helices), the role the DS plays in determining the supramolecular properties of cellulose derivatives with liquid crystalline ordering is largely an unexplored area.

4.3.4.1 Effect of DS on the Cholesteric Twist Sense and Reflection Wavelength of EC Mesophases

Mesophases were prepared from EC samples with DS varying from 2.29 to 3.00 in several solvents and the CR technique was used to monitor the reflection wavelength and cholesteric twist senses of the various mesophase systems. EC solubility is closely linked to the DS (83) so the very highly substituted EC samples cannot be examined in the same selection of solvents as the commercial product. Table 4.4 lists how the DS affects the cholesteric twist sense for several solvents.

Table 4.4

Cholesteric Twist Sense of EC in Several Solvents as a Function of DS

	Degree of Substitution						
Solvent	2.29	2.55	2.65	2.70	2.80	2.88	3.00
Aqueous Phenol	Left	Left	Left	Left	Left	-	-
Bromoform	Left	Left	Left	Left	Left	-	-
Chloroform	Left	Left	Left	Left	Left	-	Right
m-Cresol	Left	Left	Left	Left	Left	-	-
Dichloromethane	Left	Left	Left	Left	Left	-	Right
DCA	Right	Right	Right	Right	Right	Right	Right

The impact of the DS on the cholesteric twist sense is most explicitly illustrated using chloroform or dichloromethane as the solvent. Only the sample with DS of 3.00 in chloroform and dichloromethane forms mesophases whose cholesteric twist senses are right-handed in contrast to the samples of lower DS that form left-handed mesophases in these same solvents. The critical DS at which the switch from a left-handed to a right-handed cholesteric twist sense occurs for these solvents is approximately 2.88. This assignment is based on the fact that of all the EC samples examined in these solvents, only samples with a DS of less than 2.88 form left-handed mesophases with reflection colours while the sample with DS of 3.00 forms right-handed mesophases with reflection colours. As the polymer concentration of sample with DS of 2.88 is increased from that of an isotropic solution to the pure film, there is no appearance of visible reflection colours or even of fingerprint texture when viewed under a polarizing microscope. The switch in the twist sense from left-handed to right-handed cholesteric structure with increasing DS produces no radical change in the plot of reflection wavelength versus concentration; Figure 4.11 shows that like the sample with DS of 2.29, increasing the concentration of the sample with DS of 3.00 in chloroform still reduces the reflection wavelength of the mesophase. Lyotropic mesophases of CA in TFA (29) and thermotropic mesophases of the propionic acid ester of HPC (PPC) (25, 26) are two other rare examples of cellulose derivatives whose properties have been examined at more than

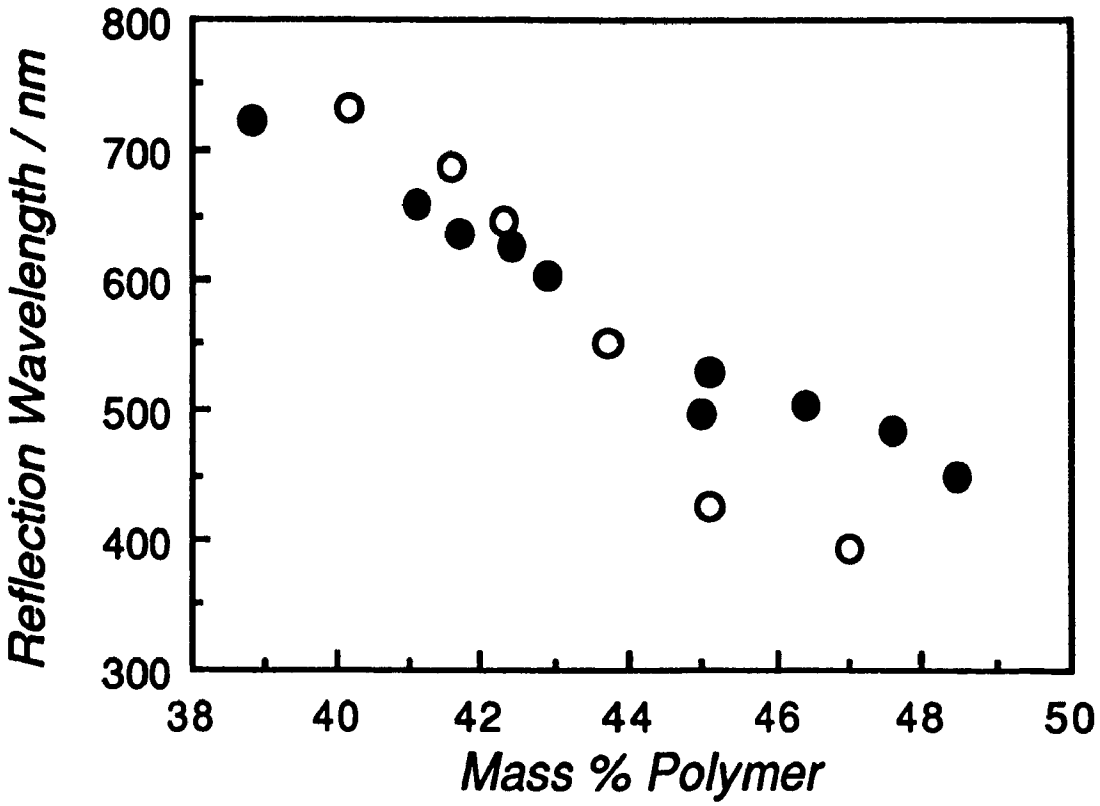

Figure 4.11 Variation of reflection wavelength with concentration for right-handed EC (DS = 3.0, filled circles) and left-handed (DS = 2.29, open circles) mesophases of EC in chloroform.

one DS. At identical temperatures, increases in the DS of PPC were found to produce moderate decreases in the reflection wavelengths of the right-handed thermotropic mesophases. The fact that CA of low DS reacts with TFA makes assignments of the effect of a change in DS of CA mesophases difficult to assess accurately, but it has been established that for CA of both high and low DS in TFA that the cholesteric twist sense is left-handed. The solvents employed here are for the most part comparatively benign which means that an accurate assessment of the effect of DS on the cholesteric twist sense, reflection wavelength and temperature dependence of the reflection wavelength is possible.

The effect of solvents on mesophases in which an increase in DS does not reverse the cholesteric twist sense offers the opportunity to observe the effect of the DS on the reflection wavelength of mesophases of left-handed cholesteric twist sense. Bromoform, aqueous phenol and m-cresol samples of EC are featured. Table 4.2 reported that in all these solvents EC with DS of 2.29 forms left-handed mesophases. Figure 4.12 shows that if the polymer content in the mesophases is maintained at fixed concentration and temperature then an increase in the DS produces an increase in the reflection wavelength for all solvent systems. The greatest sensitivity of the reflection wavelength to DS is observed in the m-cresol systems; the variation in the reflection wavelength for the bromoform and aqueous phenol systems are comparatively small. The degree to which changes in the DS of the EC / m-cresol mesophases can affect the reflection wavelength are illustrated by Figure 4.13 which shows that an increase in the DS of 0.5 at constant concentration can have as have much influence on the reflection wavelength as significant changes in concentration at a single DS. There has been no significant decrease in the molar mass during the preparation of the EC derivatives (84) so the increase is due exclusively to the change in DS. Preparing mesophases of EC in DCA as a function of DS at constant concentration presents the opportunity to observe the effect of DS on the reflection wavelength of lyotropic mesophase systems whose cholesteric twist senses are exclusively right-handed. CR measurements show that as the DS is increased a decrease is observed in the reflection wavelength of the mesophase. This behaviour corresponds to that observed for PPC thermotropic mesophases (25, 26) but is opposite to the effect

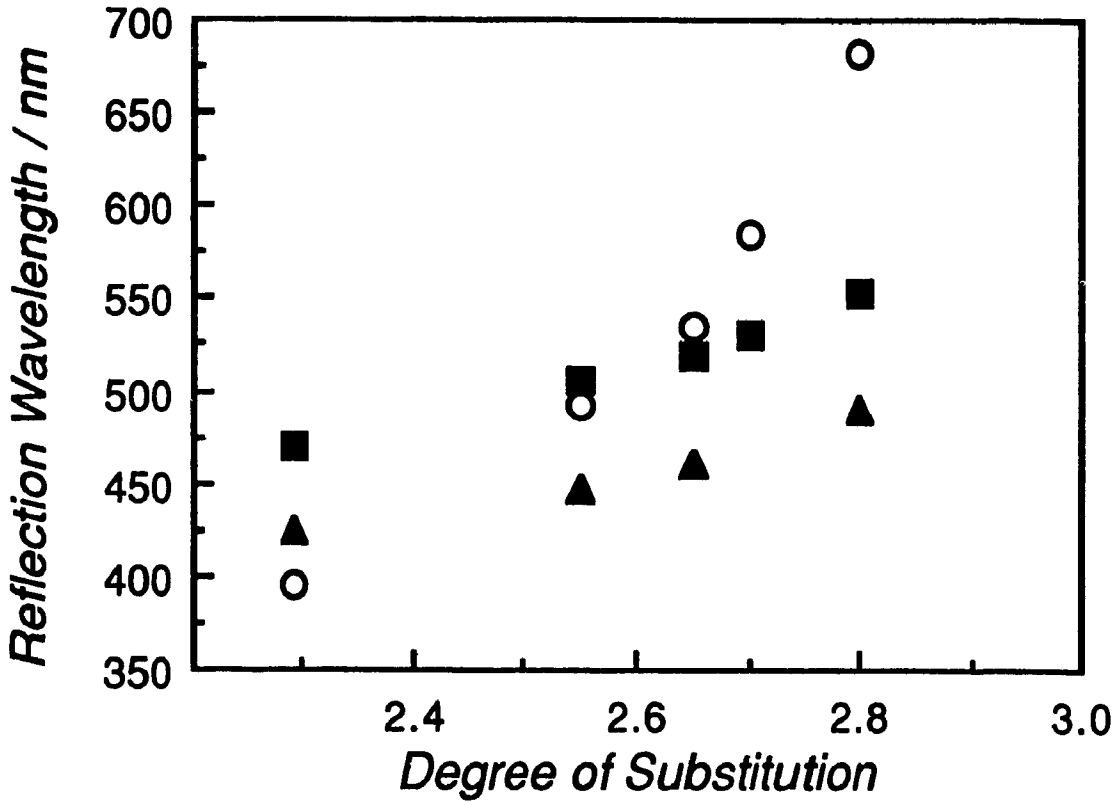

Figure 4.12 Variation of reflection wavelength with DS for EC mesophases at 30 °C. EC in m-cresol (54.4% w/w, open circles), aqueous phenol (50.9% w/w, squares) and bromoform (25.1% w/w, triangles).

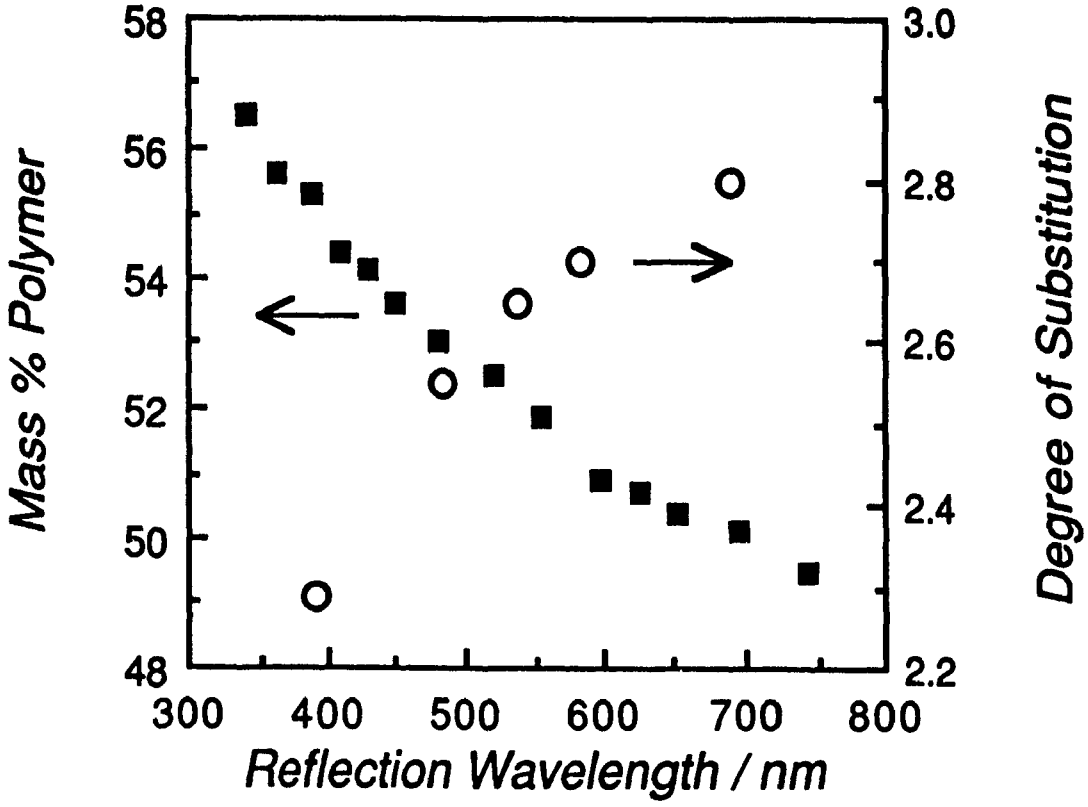

Figure 4.13 Relative effect of changes in concentration at DS = 2.29 and changes in DS at 54.5% (w/w) on the reflection wavelengths of EC / m-cresol mesophases.

observed for left-handed mesophases where increases in DS produce increases in the reflection wavelength. The cholesteric twist sense can be loosely viewed as an extreme case of pitch variation where right-handed structures are assigned positive pitch values while left-handed cholesteric structures are assigned negative values. Infinite pitch therefore corresponds to a perfect nematic structure. If the effect of the DS on the cholesteric structure is examined as reciprocal reflection wavelength versus DS then the coefficient of $d(1/\lambda_0) / d(DS)$ is positive for all samples (Figure 4.14).

4.3.4.2 Effect of DS on the Temperature Dependence of the Reflection Wavelength of EC Mesophases

Another significant feature of these variable DS mesophases is the effect of the DS on the temperature dependence of the reflection wavelength. The effect of temperature on the reflection wavelengths of EC samples with DS of 2.29 and 3.00 in chloroform can be seen from Figure 4.15. The reflection wavelength of the right-handed trisubstituted sample is more sensitive to a change in temperature than the left-handed sample of lower DS. The fact that in the sample with DS of 3.00 the reflection wavelength increases with increasing temperature whereas the reflection wavelength of the lower DS sample decreases does not mean that the temperature behaviour of the two analogs is unrelated. By replotting Figure 4.15 as reciprocal reflection wavelength versus temperature where left-handed structures are assigned negative values and right-handed ones are assigned positive values, it can be seen that the all samples have negative slopes (Figure 4.16).

Examination of the effect of the DS on the temperature dependence of the reflection wavelength for the samples that are exclusivley left-handed also reveals unusual behaviour. In the EC / bromoform (Figure 4.17) and EC / aqueous phenol (Figure 4.18) samples there is only a minor change in the mesophase behaviour as a function of DS; mesophases of EC in bromoform all decrease in reflection wavelength while mesophases of EC in aqueous phenol increase. However, like the effect on the reflection wavelength at a fixed temperature, the DS plays a major role in determining the temperature dependence of the reflection wavelength in the EC / m-cresol samples. Figure 4.19

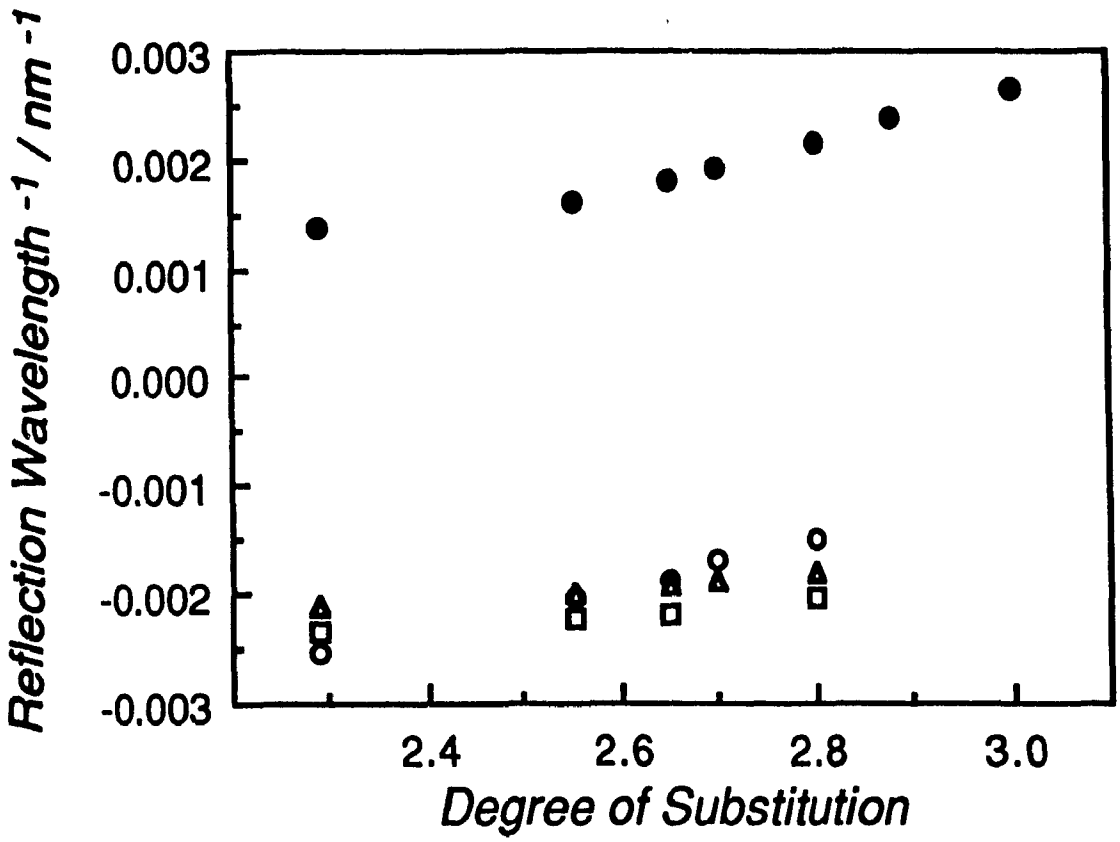

Figure 4.14 Variation of reciprocal reflection wavelength with DS for mesophases of EC. EC in DCA (24.9% w/w, filled circle), EC in aqueous phenol (50.9% w/w, open triangle), EC in bromoform (25.1% w/w, open squares) and EC in m-cresol (54.4% w/w, open circles). Zero represents the nematic state.

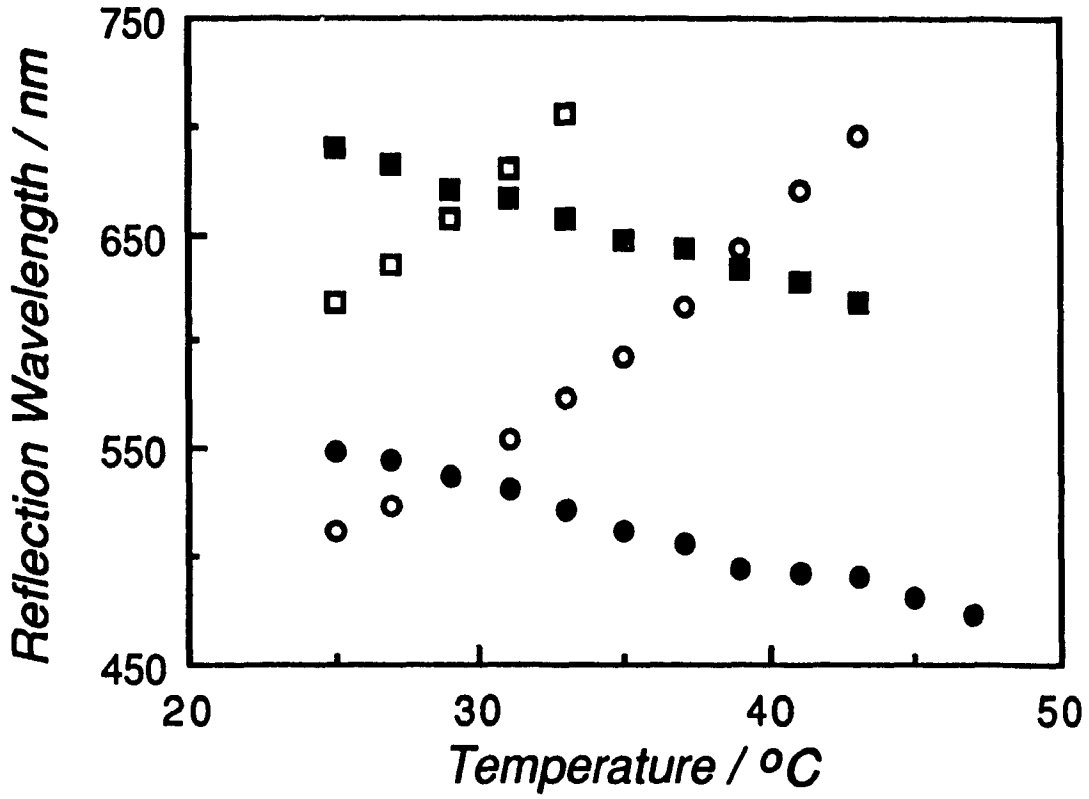

Figure 4.15 Variation of reflection wavelength with temperature for mesophases of EC with DS of 2.29 and 3.00 in chloroform. EC with DS of 2.29 (43.7% w/w, filled circle), EC with DS of 2.29 (41.6% w/w, filled square), EC with DS of 3.00 (47.6% w/w, open circle) and EC with DS of 3.00 (42.9% w/w, open square). Mesophases of EC with DS of 2.29 and 3.00 in chloroform are left-handed and right-handed, respectively.

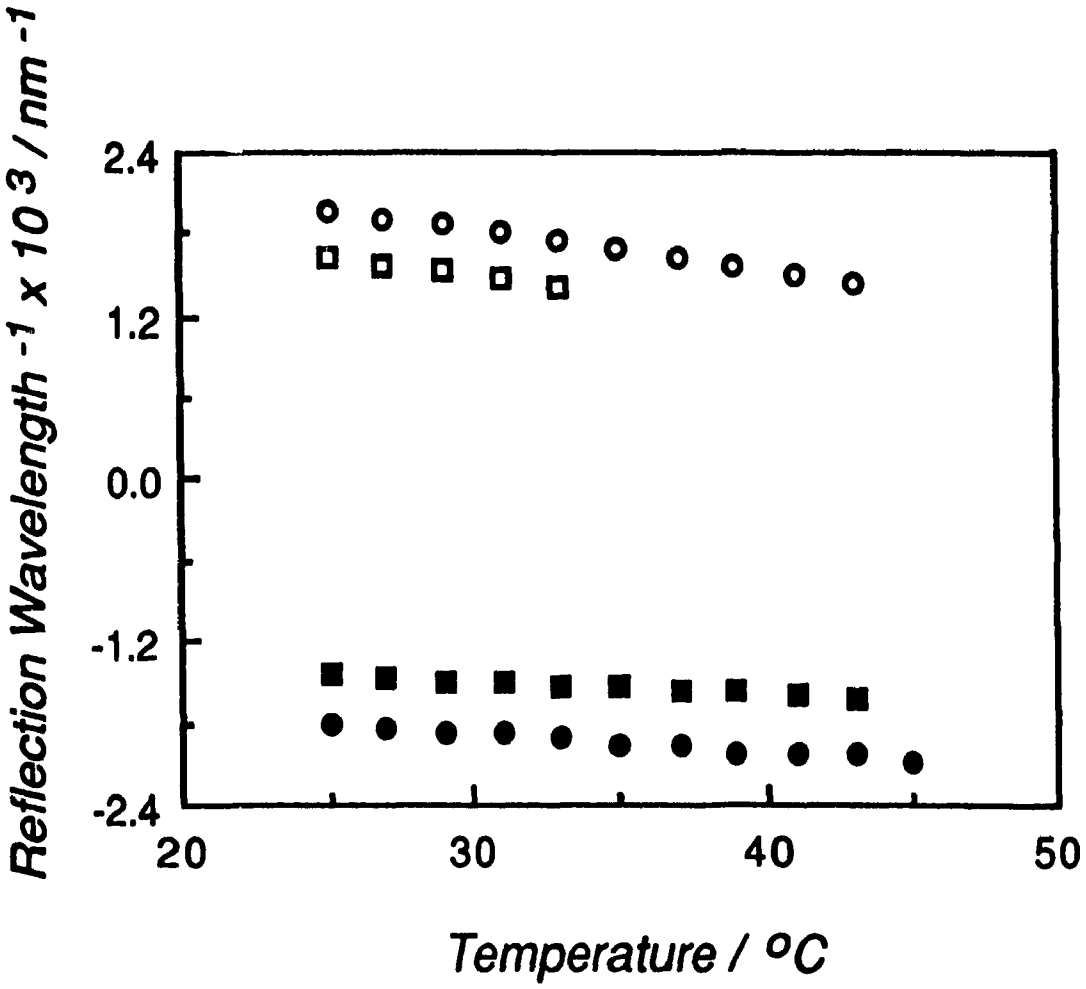

Figure 4.16 Variation of reciprocal reflection wavelength with temperature for mesophases of EC with DS of 2.29 and 3.00 in chloroform. EC with DS of 2.29 (43.7% w/w, filled circle), EC with DS of 2.29 (41.6% w/w, filled square), EC with DS of 3.00 (47.6% w/w, open circle) and EC with DS of 3.00 (42.9% w/w, open square). Zero represents the nematic state. Despite having opposite cholesteric twist senses (open points, right-handed; closed points, left-handed) the slopes are negative for both types of mesophases.

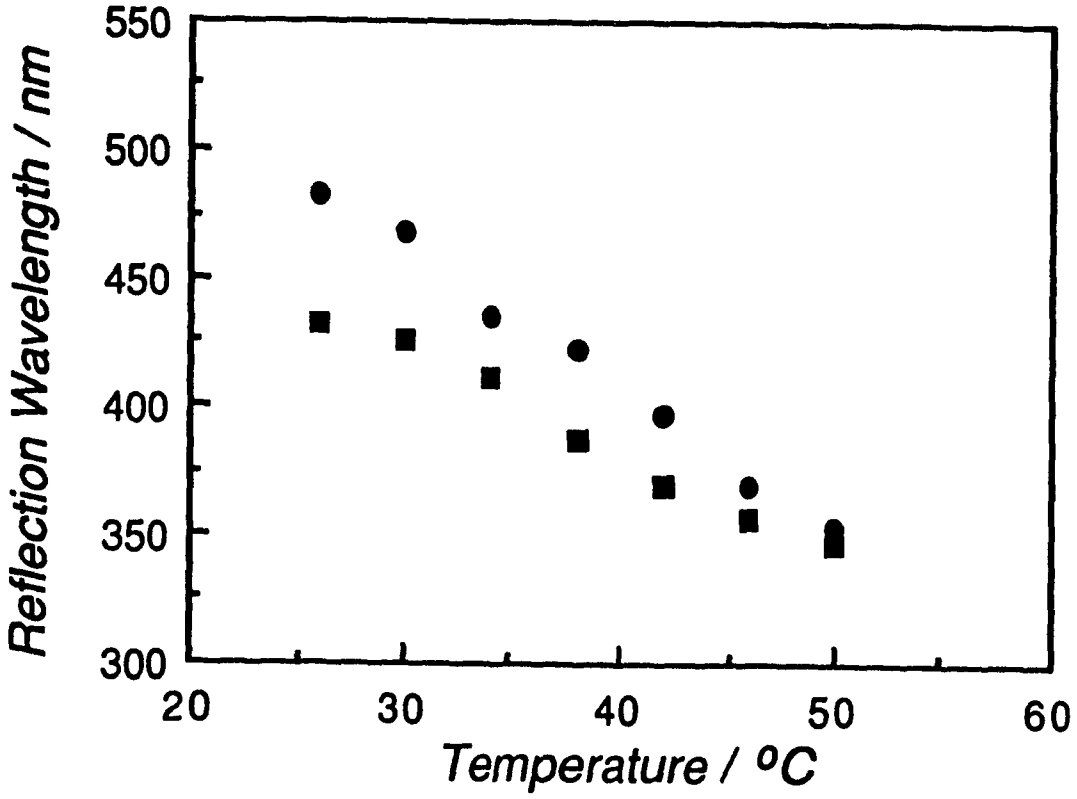

Figure 4.17 Effect of temperature on the reflection wavelength of EC / bromoform mesophases. DS = 2.29 (25.1% w/w, squares), DS = 2.80 (25.1% w/w, circles)

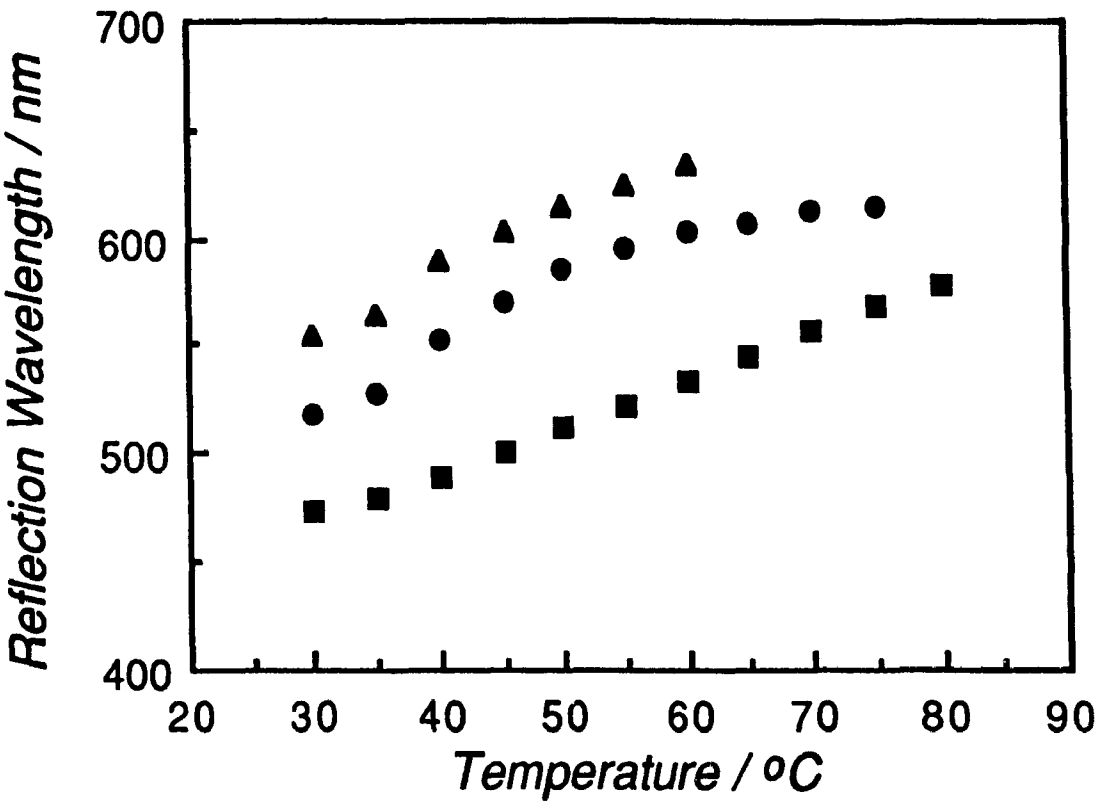

Figure 4.18 Effect of temperature on the reflection wavelength of EC / aqueous phenol mesophases. DS = 2.29 (50.9% w/w, squares), DS = 2.65 (50.9% w/w, circles) and DS = 2.80 (50.9% w/w, triangles).

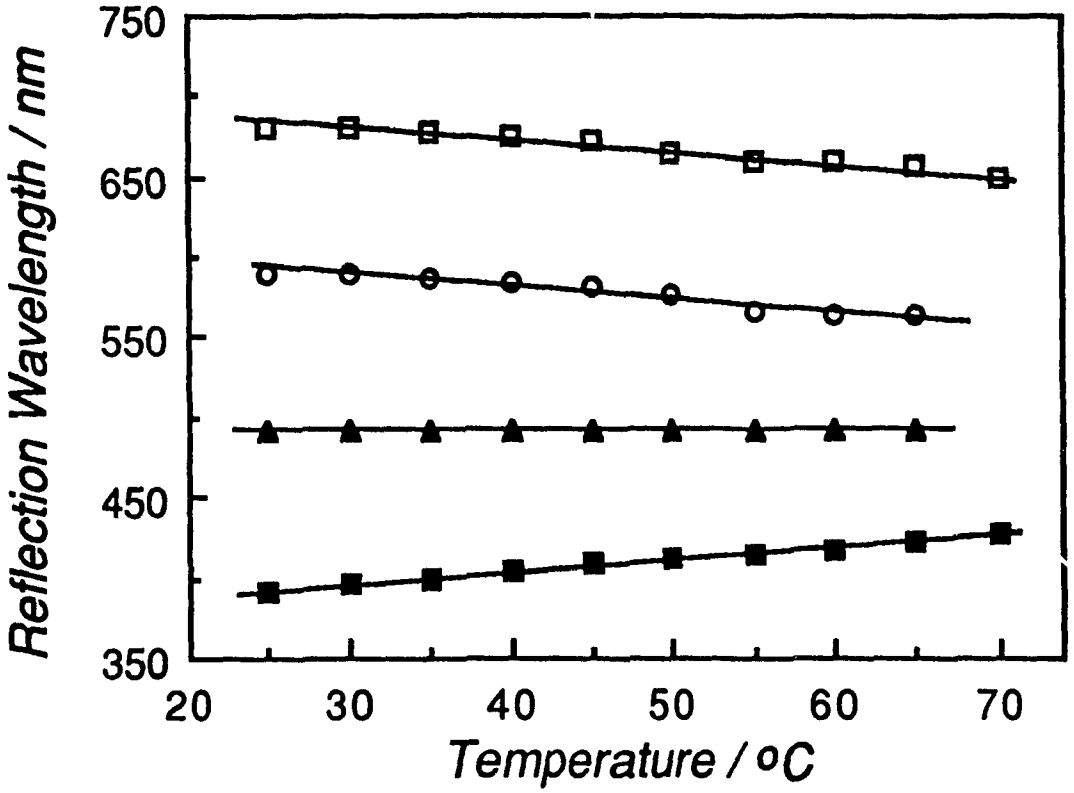

Figure 4.19 Effect of temperature on the reflection wavelength of EC / m-cresol mesophases. DS = 2.29 (54.4% w/w, squares), DS = 2.55 (54.4% w/w, triangles), DS = 2.65 (54.4% w/w, open circles) and DS = 2.80 (54.4% w/w, open squares). The lines indicate the trend of the data.

shows that not only is the DS responsible for determining the reflection wavelength of EC / m-cresol mesophases, but it also controls the sign of $d\lambda_0 / dT$. For samples with DS of 2.29 the reflection wavelength increases slightly with increasing temperature while the reflection wavelength decreases with increasing temperature for samples with DS of 2.70 and 2.80. The mesophase behaviour of EC at high DS in m-cresol now matches that of those solvents which decrease in reflection wavelength with increasing temperature for samples with DS of 2.29. At an intermediate DS of 2.55 the reflection wavelength is independent of temperature.

An interesting element of the effect of the DS on the reflection wavelength or twist sense of the mesophase and the temperature dependence of the reflection wavelength is the fact that the DS has a large effect on both of these parameters for EC in m-cresol and chloroform but has only a comparatively moderate effect on the EC / bromoform and EC / aqueous phenol mesophases. These results suggest that the forces responsible for determining the pitch and its temperature dependence are closely related. The original theories describing the formation of the cholesteric mesophase predicted that while chirality was necessary for cholesteric formation, the pitch was independent of temperature. Later theories resolved this inadequacy and found that the pitch could be affected in by variations in temperature. The interdependence of the pitch and the temperature is an important feature but the relevant topic of interest to the results found here is the prediction by Lin-Liu et al. (9, 10) that the manner in which the pitch is affected by temperature depends on the initial conditions of the mean field describing the potential function. Not only is the pitch a function of the initial conditions, but also the temperature dependence of the pitch can be similarly affected. It is therefore possible that the conditions responsible for the large increases in the pitch of EC mesophases that are observed with increases in the DS are also responsible for the variations in the temperature dependence of the pitch.

4.3.5 Other Alkyl Derivatives of Ethyl Cellulose

It is apparent from Section 4.3.4 that very high levels of substitution of

commercial grade EC by ethyl groups are required to change the cholesteric twist sense from left-handed to right-handed. Recent research has shown that twist sense reversal is also seen if acetyl groups are introduced onto the EC chain, but complete substitution is not required for the change to occur (51, 52). Given the effects of DCA and TFA on the twist sense of EC and CA, it is possible that the acetyl groups on the EC chain act in the same capacity as these solvents. However, it is also possible that the reversal in twist sense is related to the size of the substituent group or the total DS of the polymer. By introducing other alkyl groups onto the EC commercial sample, it is possible to assess whether the variation in cholesteric twist sense with increasing levels of substitution is related merely to the level of substitution of the EC chain or if the size of the alkyl substituent plays a role.

Introducing methyl groups onto the EC chain produces O-(ethyl)(methyl)cellulose (EMC) while the introduction of n-butyl groups gives O-(n-butyl)(ethyl)cellulose (BEC) (84). Table 4.5 lists the total DS of the samples examined and the cholesteric twist sense of their mesophases in three solvents.

Table 4.5

Cholesteric Twist Sense of EC, EMC and BEC Mesophases as a Function of DS

	Polymer (Total Degree of Substitution)					
Solvent	EC (2.29)	EC (3.00)	EMC (3.0)	BEC (2.6)	BEC (2.9)	BEC (3.0)
Chloroform	Left	Right	Left	Left	Left	Right
Dichloromethane	Left	Right	Left	Left	Left	Right
DCA	Right	Right	Right	-	-	Right

Table 4.5 shows that unlike the other trisubstituted derivatives, EMC in chloroform and dichloromethane establishes a left-handed mesophase. This suggests that the complete substitution of the hydroxyl groups is not necessarily sufficient to induce a reversal in twist change. For the BEC samples with total DS of 2.6, 2.9 and 3.0, only the trisubstituted derivative possesses a right-handed twist sense in chloroform and dichloromethane. While interpretations of the comparative effects of acetyl and ethyl

sidechains on the twist sense are limited due to large differences in the chemical nature of the substituents, it would appear that for the alkyl analogs, where the chemical behaviour is comparatively more uniform, the size of the substituent introduced onto the EC chain does play a role in determining the twist sense.

Given that DCA is the only known solvent in which EC with a DS of 2.29 forms a right-handed mesophase and the possibility exists that this is due to the interaction of the solvent with the hydroxyl groups, it is instructive to examine the effect of DCA on the trisubstituted derivatives where the possibility of hydroxyl group interaction is eliminated. Table 4.5 shows that like EC with DS of 2.29, EMC, tri-O-ethyl cellulose and BEC with total DS of 3.0 in DCA all produce right-handed cholesteric structures. These results are of particular importance to EMC because it means that the cholesteric twist sense for this polymer is truly solvent dependent; it forms a left-handed cholesteric mesophase in chloroform and dichloromethane and a right-handed one in DCA.

Solutions of EC with DS of 3.00 in DCA in the concentration range of 17.8% to 19.8% (w/w) are biphasic. Examination of these samples by CR spectroscopy found that the anisotropic regions of biphasic samples show the unusual feature of reflection colours (Figure 4.20) and that like the fully anisotropic samples these reflection wavelengths are sensitive to temperature (Figure 4.21). Only a small temperature range was investigated for the biphasic sample because the anisotropic regions rapidly turn isotropic with increasing temperature. The slight variation in the wavelength of the concentration dependence observed for other samples within the biphasic region is not unexpected as theory predicts that the high molar mass fractions of a sample should preferentially phase separate (85) and a relationship is known to exist between the reflection wavelength and molar mass (24, 53). (Samples at 19.3% and 19.8% concentration in Figure 4.20 are probably misplaced from the trend of the data because of degradation effects. Like CA in TFA, degradation of EC is a problem as the DCA solutions will turn black in a matter of days.) The phase rule states that an increase in the concentration of the anisotropic regions should not occur until the system is fully anisotropic which means that the liquid crystalline system is established with a well developed cholesteric structure already in place. This effect of visible reflection in the biphasic gap is noteworthy because most

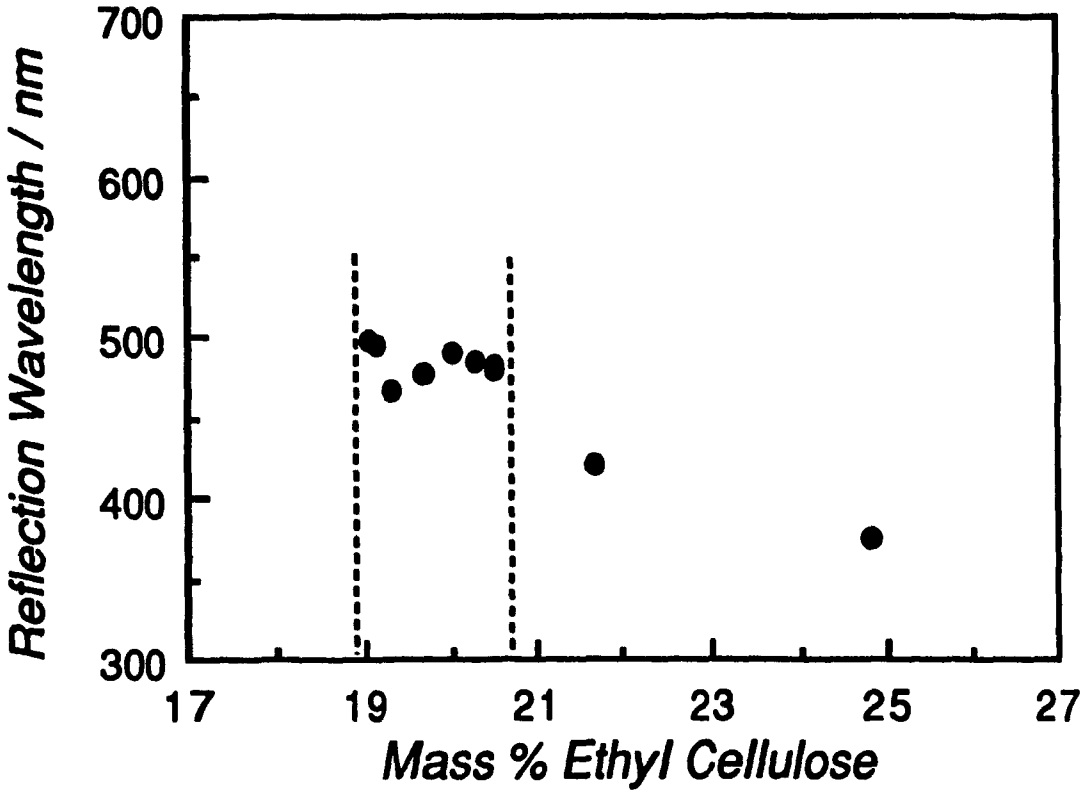

Figure 4.20 Variation of reflection wavelength with concentration for EC with DS of 3.00 in dichloroacetic acid. This system is unusual in that the anisotropic regions of the biphasic gap (indicated by the dashed lines) possess reflection colours.

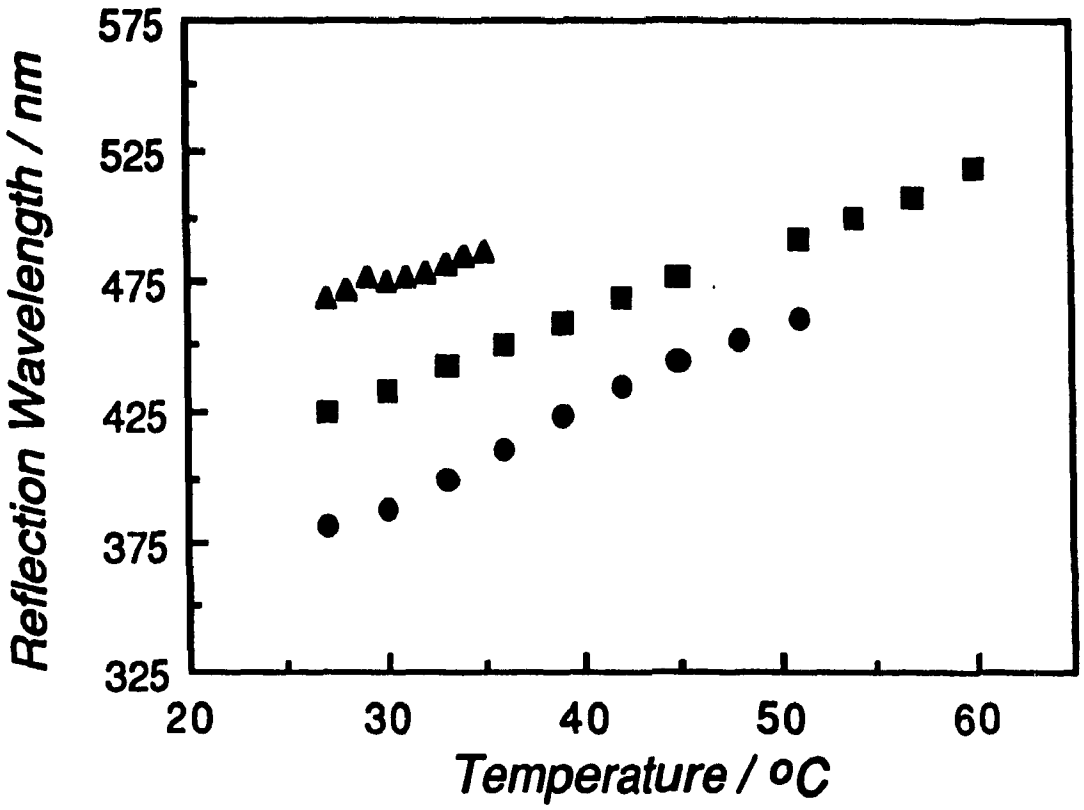

Figure 4.21 Response of the reflection wavelength to increasing temperature for mesophases of EC with DS of 3.00 in dichloroacetic acid. The 19.3% w/w sample (triangles) is biphasic while the 21.7% w/w (squares) and 24.9% w/w (circles) samples are fully anisotropic.

cholesteric systems phase separate initially as quasi-nematic structures that tighten into a cholesteric arrangements with increasing concentration. The fact that it is possible for a mesophase with reflection colours to establish itself at the inception of mesophase formation means that the chiral forces responsible for the twist are highly established in this polymer / solvent system.

4.3.6 Cholesteric Films of Trisubstituted EC Derivatives

Given the volatility of chloroform and the fact that EMC forms left-handed mesophases in this solvent while EC with DS of 3.00 and the trisubstituted BEC derivative form right-handed ones, it is possible to cast films of these polymers that possess "frozen-in" cholesteric structure. By observing the effect of temperature on these films it is possible to determine if a thermotropic or pseudo-thermotropic effect exists. The size of the sidechain in cellulose derivatives appears to play a role in determining whether the cellulosic compound is thermotropic. For example, Table 4.1 shows that all the cellulosics that possess large sidechains such as the ester or ether derivatives of HPC are capable of forming thermotropic liquid crystals with reflection colours. HPC appears to be at the borderline of pure thermotropicity as it does not produce reflection colours when heated in bulk form, but if cast from water to form films that possess right-handed cholesteric structure then these films will irreversibily increase their reflection wavelength with increasing temperature (46). One of the controlling features of HPC cholesteric films is the need to overcome intermolecular hydrogen bonding before an increase in reflection wavelength can occur. The trisubstituted EMC, EC and BEC polymers do not possess this hydrogen bonding restriction so these polymers allow an investigation into the ability of a cellulose derivative to behave as a pseudo-thermotropic as a function of twist sense and size of the sidechain substituents.

Figure 4.22 shows there is no change in the reflection wavelength of the cholesteric films of BEC as the temperature is increased up to the clearing temperature. Similar behaviour is also observed for tri-O-ethyl cellulose and EMC with the exception that the ellipticities of the EMC spectra are positive. The clearing temperatures of these

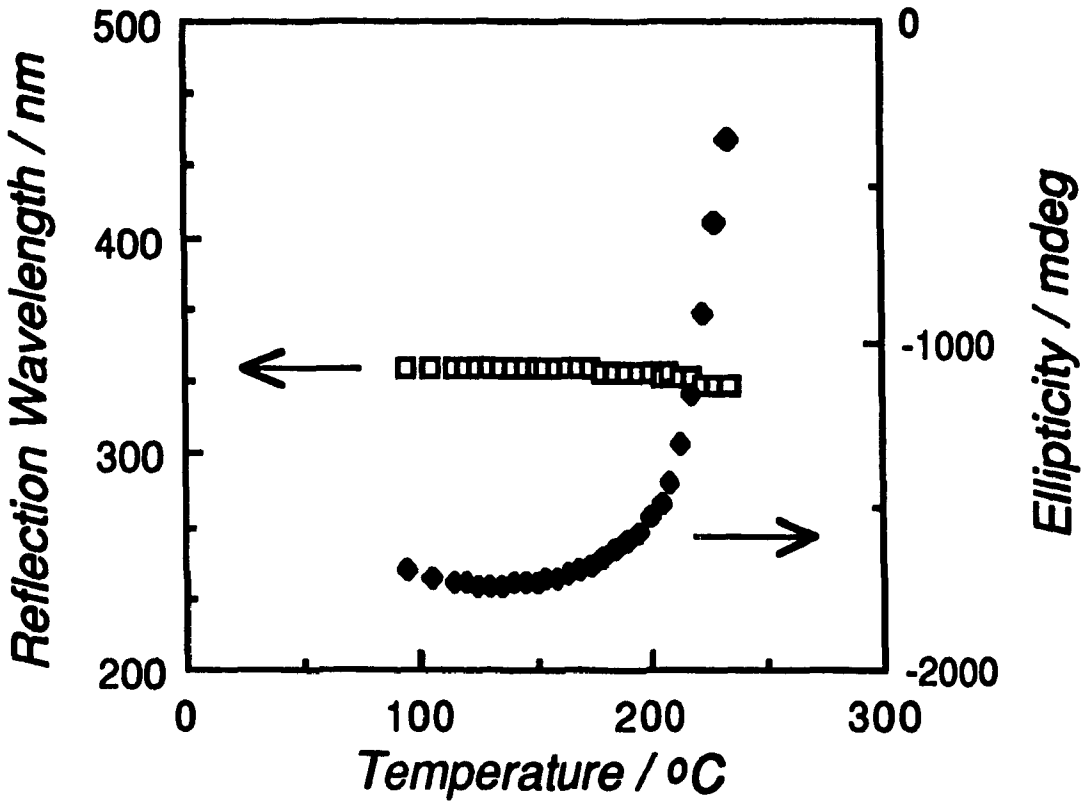

Figure 4.22 Effect of temperature on the reflection wavelength and ellipticity of the CRS peak for a cholesteric (butyl)(ethyl)cellulose film. The lack of response of the reflection wavelength to increasing temperature means that the sidechains of this cellulose derivative are not sufficiently large to induce thermotropic behaviour.

cholesteric films are identifiable by the sudden drop in the ellipticity of the CR spectra. It would therefore appear that even for the derivatives of EC in which hydrogen bonding does not exist, the sidechains of these derivatives are insufficiently large to induce pseudo-thermotropic behaviour.

4.3.7 The Search for a Polymeric Blue Phase

The previous sections of this chapter have shown that changes in temperature can produce a variety of behaviours in EC mesophases depending on the DS and solvent employed. An interesting effect of temperature on the structure of low molar mass cholesteric liquid crystals that can sometimes be observed just below their clearing temperatures is the production of a unique stable structure called the "blue phase" (86, 87, 88, 89). The clearing temperature of a liquid crystal is considered to be the temperature at which the forces responsible for orienting the liquid crystal components are just exceeded by the destructive influences of the components' vibrational, translational and rotational motions. When this temperature is reached the oriented system collapses to an isotropic state. For nematic liquid crystals the change from an oriented system to a disordered one is direct, but for many low molar mass cholesteric liquid crystals the blue phase is encountered. The blue phase was first identified as a stable oriented system which is not equivalent to the cholesteric phase in 1906 by Lehmann (90). Blue phase is a trivial name that was applied because of one of the optical properties that appears to be characteristic of the medium; selective reflection of light in the visible region, usually in the blue end of the spectrum. The other optical properties associated with blue phases are high optical activity and the absence of birefringence. The structure of the blue phase is still unresolved, but cubic structures derived from highly chiral cholesteric structures have been most commonly postulated (88). Any complete theory of the blue phase structure must account for both the absence of birefringence and the cholesteric-like reflection of the phase.

To date, no chiral polymer has been found to exhibit a blue phase. There are two main reasons for this: (i) many chiral polymers that form cholesteric systems, such as

some polypeptides, frequently form only long pitch mesophases and there appears to be an upper limit to the pitch of a mesophase that can form a blue phase (88) and (ii) other polymers such as many cellulose derivatives and some polypeptides which form short pitch cholesteric systems increase in pitch with an increase in temperature thereby untwisting the cholesteric structure rather than tightening towards the highly chiral blue phase. A blue phase might therefore be expected for a short pitch cholesteric mesophase whose twist decreases with increasing temperature. EC meets these criteria.

The search for the blue phase was conducted using CR spectroscopy. An EC / chloroform mesophase, 47.6 % (w/w), in a sealed microslide was placed in the Mettler Hot Stage and the sample temperature was held at 40 ^{o}C for one day and then raised at the rate of 1 ^{o}C per day. This slow heating rate was chosen so that the long cellulosic chains would have the time to take up their equilibrium cholesteric conformation. The sample was scanned once each day until the clearing temperature of the mesophase was reached. At this point the temperature was reduced at the rate of 1 ^{o}C per day and the sample scanned until the cholesteric mesophase reformed. It was expected that the presence of the blue phase would be revealed by a CR spectrum that contained two peaks: one at shorter wavelength which corresponded to the residual cholesteric structure and the second at a longer wavelength which was the result of the presence of a blue phase (88). However, despite meeting the criteria listed above no evidence for the existence of a blue phase was found. Possible reasons why a blue phase might not be observed in this polymer system under the conditions employed include: (i) It does not or cannot exist; the polymer chains are so long that topological restraints may prevent the chains from rearranging themselves into the blue phase structure; (ii) The conditions employed were not sufficiently rigorous. For example, topological restraints may in fact only slow the formation of the phase but not prevent it. Another possibility is that because the blue phase is frequently encountered in only a small temperature region, the temperature intervals used here were too large.

4.3.8 The Search for Induced Optical Activity

In an attempt to discern why the unusual behaviour of many of the polymer / solvent systems described in the previous sections occurs, a technique was employed that involves adding an optically inactive dye to the cholesteric mesophases. When this technique has been applied to other polymers the dye has sometimes become optically active and the liquid crystal induced CD absorption bands of the dye molecule can be studied (91, 92, 93). This technique is employed because the electronic transitions of many polymers, including EC, are rarely directly accessible. While caution must be exercised when attempting to interpret the data due to the possibility of artifacts (94, 95) the technique holds the potential to provide useful conformational information. This method would appear to be attractive for EC mesophases because of the possibility of comparative examinations of any induced CD bands of the dye in different types of EC mesophases. For example, mesophases that respond differently to temperature based on solvent, such as the low DS EC sample in chloroform and m-cresol, and mesophases that differ only in DS but have different cholesteric twist senses such as EC of DS equal to 2.29 and 3.0 in chloroform, might induce different CD bands that could provide information about relative chain conformations in the various mesophases.

A major difficulty encountered with dissolving dyes in the EC mesophases was that most water soluble dyes show limited solubility in the solvents for EC employed in this study. Complete solubility is a prerequisite for a dye because if particulate matter is present then light scattered from the aggregates can produce artificial signals. An alternative approach that was explored was to use a reactive achiral dye and attach it to the backbone of the EC chain. The dye chromophores of the resultant EC derivative should in principle become optically active because they are attached to a chiral chain. By introducing a small number of dye molecules along the backbone the solubility problem previuosly described should be overcome and any absorption bands due to the dye can be examined by CD. After reaction with the dye, the polymer could then be fully ethylated and this would allow a study of all types of EC mesophases in terms of solvent effects and cholesteric twist sense. The dye employed, Reactive Blue 4, was attached to EC by

reaction in a THF / sodium hydride medium and gave the derivative shown in Figure 4.23. However, while mesophases of this polymer could be prepared there was no evidence found of any CD bands due to the dye. Presumably the dye molecules are so far physically removed from the chiral cellulose backbone that their orientations are effectively isotropic and therefore contribute nothing to the chiroptical spectrum.

Another approach involved incorporating a smaller molecular probe, 4-chloro-2-nitrobenzenesuphonyl chloride, onto the EC chain using N,N-dimethylacetamide and pyridine as the reaction medium. The hope was that the smaller molecule would be sufficiently close to the chiral backbone to become optically active. However, while only minor substitution occurred, the properties of this EC derivative compound were such that it would not form a mesophase in the solvents of interest and showed no CD peaks in the isotropic state.

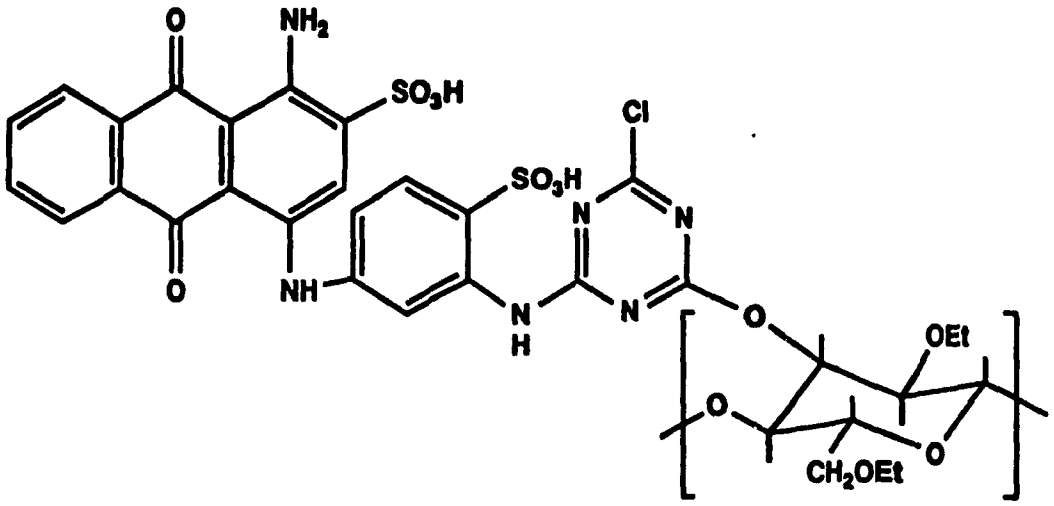

Figure 4.23 Monomer unit of an EC chain with attached Reactive Blue dye. In principle, the achiral dye should become optically active when attached to the chiral polymer backbone.

4.4 CONCLUSION

This chapter involved a study of the cholesteric structure of ethyl cellulose (EC) and several prepared EC derivative mesophases by studying the associated optical properties using a Circular Reflectance (CR) spectroscopy technique. A wide range of behaviour was found depending on the degree of substitution (DS), temperature and solvent employed. Although the cholesteric twist sense of commercial grade EC with DS of 2.29 is solvent dependent, the usual cholesteric twist sense is left-handed. The twist sense and temperature dependence of the reflection wavelength of EC mesophases are very sensitive to the DS and solvent employed. At a DS of 2.29 mesophases of EC in most solvents are left-handed, but at a DS of 3.00 the mesophases are right-handed in all solvents examined. For EC in solvents that do not change their twist sense, minor changes in DS strongly influence the reflection wavelength: left-handed EC mesophases increase in reflection wavelength as the DS is increased under constant conditions while right-handed mesophases decrease in reflection wavelength.

The temperature dependence of the reflection wavelength ($d\lambda_0 / dT$) of EC mesophases is also determined by the DS; for samples with DS of 2.29 the sign of $d\lambda_0/dT$ is determined by the solvent as both increases and decreases in pitch are observed despite the various mesophases possessing the same cholesteric twist sense. For EC with DS of 2.29 and 3.00 in chloroform the cholesteric twist senses are left-handed and right-handed, respectively, and the left-handed mesophase decreases in reflection wavelength with increasing temperature while the right-handed mesophase increases in reflection wavelength. For the EC / solvent systems that retain their left-handed twist sense with increasing DS, the sign of dP / dT remains the same as the DS is increased for mesophases of EC in bromoform and aqueous phenol, but dP/ dT changes from positive to negative for EC / m-cresol mesophases.

Mesophase samples of trisubstituted O-(ethyl)(methyl)cellulose (EMC), tri-O-ethyl cellulose and O-(n-butyl)(ethyl)cellulose (BEC) in chloroform were examined and it was determined that EMC forms a left-handed mesophase whereas TEC and BEC form right-handed ones. All these samples were found to form right-handed mesophases in

dichloroacetic acid (DCA). Examination of the biphasic region of tri-O-ethyl cellulose / DCA solutions by CR spectroscopy found that the anisotropic regions possess temperature sensitive reflection colours. Films of EC, EMC, TEC and BEC cast from chloroform solutions were found to possess frozen-in cholesteric structure and possess measurable CR peaks. These reflection peaks are insensitive to temperature up to their clearing temperatures.

4.5 REFERENCES

(1) P.N. Keating, *Mol. Cryst. Liq. Cryst.*, **8**, 315 (1969).

(2) B. Böttcher, *Chem. Ztg.*, **96**, 214 (1972).

(3) H.W. Gibson, "Liquid Crystals The Fourth State of Matter", (F. D. Saeva, ed.), Marcel Decker Inc., New York, 1979, pp. 99.

(4) W.J.A. Goossens, *Phys. Lett. A*, **31**, 413 (1970).

(5) A. Wulf, *J. Chem. Phys.*, **59**, 1487 (1973).

(6) W. Maier and A. Saupe, *Z. Naturforsch. A*, **14**, 882 (1959).

(7) H. Stegemeyer and H. Finkelmann, *Naturwissenschaften*, **62**, 436 (1975).

(8) H. Finkelmann and H. Stegemeyer, *Ber. Bunsenges. Phys. Chem.*, **82**, 1302 (1978).

(9) Y.R. Lin-Liu, Y.M. Shih and C.-W. Woo, *Phys. Rev. A*, **14**, 445 (1976).

(10) Y.R. Lin-Liu, Y.M. Shih and C.-W. Woo, *Phys. Rev. A*, **15**, 2550 (1977).

(11) T. Mori, *Polym. J.*, **17**, 1145 (1985).

(12) J. Watanabe and T. Nagase, *Macromolecules*, **21**, 171 (1988).

(13) Y.H. Kim, *J. Phys. (Paris)*, **43**, 559 (1982).

(14) H. Kimura, M. Hoshino and H. Nakano, *J. Phys. Soc. Jpn.*, **51**, 1584 (1982).

(15) A. Sikora, T.A. Siromyatnikova, B.M. Ginzburg, Y.A. Alumyan, A.A. Shepelevskii and S. Ya. Frenkel, *Die Makromol. Chem.*, **189**, 201 (1979).

(16) T.V. Samulski and E.T. Samulski, *J. Chem. Phys.*, **67**, 824 (1977).

(17) M.A. Osipov, *Chem. Phys.*, **96**, 259 (1985).

(18) HL. de Vries, *Acta Crystallogr.*, **4**, 219 (1951).

(19) D.M. Makow, *Color Res. Applic.*, **4**, 25 (1979).

(20) J.L. Fergason, *Mol. Cryst.*, **1**, 293 (1966).

(21) G.S. Chilaya and L.N. Lisetski, *Mol. Cryst. Liq. Cryst.*, **140**, 243 (1986).

(22) R.S. Werbowyj and D.G. Gray, *Mol. Cryst. Liq. Cryst.*, **34**, 97 (1976).

(23) S.-L. Tseng, A.Valente and D.G. Gray, *Macromolecules*, **14**, 715 (1981).

(24) G.V. Laivins and D.G. Gray, *Polymer*, **26**, 1435 (1985).

(25) S.-L. Tseng, G.V. Laivins and D.G. Gray, *Macromolecules*, **15**, 1262 (1982).

(26) S.N. Bhadani and D.G. Gray, *Mol. Cryst. Liq. Cryst.*, **99**, 29 (1983).

(27) S.N. Bhadani and D.G. Gray, *Mol. Cryst. Liq. Cryst.*, **102**, 255 (1984).

(28) A.M. Ritcey and D.G. Gray, *Macromolecules*, **21**, 1251 (1988).

(29) A.M. Ritcey, K.R. Holmes and D.G. Gray, *Macromolecules*, **21**, 2914 (1988).

(30) J. Lematre, S. Dayan and P. Sixou, *Mol. Cryst. Liq. Cryst.*, **84**, 267 (1982).

(31) J.-X. Guo and D.G. Gray, unpublished results.

(32) D.G. Gray, *J. Appl. Polym. Sci: Appl. Polym. Symp.*, **37**, 179 (1983).

(33) J.H.M. Willison and R.M. Abeysekera, *J. Polym. Sci.*, **26**, 71 (1988).

(34) H. Chanzy, A. Peguy, S. Chaunis and P. Monzie, *J. Polym. Sci., Polym. Phys. Ed.*, **18**, 1137 (1980).

(35) D.L. Patel and R.D. Gilbert, *J. Polym. Sci., Polym. Phys. Ed.*, **19**, 1231 (1981).

(36) C.L. McCormick, P.A. Callais and B.H. Hutchinson Jr., *Macromolecules*, **18**, 2394 (1985).

(37) Y.-S. Chen and J.A. Cuculo, *J. Polym. Sci., Polym. Phys. Ed.*, **24**, 2075 (1986).

(38) H. Baessler and M.M. Labes, *J. Chem. Phys.*, **52**, 631 (1970).

(39) M. Panar and L.F. Beste, *Macromolecules*, **10**, 1401 (1977).

(40) D.L. Patel and D.B. Dupré, *J. Chem. Phys.*, **72**, 2515 (1980).

(41) A.M. Ritcey, Ph.D. Thesis, McGill University, 1987.

(42) M. Panar and O.B. Willcox, Belgium Patent 656,359 (1976), German Federal Republic Patent 2,705,381(1977), France Patent 2,340,344 (1977).

(43) J. Maeno, United States Patent 4,132,464 (1979).

(44) S. Fortin and G. Charlet, *Macromolecules*, **22**, 2286 (1989).

(45) R.S. Werbowyj and D.G. Gray, *Macromolecules*, **17**, 1512 (1984).

(46) G. Charlet and D.G. Gray, *Macromolecules*, **20**, 33 (1987).

(47) A.M. Ritcey and D.G. Gray, unpublished results.

(48) H. Yokota, *Cellulose Chem. Technol.*, **20**, 487 (1986).

(49) P. Zugenmaier and P. Haurand, *Carbohydr. Res.*, **160**, 369 (1987).

(50) U. Vogt and P. Zugenmaier, *Ber. Bunsenges. Phys. Chem.*, **69**, 1217 (1985).

(51) J.-X. Guo and D.G. Gray, *Macromolecules*, **22**, 2082 (1989).

(52) J.-X. Guo and D.G. Gray, *Macromolecules*, **22**, 2089 (1989).

(53) M. Siekmeyer and P. Zugenmaier, *Die Makromol. Chem., Rapid Commun.*, **28**, 173 (1987).

(54) H. Steinmeier and P. Zugenmaier, *Carbohydr. Res.*, **173**, 75 (1988).

(55) W.A. Pawlowski, R.D. Gilbert, R.E. Fornes and S.T. Purrington, *J. Polym. Sci.: Part B*, **25**, 2293 (1987).

(56) T. Yamagishi, T. Fukuda, T. Miyamoto and J. Watanabe, *Cellucon Jpn. Proceed.*, in press.

(57) B.R. Harkness and D.G. Gray, *Macromolecules*, accepted for publication.

(58) B.R. Harkness and D.G. Gray, unpublished results.

(59) S. Ambrosino, T. Khallala, M. J. Seurin, A. Ten Bosch, F. Fried, P. Maissa and P. Sixou, *J. Polym. Sci.: Part C*, **25**, 351 (1987).

(60) Y. Nishio, Y. Fujiki and T. Takahashi, *Polym. Prep. (Jpn.)*, **37**, 457 (1988).

(61) K. Araki, Y. Iida and Y. Imamura, *Die Makromol. Chem., Rapid Commun.*, **5**, 99 (1984).

(62) S. Suto, H. Ise and M. Karasawa, *J. Polym. Sci.: Polym. Phys. Ed.*, **24**, 1515 (1986).

(63) S. Suto, S. Kimura and M. Karasawa, *J. Appl. Polym. Sci.*, **33**, 379 (1987).

(64) J. Bheda, J.F. Fellers and J.L. White, *Coll. Polym. Sci.*, **258**, 1335 (1980).

(65) S. Suto, J.L. White and J.F. Fellers, *Rheol. Acta*, **21**, 62 (1982).

(66) S. Suto, *J. Polym. Sci.: Polym. Chem. Ed.*, **22**, 637 (1984).

(67) S. Suto, M. Ohshiro, W. Nishibori, H. Tomita and M. Karasawa, *J. Appl. Polym. Sci.*, **35**, 407 (1988).

(68) Y. Nishio, S. Susuki and T. Takahashi, *Polym. J.*, **6**, 753 (1985).

(69) K. Kamide, K. Okajima, T. Matsui and S. Kajita, *Polym J.*, **18**, 273 (1986).

(70) Y. Huang, *J. Macromol. Sci.: B*, **28**, 131 (1989)

(71) W.R. Moore and A.M. Brown, *J. appl. Chem.*, **8**, 363 (1958).

(72) A.M. Ritcey, G. Charlet and D.G. Gray, *Can. J. Chem.*, **66**, 2229 (1988).

(73) CRC Handbook of Chemistry and Physics, (R. C Weast, ed.), CRC Press, Cleveland, 56th Edition 1976, pp. E-55.

(74) P.A. Patton and R.D. Gilbert, *J. Polym. Sci.: Polym. Phys. Ed.*, **21**, 1515 (1983).

(75) R.D. Gilbert and R.E. Fornes, *J. Polym. Sci.: Polym. Phys. Ed.*, **27**, 1949 (1989).

(76) C. Robinson, *Tetrahedron*, **13**, 219 (1961).

(77) H. Toriumi, S. Minakuchi, Y. Uematsu and I. Uematsu, *Polym. J.*, **12**, 431 (1980).

(78) H. Toriumi, Y. Kusumi, I. Uematsu and Y. Uematsu, *Polym. J.*, **11**, 836 (1979).

(79) J.B. Milstien and E. Charney, *Biopolymers*, **9**, 991 (1970).

(80) D.B. Dupré and R.W. Duke, *J. Chem. Phys.*, **163**, 143 (1975).

(81) K. Czarniecka and E.T. Samulski, *Mol. Cryst. Liq. Cryst.*, **63**, 205 (1981).

(82) H. Toriumi, S. Minakuchi and I. Uematsu, J. *Polym. Sci.: Polym. Phys. Ed.*, **19**, 1167 (1980).

(83) "Ethyl Cellulose - Properties and Uses", Hercules Powder Co., Wilmington, Del., 1962.

(84) Chapter 2, this thesis.

(85) P.J. Flory and A. Abe, *Macromolecules*, **11**, 1119 (1978).

(86) P.P. Crooker, *Mol. Cryst. Liq. Cryst.*, **98**, 31 (1983).

(87) K. Bergmann and H. Stegemeyer, *Ber. Bunsenges. Phys. Chem.*, **82**, 1309 (1978).

(88) H. Stegemeyer, Th. Blümel, K. Hiltrop, H. Onusseit and F. Porsch, *Liq. Cryst.*, **1**, 3 (1986).

(89) TK. Brog and P.J. Collings, *Mol. Cryst. Liq. Cryst.*, **60**, 65 (1980).

(90) O. Lehmann, *Z. Phys. Chem.*, **56**, 750 (1906); as reported by H. Stegemeyer, Th. Blümel, K. Hiltrop, H. Onusseit and F. Porsch, *Liq. Cryst.*, **1**, 3 (1986).

(91) F.D. Saeva and J.J. Wysocki, *J. Am. Chem. Soc.*, **93**, 5928 (1971).

(92) E. Sackmann and J. Voss, *Chem. Phys. Lett.*, **14**, 528 (1972)

(93) F.D. Saeva and G.R. Olin, *J. Am. Chem. Soc.*, **95**, 782 (1973).

(94) Y. Shindo and Y. Ohmi, *J. Am. Chem. Soc.*, **107**, 91 (1985).

(95) Y. Shindo, M. Nakagawa and Y. Ohmi, *Appl. Spectrosc.*, **39**, 860 (1985).

CHAPTER 5

OPTICAL ROTATORY DISPERSION STUDIES

5.1 INTRODUCTION

A Circular Reflectance spectroscopy study of mesophases of ethyl cellulose (EC) and some of its derivatives demonstrated that the effects of degree of substitution (DS) and solvent type are significant in determining the liquid crystalline properties (1). A natural extension of this line of research is to examine the Optical Rotatory Dispersion (ORD) spectra of isotropic and anisotropic solutions of EC.

5.1.1 ORD Studies of Isotropic Solutions

Isotropic solutions of chiral molecules possess an inherent optical activity due to the chromophores of the individual molecules. The optical activity of an isolated chromophore has been described by Drude (2) who related the specific optical rotation, $[\alpha]$, to the wavelength of the incident light, λ, by Equation [5.1].

$$[\alpha] = \frac{A}{\lambda^2 - \lambda_o^2} \qquad [5.1]$$

where λ_0 is the wavelength of the absorption maximum and A is a constant. Equation [5.1] is considered to be valid at wavelengths far removed from λ_0. The major feature of an ORD spectrum for an isotropic solution is a sudden reversal in the sign of the optical rotation as the wavelength of the incident light traverses the wavelength of the absorption maximum (Figure 1.9). This anomaly is known as a Cotton Effect. In contrast to Circular Dichroism (CD) signals, ORD signals persist at wavelengths far removed from λ_0. For wavelengths longer than λ_0 a positive (negative) ORD curve that rises (falls) monotonically from long to short wavelengths is called a plain positive (negative) ORD curve. Based on Equation [5.1] a plot of $[\alpha]\lambda^2$ versus $[\alpha]$ is called a Drude plot and is predicted to be linear; the slope of the plot corresponds to the square of λ_0.

If an interaction of chromophores exists due to molecular helicity then more complex ORD spectra are observed. In this case the CD and ORD spectra are anomalous (Figure 5.1) and the relationship derived by Moffitt and Yang (3) is used to relate $[\alpha]$ and λ (Equation [5.2]).

$$[\alpha]_\lambda = \frac{100}{M}\left[(a_0)\frac{\lambda_0^{\,2}}{\lambda^2-\lambda_0^{\,2}} + (b_0)\frac{\lambda_0^{\,4}}{(\lambda^2-\lambda_0^{\,2})^2}\right] \qquad [5.2]$$

where M = the molar mass per monomer residue
a_0 = a nonexciton constant
b_0 = an exciton constant.

The anomalous curve shapes are the result of a splitting of the excited state into two energy levels each of which gives a Cotton Effect of opposite sign. Summation of these curves produces the complex curves shown in Figure 5.1. A Moffitt-Yang plot, ([α] M / 100) $(\lambda^2 - \lambda_0^2) / \lambda_0^2$ versus $\lambda_0^2 / (\lambda^2 - \lambda_0^2)$, is predicted to be linear for these anomalous spectra.

If a molecule has only a single major electronic transition that dominates the accessible part of the spectrum then an examination of an isotropic solution by ORD affords the possibility of discerning the wavelength of the major electronic transition of that molecule even if direct measurement of λ_0 is impossible. The fact that this can be accomplished at wavelengths far removed from λ_0 means that the technique can supply information not generally available through direct CD measurement.

5.1.2 ORD Studies of Anisotropic Solutions

In Chapter 4.1.2 it was reported that de Vries (4) had derived the relationship between the optical properties of a cholesteric liquid crystal and its physical structure. As part of this theory de Vries also described the relationship between the optical rotation of plane polarized light, α, and the wavelength of the incident light for a planar cholesteric liquid crystal (Equation [5.3]).

$$\alpha = -\frac{\pi \Delta n^2 b P}{4\lambda^2[1 - (\lambda / \lambda_0)]} \qquad [5.3]$$

where Δn = layer birefringence
b = thickness of sample
P = pitch.

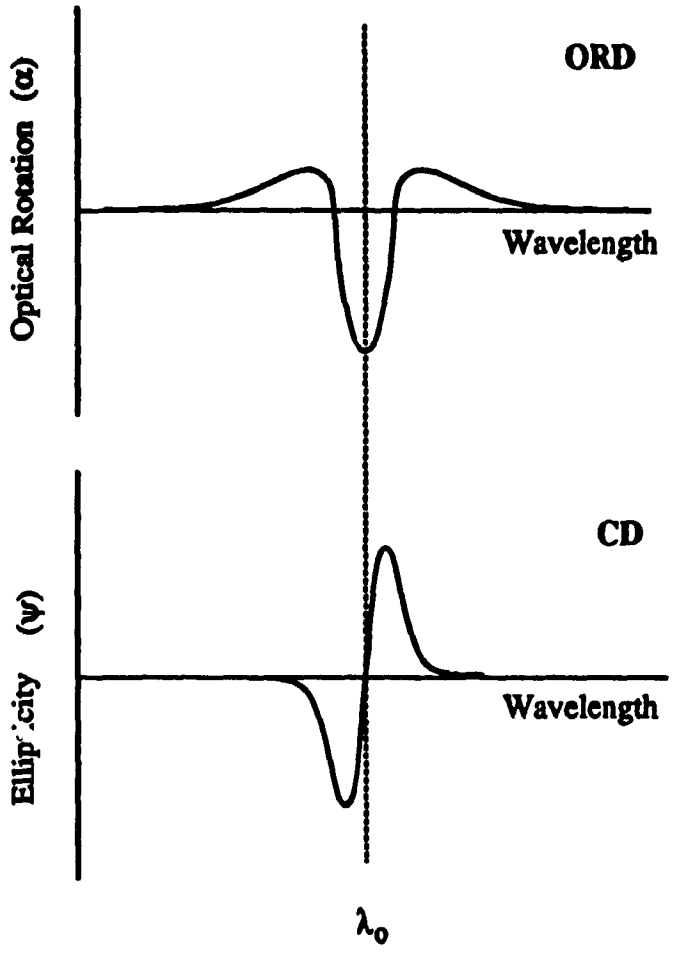

Figure 5.1 Typical ORD and CD spectra for chromophores in a helical environment. Compare with Figure 1.9. The ORD signal persists at wavelengths far removed from λ_0 which makes it an attractive technique for investigating chiral absorptions that are obscured by optically opaque solvents.

Equation [5.3] shows that like isotropic solutions, the optical rotation of a cholesteric liquid crystal is also sensitive to the difference of the squares of the wavelength of the incident light wave and the absorption maximum corresponding to the pitch, so like the Cotton Effect seen in isotropic media, an anomaly also exists for the ORD spectra of cholesteric liquid crystals. This type of anomaly is called a pseudo-Cotton Effect.

5.1.3 Cellulose Derivatives

Recent research into the origin of the observed ORD curves of unsubstituted monosaccharides has been pursued primarily by the use of vacuum-ultraviolet CD (UVCD). These studies have determined that the transitions occurring in the range of 160 - 185 nm contribute little or nothing to the ORD signal observed at higher wavelengths and that it is the electronic transition at ~150 nm that dominates the ORD spectrum at higher wavelengths (5, 6). Cellulose acetate (CA) films with isotropic ordering have been examined by UVCD and have been found to possess strong electronic transitions at 195 nm and ~160 nm (7). The transition at 195 nm is due to the acetate moiety. When the degree of substitution (DS) of the CA is decreased, the ellipticity of the acetate band decreases but there is no corresponding appearance of an electronic band due to the hydroxyl groups. This result is interpreted as meaning that despite being attached to a chiral backbone, the orientations of the hydroxyl groups are effectively isotropic and they therefore not sensitive to chiroptical techniques. Isotropic solutions of (hydroxypropyl) cellulose in methanol have recently been examined and based on Drude plots have been calculated to possess a transition at ~175 nm (8). This electronic absorption is assigned to an $n \rightarrow \sigma^*$ transition of the lone pair of electrons on the ring and linkage oxygen atoms. Other electronic transitions for the cellulose backbone bonds such as those associated with C-C and C-H bonds are of higher energy and occur at much shorter wavelengths than those of the oxygen atom lone pair electrons (5, 6). It therefore appears that there is a single dominating influence in the observable ORD spectrum of an isotropic cellulose ether.

At present it is not known which features of the cellulose derivative or solvent are responsible for the cholesteric twist sense or temperature dependence of the mesophase structure. As was demonstrated in Table 4.1 and in Chapters 3 and 4, very closely related cellulose derivatives or even a single cellulose derivative in different solvents can have markedly different liquid crystalline properties. Although limited in its application to isotropic solutions of cellulose derivatives because it cannot scan the wavelengths where electronic absorptions occur, conventional ORD spectroscopy has previously offered some interesting insights into the solution and liquid crystalline behaviour of polybenzyl-L-glutamate (PBLG) (9). This study examines the ORD spectra of isotropic and anisotropic EC solutions in several solvents to determine the effect of concentration, solvent, DS and temperature on the solution properties.

5.2 EXPERIMENTAL

ORD spectra were recorded with a modified Jasco ORD / UV-5 Spectrometer. The sample cells for isotropic measurements were 1 cm quartz cells. When required, a 9 mm spacer was used to reduce the thickness of the 1 cm cells to 1 mm. Quartz plates with 0.1 mm spacer were used for anisotropic measurements. When temperature control was required, a jacketed 1 cm quartz cell attached to a water recirculation bath was employed. The samples employed include those listed in Table 2.2.

5.3 RESULTS AND DISCUSSION

5.3.1 Isotropic Solutions

As all the solvents employed for EC in this study are spectrally opaque until wavelengths far above the anticipated λ_0 of EC, ORD is the best chiroptical technique for investigating the isotropic solutions of EC.

5.3.1.1 Effect of Solvent and Temperature

Figure 5.2 shows that both complex positive and plain negative ORD curves may be obtained for isotropic solutions of EC with a DS of 2.29 depending on the solvent employed. In m-cresol, aqueous phenol and dichloroacetic acid (DCA) plain negative dispersion curves are found while for chloroform, acetic acid, pyridine and dichloromethane positive dispersion curves are found. CA is also reported to have solvent dependent curve shapes (10), but this polymer has two electronic transitions contributing to the observed ORD signal and the sign of the acetate CD band of CA is known to be solvent dependent (8), so the anomalous ORD curves may be the result of variations in the sign and signal strength of the individual transitions. The question therefore arises as to what is the cause of these variations in the ORD curve shapes of EC where only a single band should contribute to the observed spectrum: is it a purely a structural effect or is some other mechanism at work? Whereas a Drude plot for the ORD spectrum of EC with DS of 2.29 in chloroform (Figure 5.3) is not linear, which suggests that the polymer is not in a random configuration, a Moffitt - Yang plot is linear when λ_0 is taken as 150 nm (Figure 5.4). Linear Moffitt - Yang plots of an ORD curve that have only a single band contributing to the observed signal are usually indicative of exciton coupling which is considered to be a feature of a helical structure. Figure 5.5 shows that the optical rotation of the EC solutions are affected by temperature, but while the optical activity of a polymer in a helical form would be expected to be sensitive to temperature these data do not prove the existence of a helical conformation for EC in chloroform because the anomalous curve does not change to a plain dispersion curve when the temperature is increased to 50 °C. An increase in temperature should cause a disruption

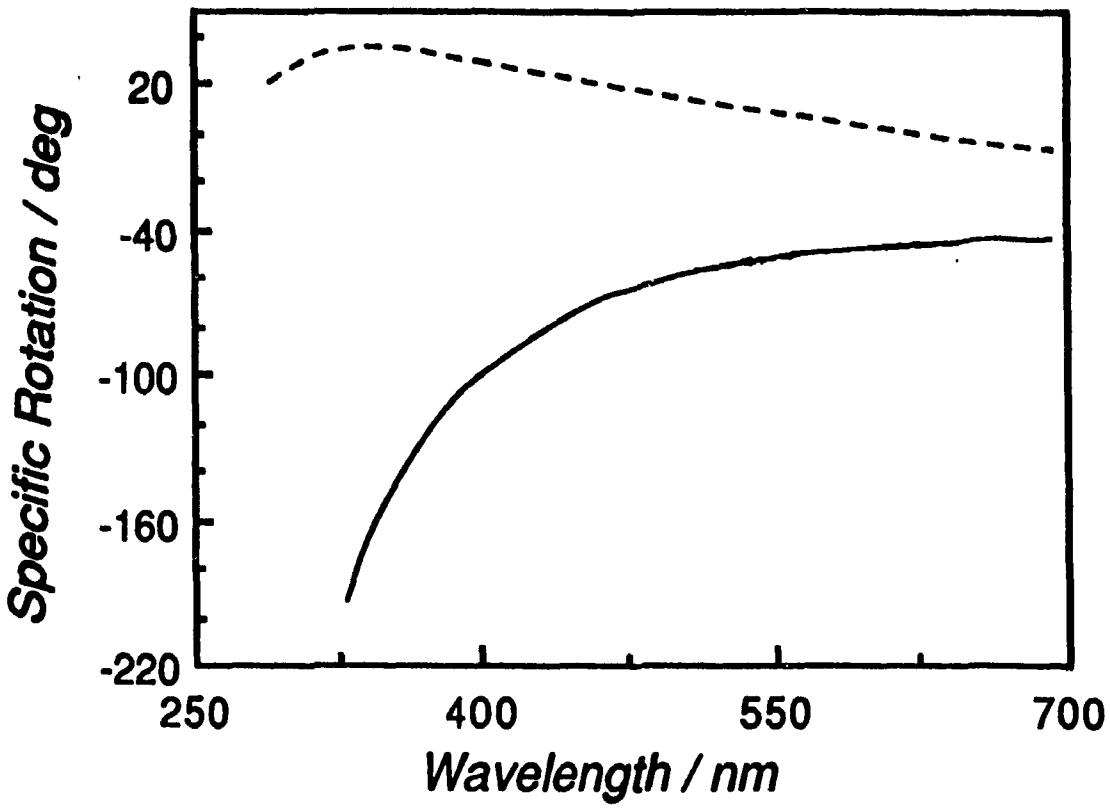

Figure 5.2 ORD curves for EC with DS of 2.29 in chloroform (2.0% w/w, dashed line) and in m-cresol (2.0% w/w, solid line). The ORD curve for EC in chloroform is anomalous while that for EC in m-cresol is plain negative.

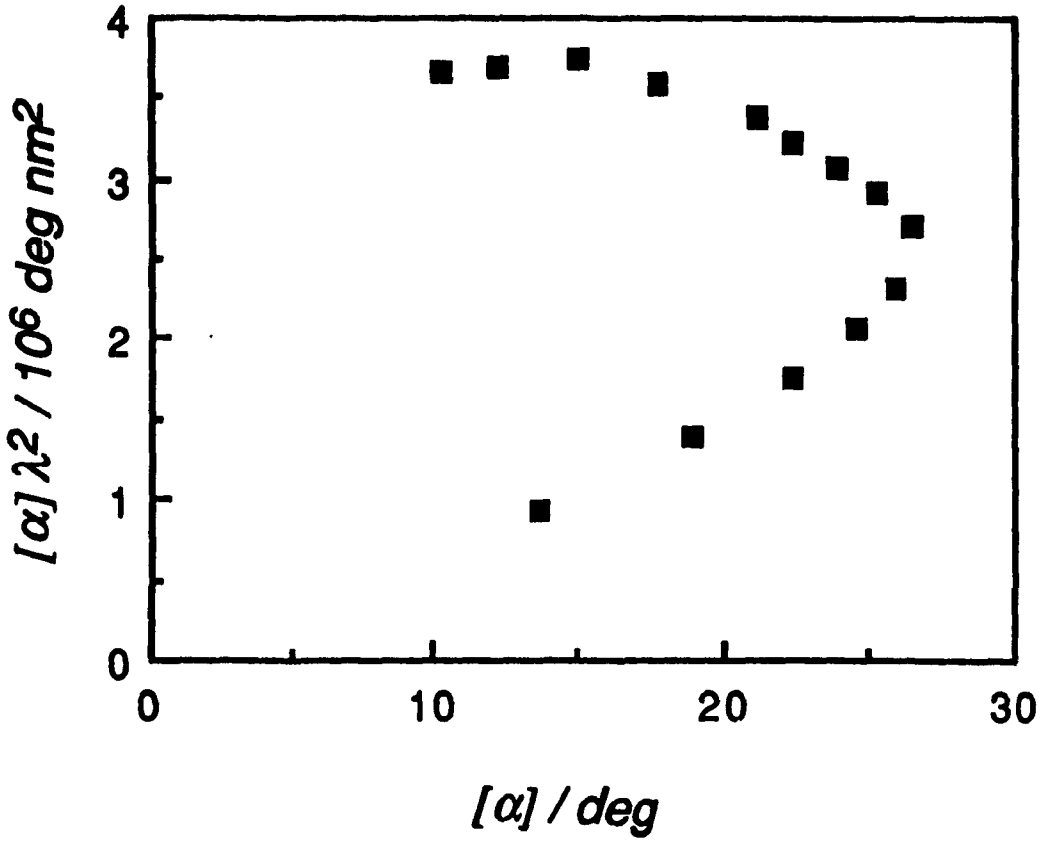

Figure 5.3 Drude plot for EC with DS of 2.29 in chloroform (2.0% w/w). The extreme nonlinearity of the plot suggests that EC is not in a random coil configuration.

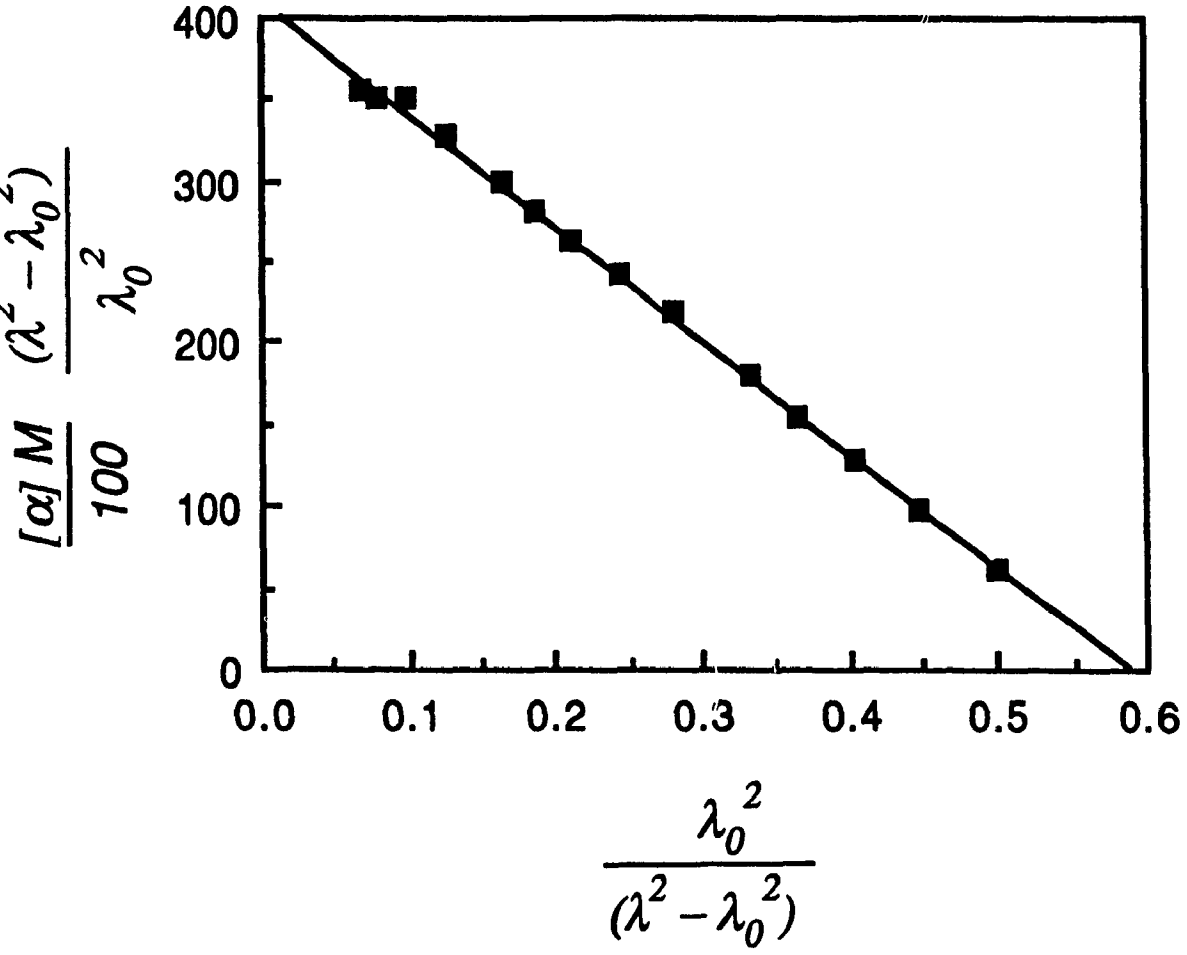

Figure 5.4 Moffitt-Yang plot for EC with DS of 2.29 in chloroform (2.0% w/w). Linear Moffitt-Yang plots are usually considered to be due to contributions to optical activity from chromophores in a helical environment.

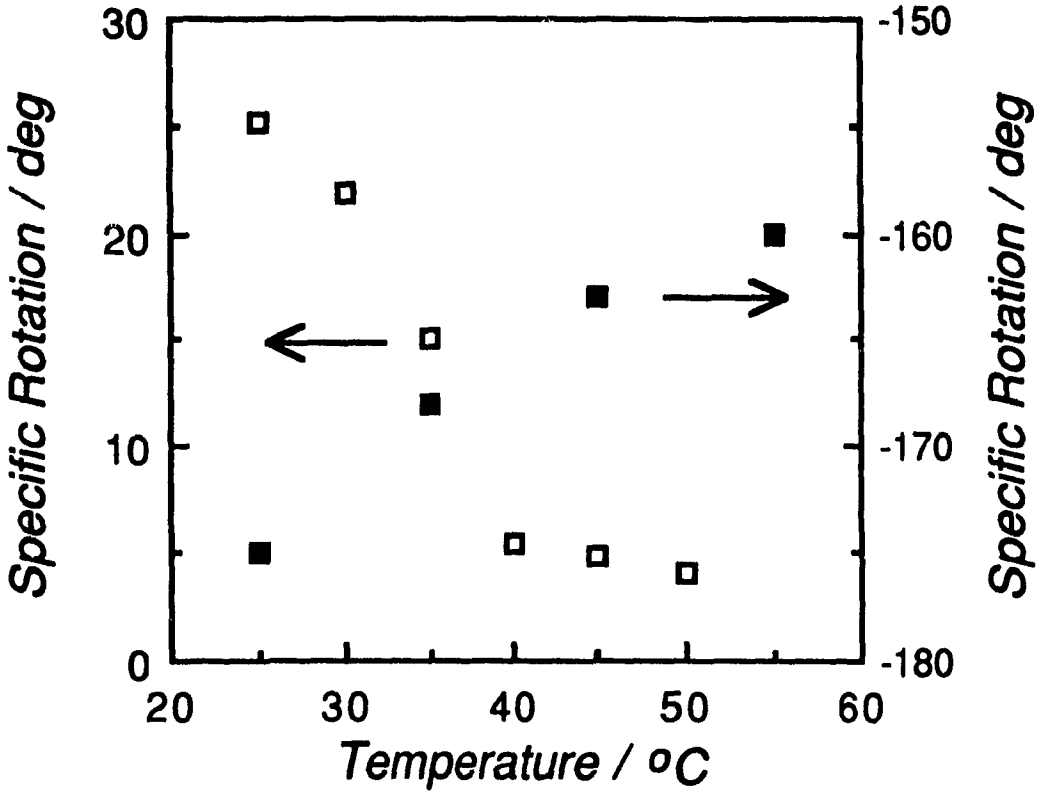

Figure 5.5 The effect of temperature on the optical activity (λ = 320 nm) of EC with DS of 2.29 in chloroform (2.0% w/w, open squares) and EC in m-cresol (2.0% w/w, closed squares). EC in chloroform still exhibits postive dispersion curves at elevated temperatures.

of the helix and a collapse to a less ordered structure. A change from an anomalous to a plain dispersion curve would be expected for a collapse of the helix as the exciton contributions to the optical activity would be lost. Further evidence suggesting that a helical structure does not exist for EC in chloroform is that if the helix did exist then it would have to be well established to survive at a temperature of 50 °C and thus would be expected to be very stiff at room temperature. This would be dramatically reflected in dilute solution viscosity measurements but it has already been demonstrated that the calculated molecular dimensions and the predicted and observed liquid crystalline phase separation volume fractions are in approximately the same range for those solvents in which EC produces both anomalous and plain negative dispersion spectra (11).

A possible explanation for the origin of the anomalous curves is that the solvent itself may interact with the chiral polymer chain to such an extent that it becomes slightly optically active and introduces a new chromophore to the chiroptical spectrum. The possibility of solvent interaction with the polymer would also appear to be the case for solutions of EC with DS of 2.29 in m-cresol as the Drude plot gives a calculated λ_0 value for EC of ~223 nm (Figure 5.6). This value is much higher than the anticipated value of 150 - 160 nm. The aromatic chromophore of m-cresol is a strongly absorbing species so only a minor chiroptical contribution from this solvent would be required to produce this effect.

The possibility of solvent interaction with EC was discussed in Chapter 4.3.1 as a potential reason for the nonviability of a dielectric theory (12) that attempts to relate the cholesteric twist sense of lyotropic mesophases to the solvent employed. The results found here suggest that this solvent interaction may, in fact, exist for solutions of EC. As the dielectric theory works on the assumption of noninteraction between solvent and polymer, its inability to differentiate between the various twist senses of the EC mesophases could be attributed to solvent interaction effects that affect the values of the dielectric constants of the polymer in solution.

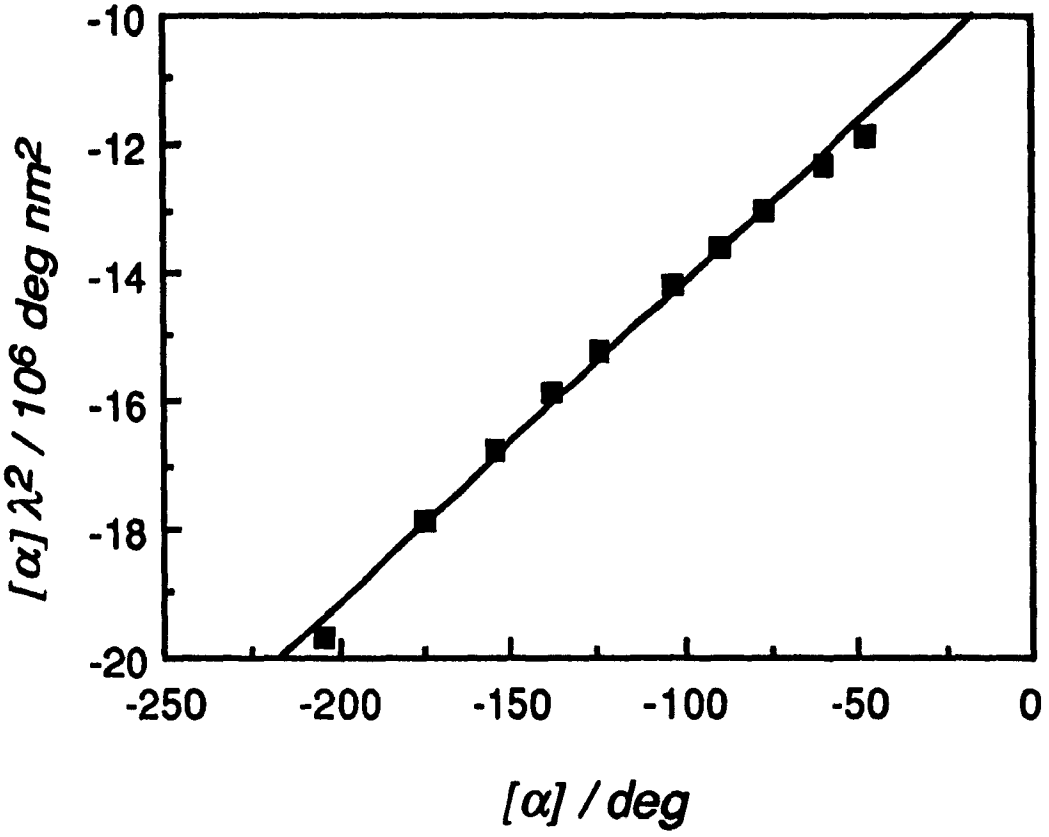

Figure 5.6 Drude plot for EC with DS of 2.29 in m-cresol (2.0% w/w). The wavelength of maximum absorption calculated from this plot is ~223 nm. This value is higher than the expected value of 150 to 160 nm. An induced optical activity effect involving the solvent may be responsible.

5.3.1.2 Effect of Degree of Substitution

It was reported that minor changes in the DS can have significant effects on the liquid crystalline properties of EC (1). The feature that is of interest here is the effect of the complete substitution of the hydroxyl groups by ethyl substituents on the ORD spectra of isotropic solutions. Removal of the unreacted hydroxyl groups eliminates a potential source of solvent interaction. Figure 5.7 shows that the intensity of the optical rotation of EC in chloroform is diminished by an increase in the DS but that the ORD spectrum is still positive. This suggests that there are no major conformational changes as a function of DS.

For EC in m-cresol, the intensity of the specific optical rotation is also affected by the DS (Figure 5.8), but a Drude plot of a 2% solution of EC with DS of 3.00 in m-cresol shows that the calculated value of λ_0 is ~218, still far above the anticipated value. This suggests that if an interaction between solvent and polymer does exist then it is not occur through an association with the hydroxyl groups of the EC chain.

5.3.2 The Search for a Pretransitional Effect

It was reported that EC with DS of 3.00 (TEC) in DCA forms a mesophase with a well developed cholesteric structure already in place (1). As the impetus for the development of the cholesteric twist is related to the chirality of the component molecules, the question that arises is does TEC in DCA form a liquid crystal with a cholesteric order already in place because of a pretransitional ordering of the molecules? Polybenzyl-L-glutamate (PBLG) has been found to show an ordering of its molecules at a concentration below that of its critical concentration for mesophase formation (10). At this concentration the PBLG solutions show an absence of birefringence but possesses high optical rotatory powers. ORD is an ideal technique to follow the optical rotation of a polymer as a function of concentration. Figure 5.9 shows the specific rotation of the TEC / DCA system as a function of concentration. It can be seen that there is no apparent increase in the specific optical rotation just below the critical concentration for mesophase formation. This means that there is no evidence for a pretransitional effect.

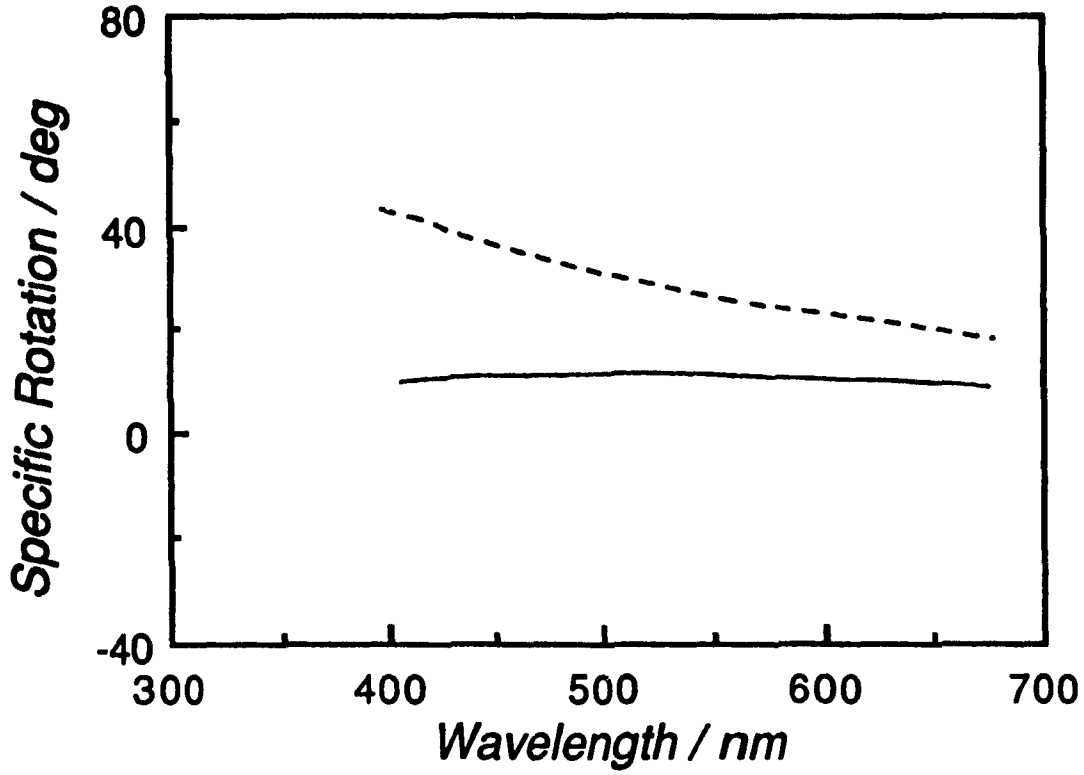

Figure 5.7 The effect of DS of the optical activity of EC in chloroform. EC with DS of 2.29 (4.1% w/w, dashed line) and EC with DS of 3.00 (4.1% w/w, solid line).

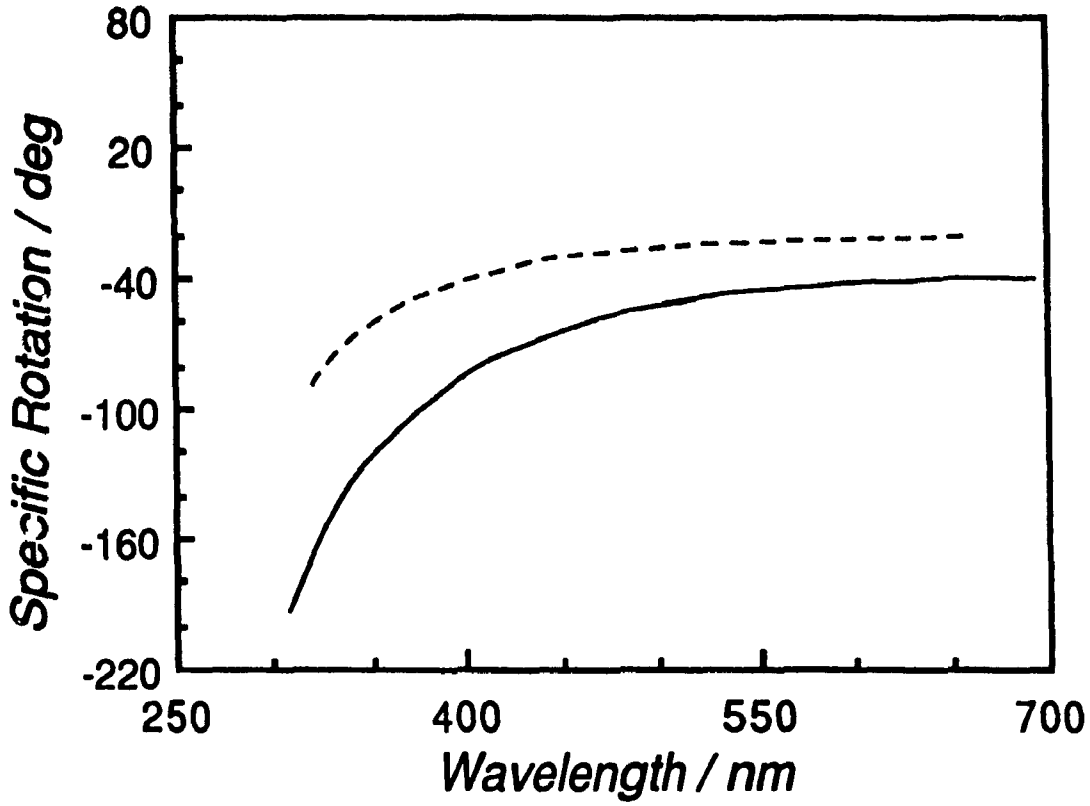

Figure 5.8 The effect of DS of the optical activity of EC in m-cresol. EC with DS of 2.29 (2.0% w/w, solid line) and EC with DS of 3.00 (2.0% w/w, dashed line).

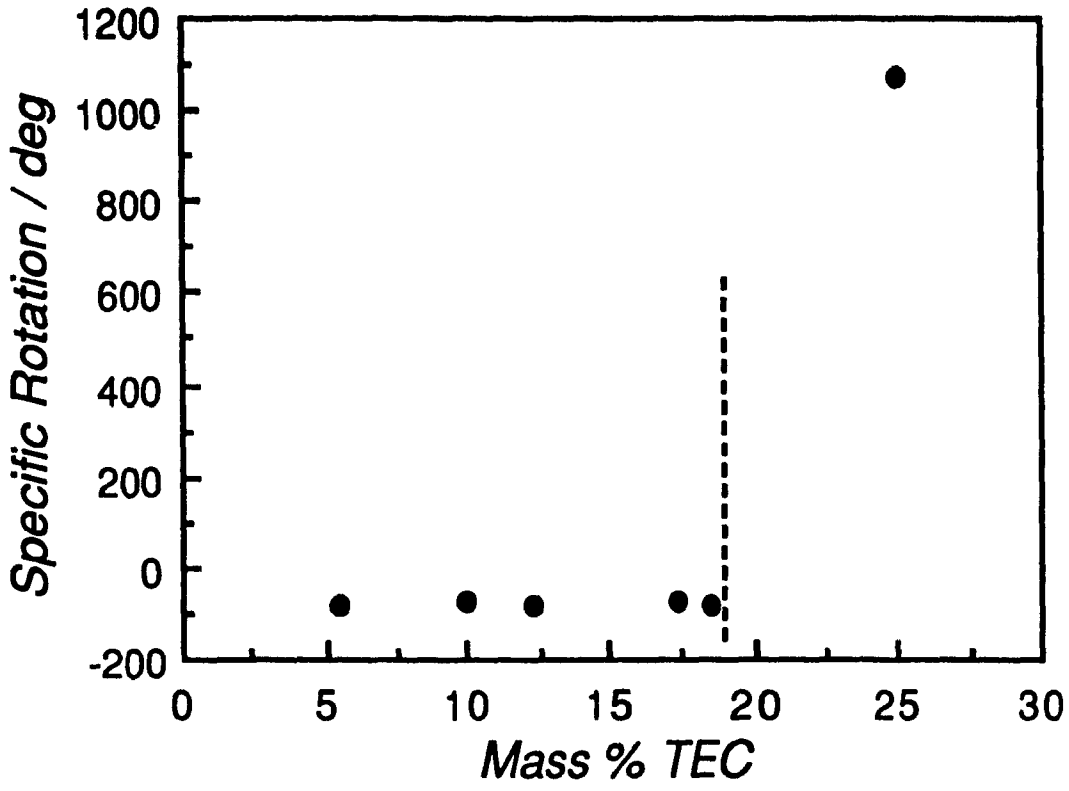

Figure 5.9 The effect of concentration on the specific optical activity of EC with DS of 3.00 in dichloroacetic acid. The absence of an increase in the optical activity at a concentration just below the critical concentration (dashed line) means that a pretransitional ordering of the molecules does not occur.

5.3.3 Anisotropic Solutions

ORD is frequently employed to assign the cholesteric twist sense of a liquid crystals with a pitch above the visible region of the spectrum. Twist sense assignment by ORD curve tailing is a function of the sign of the ORD spectrum; if the curve tailing is positive (negative) then the cholesteric twist sense is left-handed (right-handed). However, as previously discussed (Chapter 4.3.2), this method of assigning the twist sense is potentially open to error if the dilute solution contributions to the observed ORD signal are stronger than those associated with the liquid crystalline ordering of the long pitch mesophase. Section 5.3.1 reported that for isotropic solutions of EC the sign of the optical rotation is solvent dependent and while no evidence is found for the signal strength of the dilute solution optical activity overwhelming that of the mesophase, the variability of the sign of the ORD spectra of a simple cellulose ether provides an excellent example of the reason caution must be employed when using ORD to identify the twist sense of long pitch samples.

If reflection colours are visible then the twist sense of a cholesteric liquid crystal can be easily identified by ORD. Figures 5.10 shows the ORD spectra of EC with DS of 2.29 in monochloroacetic acid and TEC in DCA. The opposite helicoidal twist senses of these two mesophases, left-handed and right-handed respectively, are reflected in the shapes of the observed pseudo-Cotton Effects.

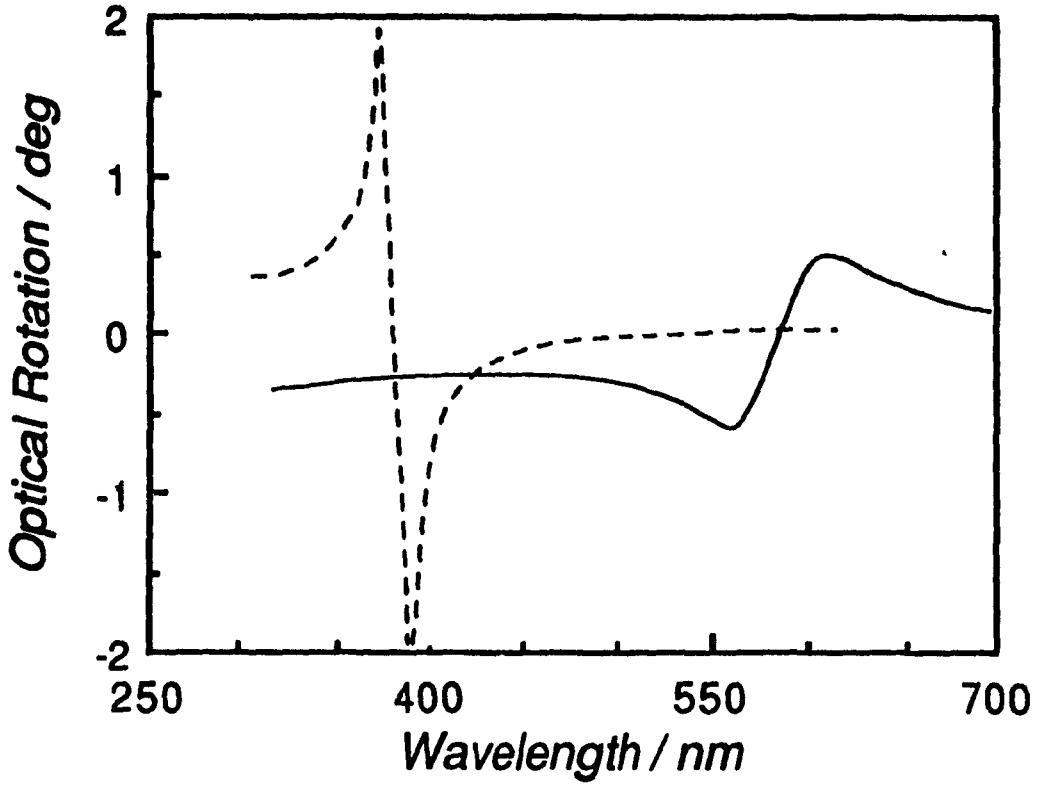

Figure 5.10 ORD spectra of mesophases of EC with DS of 2.29 in monochloroacteic acid (~45% w/w, solid line) and EC with DS of 3.00 in dichloroacetic acid (24.9% w/w, dashed line). The EC / monochloroacetic acid sample is left-handed while the EC / dichloroacetic acid sample is right-handed.

5.4 CONCLUSION

Optical Rotatory Dispersion (ORD) spectroscopy has been employed to examine isotropic and anisotropic solutions of ethyl cellulose (EC). Solvent effects are found to strongly affect the observed ORD spectra as both positive and negative dispersion curves occur, depending on the solvent employed. The degree of substitution (DS) is shown to affect the intensity of the observed optical rotations but the sign of the rotation remains the same at both high and low DS values. The optical activity of EC in chloroform and m-cresol is also affected by temperature. The possibility of solvent interaction with EC resulting in induced optical activity of the solvent molecules must be considered not only because of the anomalous dispersion curve produced by the chloroform solutions, but also because the plain negative dispersion curves provide estimates of the wavelength of maximum absorbance which are much higher than expected.

No evidence was found for a pretransitional ordering of the EC molecules prior to mesophase formation in dichloroacetic acid.

5.5 REFERENCES

(1) Chapter 4, this thesis.

(2) P. Drude, "Lehibuch der Optik, ed 2", S. Hirzel Verlas, Liepzig, 1906; as reported by G.D. Fasman, *Methods Enzymol.*, **6**, 928 (1963).

(3) W. Moffitt and J.T. Yang, *Proc Natl. Acad. Sci.*, (Wash.), **42**, 596 (1956); as reported by E. Charney, "The Molecular Basis of Optical Activity", Robert E. Krieger Publishing Company, Malabar, Florida, 1985, pp. 285.

(4) HL. de Vries, *Acta Crystallogr.*, **4**, 219 (1951).

(5) E.S. Stevens and B.K. Sathyanarayana, *Carbohydr. Res.*, **166**, 181 (1987).

(6) E.S. Stevens and B.K. Sathyanarayana, *Biopolymers*, **27**, 415 (1988).

(7) A.J. Stipanovic and E.S. Stevens, *J. Appl. Polym. Sci.: Appl. Polym. Symp.*, **37**, 277 (1983).

(8) A.M. Ritcey, Ph.D. Thesis, McGill University, 1987.

(9) D.L. Patel and D.B. Dupré, *Mol. Cryst. Liq. Cryst.*, **53**, 323 (1979).

(10) A.S. Buntjakov and V.M. Averyanova, *J. Polym. Sci.: Part C*, **38**, 109 (1972).

(11) Chapter 3, this thesis.

(12) T.V. Samulski and E.T. Samulski, *J. Chem. Phys.*, **67**, 824 (1977).

CHAPTER 6

CONCLUSION

6.1 GENERAL SUMMARY AND CONCLUSIONS

All cellulose derivatives possess the same chiral backbone, but a survey of the literature on the liquid crystalline properties of different cellulosics reveals a variety of chiroptical behaviours. It is therefore difficult to develop a set of criteria that would permit reliable predictions to be made about the behaviour of new cellulose derivatives. What are the factors that determine the liquid crystalline behaviour and how sensitive are mesophases to variations in these factors? This question has never been suitably addressed, but by studying a single cellulose derivative under a variety of conditions this thesis has demonstrated that the liquid crystalline properties are so sensitive to minor variations in the solution matrix that the supposition of a predictable behaviour based on the existence of a common backbone or even by the presence of a particular sidechain type is unfounded.

The primary polymer of interest to this study is ethyl cellulose (EC). As a first step towards examining the chain stiffness and liquid crystalline phase separation behaviour of EC in a variety of solvents, literature data on the intrinsic viscosity / molar mass relationship of several cellulose derivatives was employed to establish that (i) the Bohdanecky hydrodynamic theory is a viable adaptation of the Yamakawa and Fujii model for estimating the molecular dimensions of cellulosic chains in solution and that (ii) the freely-jointed lattice theory of Flory and the freely-jointed virial expansion theory of Grosberg and Khokhlov provide better estimates of the critical volume fractions for liquid crystalline phase separation than the wormlike chain theory of Odijk. No basis was found for favouring either the lattice model or the virial expansion model for these derivatives as the literature experimental results usually fall between the predicted estimates of the two theories. Literature data on the intrinsic viscosity / molar mass relationship of EC in several solvents was re-interpreted to (i) determine the Mark-Houwink-Sakurada (MHS) constants, (ii) calculate its dimensions in several solvents by measuring the apparent partial specific volume and using the Bohdanecky hydrodynamic theory and (iii) compare the predicted critical volume fractions for mesophase formation with the experimentally determined values. Potential errors in the all these data were evaluated by determining the confidence limits. Based on the confidence limits, a wide range of possible values were

obtained for the MHS exponent which means that reliable estimates of relative chain stiffness are difficult to assign. Minor scatter in the data resulted in a wide range of estimates for the equivalent Kuhn segment length and diameter, and because a wide range of estimates for the molecular dimensions exist, the predicted values for the critical volume fraction are also very broad. However, despite the breadth of the predicted possible critical volume fractions, the lattice theory of Flory was found to be superior to virial expansion theory of Grosberg and Khokhlov for all those solvents in which EC forms a mesophase. EC does not form a mesophase in several solvents in which it is calculated to have a high axial ratio. Two possible reasons for this behaviour are postulated: (i) the necessity of a thermodynamically favourable solvent in addition to chain stiffness, and (ii) a non-draining effect that affects values of $[\eta]_0$ and therefore the calculated molecular dimensions and critical volume fractions.

A commercial sample of EC was reacted with varying quantities of iodoethane to produce EC samples of with a range of DS values. Reaction of EC with iodomethane and 1-iodobutane produced samples of O-(ethyl)(methyl)cellulose (EMC) and O-(n-butyl)(ethyl) cellulose (BEC). These samples are the EC analogs and mixed ether derivatives that permit a study of the effect of minor variations in the number and size of the sidechains on the liquid crystalline properties.

Circular Reflectance (CR) spectroscopy was used to investigate the structural properties of the mesophases of EC and its derivatives in several solvents for those samples which exhibit reflection colours. The difficulty of developing a model which adequately predicts the twist sense and temperature dependence of the pitch or reflection wavelength is vividly illustrated as solvent effects and / or minor changes in the DS were found to produce an unparalleled range of behaviours. For example, EC with DS of 2.29 forms a left-handed mesophase in most solvents, but both increases and decreases in reflection wavelength with increasing temperature can be seen for these left-handed mesophases depending on the solvent employed. The extreme sensitivity of the mesophase properties to increases in the DS are best illustrated by the EC / m-cresol and EC / chloroform samples. For EC / chloroform samples, an increase in the DS produces a change in the twist sense and while the reflection wavelength of the left-handed

mesophase decreases with increasing temperature, the reflection wavelength of the right-handed mesophase increases. For EC in m-cresol, an increase in DS under constant conditions produces a substantial increase in reflection wavelength but no change in the twist sense. However, the temperature dependence of the reflection wavelength is also governed by the DS as at a DS of 2.29 the reflection wavelength increases with temperature while at DS values of 2.70 and 2.80 the reflection wavelength decreases; at an intermediate DS of 2.55 there is no change in the reflection wavelength.

CR studies of the mixed ether derivatives of EC in chloroform and dichloromethane show that the cholesteric twist sense in these solvents is not merely a function of the total DS of the polymer. The fully substituted EMC and low DS EC samples are left-handed, but the fully substituted BEC samples, like TEC, form right-handed mesophases. It therefore appears that the size of the substituent introduced to the EC chain can play a role in determining the twist sense of the mesophase. The derivatives of EC form films with frozen-in cholesteric order and reflection colours, but heating these films to their clearing temperature produces no variations in the reflection wavelength which suggests that these derivatives are below the critical size required to induce pure thermotropic behaviour.

Optical Rotatory Dispersion (ORD) spectroscopy was employed to examine EC and some of its derivatives to determine if there are equivalent behavioural differences in isotropic solutions of these polymers. The sign of the optical rotation and shape of the ORD spectra were found to be solvent dependent and evidence was found which suggests that interactions between the solvent and polymer may be occurring. The possibility of solvent interaction is a significant finding as the liquid crystalline properties have been shown to be defined by the solvent employed.

6.2 CONTRIBUTIONS TO ORIGINAL KNOWLEDGE

The data in this thesis represent the first systematic examination of the sensitivity of the liquid crystalline properties of a cellulose derivative to several variables. The following claims to original research are made:

(1) The Bohdanecky hydrodynamic theory was applied to several cellulose derivatives that have already had their molecular dimensions calculated by the Yamakawa - Fujii model and established that the Bohdanecky model is a viable adaptation of the Yamakawa - Fujii theory for determining molecular dimensions. Based on the molecular dimensions determined by the Bohdanecky theory, the liquid crystalline phase separation behaviour was examined according to three theories and a comparison was made between the predicted results and the literature values of the critical volume fraction for mesophase formation.

(2) The liquid crystalline phase separation behaviour of a single cellulose derivative in several solvents was investigated. Literature data on the intrinsic viscosity / molar mass relationship of EC in several solvents was re-interpreted to obtain the MHS constants, the molecular dimensions derived by the Bohdanecky model and the predicted critical volume fractions for mesophase formation in these solvents; a comparison was made with the experimental critical volume fraction values. It was demonstrated that EC does not form a mesophase in several solvents in which it is predicted to have an extended backbone. The calculation of confidence limits for the MHS constants, molecular dimensions and predicted critical volume fractions showed that even minor scatter in the data can have a significant impact on the calculated parameters.

(3) EC is the first polymer found to form mesophases of the same twist sense that can increase or decrease in pitch with increasing temperature depending on the solvent employed.

(4) It has been demonstrated that a cellulose derivative can display complex liquid crystalline chiroptical behaviour depending on the DS.

- The twist sense of EC in some solvents can be reversed by changing the DS.
- The reflection wavelengths of left-handed mesophases of EC (DS = 2.29) in chloroform were shown to decrease with increasing temperature while right-handed mesophases of EC (DS = 3.00) in chloroform increased in reflection wavelength.
- Under constant conditions, increases in the DS were shown to increase the reflection wavelength of left-handed mesophases while a right-handed one was shown to decrease.
- EC is found to form a mesophases of a single twist sense whose reflection wavelengths can increase or decrease with increasing temperature as a function of DS.

(5) The cholesteric twist senses of EC derivatives in chloroform and dichloromethane were shown to be affected by the size of the substituent and not just the total DS.

(6) Cast films of the EC derivatives were found to possess frozen-in cholesteric structure and measurable reflection wavelengths.

(7) The signs of the optical rotations and shapes of the ORD spectra of isotropic solutions of EC were shown to be solvent dependent.

6.3 SUGGESTIONS FOR FURTHER RESEARCH

The data in this thesis have demonstrated that solvent effects and the DS have a much greater effect on the isotropic and anisotropic properties of a cellulose derivative than previously realized. These results open numerous new avenues of investigation. Some of the topics that would yield informative data include:

(1) It is not known to what extent draining effects play a role in the viscosity measurements of the EC solutions. A non-hydrodynamic investigation of the solution conformation of EC in the various solvents employed in Chapter 3 might allow this to be established. Should draining effects prove to be negligible or identical for all the EC / solvent systems, the thermodynamic properties of the EC / solvent systems at concentrations ranging from the isotropic to the anisotropic states should be studied.

(2) A study should be conducted with other cellulose derivative mesophases as a function of DS to determine if the effects observed with EC are unique or if all cellulosics are similarly affected.

(3) Specifically substituted cellulose derivatives should be prepared and their mesophases studied to determine the role of not only DS but also of site occupation.

(4) An NMR investigation of EC with DS of 2.29 and 3.00 mesophases in deuterated chloroform would be of interest. These mesophases are left-handed and right-handed, respectively, and respond differently to increases in temperature. Due to their almost identical molecular character, it might be possible to discern information that would not be forthcoming from a comparison of cellulose derivatives possessing different sidechains and may provide clues as to the role DS plays in establishing the twist sense.

(5) The possibility of specific interactions between polymer and solvent should be investigated to determine if they do occur and if so, how they impart different mesophase properties such as cholesteric twist sense and pitch responses to variations in temperature.

(6) EMC in chloroform and EC with DS of 3.00 in chloroform form mesophases that have left-handed and right-handed twist senses, respectively. An investigation of the miscibility of these two polymers in chloroform would be of interest because preliminary optical studies of both liquid crystals and cast films prepared from mixtures of the two polymers suggest that they are miscible.

APPENDIX A

The following tables contain the data employed in this thesis to compute the molecular dimensions of several cellulose derivatives according to the Bohdanecky theory in Chapter 3. All intrinsic viscosity data are reported in units of $cm^3\ g^{-1}$.

Intrinsic Viscosity of Cellulose Triacetate in Several Solvents [a, b]

Molar Mass	TFA	Acetone	DCM	TCE	TCM	DMAC
690,000	508	480	306	270	272	607
500,000	434	398	260	243	228	490
444,000	385	357	-	214	210	451
308,000	286	282	184	168	171	350
262,000	-	265	-	163	-	327
200,000	228	211	136	129	129	256
149,000	-	154	-	98	-	195
137,000	164	143	100	95	97	183
82,200	118	110	71	73	69	131
63,600	96	-	59	60	-	102

[a] Measured by K. Kamide, Y. Miyazaki and T. Abe, *Polym. J.*, **11**, 523 (1987).

[b] TFA = trifluoroacetic acid, DCM = dichloromethane, TCE = tetrachloroethane, TCM = trichloromethane, DMAC = dimethylacetamide.
$\bar{v}$ = 0.68 in Acetone, 0.744 in TCE (as reported by M. Kurata, M. Iwama and K. Kamada, "Polymer Handbook", (J. Brandrup and E.H. Immergut, eds.), Interscience Publishers, New York, 1966, Ch. IV) and is taken as 0.744 in all other solvents.

Intrinsic Viscosity of (Acetoxypropyl)cellulose in Dimethylphthalate [a]

Molar Mass	Intrinsic Viscosity
432,000	203
352,000	146
194,000	129
133,000	96
76,700	45
21,800	14

[a] Measured by G.V. Laivins and D.G. Gray, *Macromolecules*, **18**, 1746 (1985).
$\bar{v}$ taken as 0.825

Intrinsic Viscosity of (Hydroxypropyl)cellulose in Several Solvents

Molar Mass	DMAC [a]	Ethanol [a]	DCA [b]
252,000	-	-	228
248,800	208	225	-
206,800	-	190	-
195,000	-	-	180
181,000	-	-	168
151,600	142	143	-
122,900	107.5	118	-
115,000	-	-	111
94,700	86	93	-
63,000	-	-	64
57,000	49.4	58.5	-
46,000	-	-	48.5
25,900	28.4	28.4	-
19,600	-	-	22

[a] Measured by C. Conio, E. Bianchi, A. Ciferri, A. Tealdi and A. Aden, *Macromolecules*, **16**, 1264 (1983). DMAC = dimethylacetamide.

[b] Measured by M.A. Aden, E. Bianchi, A. Ciferri, A. Conio and A. Tealdi, *Macromolecules*, **17**, 2010 (1984). DCA = dichloroacetic acid. $\bar{v} = 0.821$ in DMAC, 0.833 in Ethanol and 0.790 in DCA.

Intrinsic Viscosity of BzPC in Acetone and Benzene [a]

Molar Mass	Acetone	Benzene
1,130,000	214	281
694,000	154	185
434,000	110	140
413,000	90	127
290,000	73	98
219,000	55	69
119,000	30	39
79,700	20	25

[a] Measured by S.N. Bhadani, S.-L. Tseng and D.G. Gray, *Die Makromol. Chem.*, **184**, 1727 (1983). $\bar{v}$ is assumed to be 0.825.

Intrinsic Viscosity of Cellulose Tricarbanilate in Acetone and Dioxane [a]

Molar Mass	Acetone	Dioxane
2,665,000	910	1400
1,915,000	650	1130
1,840,000	580	-
950,000	480	830
874,000	405	750
742,000	344	595
579,000	310	520
402,000	230	415
292,000	171	274
248,000	160	262
247,000	174	310
188,000	112	180
185,000	110	172
127,000	92	138
90,700	67	97
67,200	50	68

[a] Measured by W. Burchard and E. Husemann, *Die Makromol. Chem.*, **44-46**, 358 (1961).
$\bar{v} = 0.72$ in dioxane (as reported by M. Kurata, M. Iwama and K. Kamada, "Polymer Handbook", (J. Brandrup and E.H. Immergut, eds.), Interscience Publishers, New York, 1966, Ch. IV) and is assumed to be 0.72 in acetone.

Intrinsic Viscosity of Nitrocellulose in Acetone

Molar Mass	Intrinsic Viscosity
2,490,000	5300
630,000	1530
456,000	1160
262,000	700
242,000	770
178,000	525
90,000	295
74,500	237
46,000	165
40,000	104
23,500	66
18,000	42.5
13,000	36

[a] Measured by G. Meyerhoff, *J. Polym. Sci.*, **29**, 399 (1958).
$\bar{v} = 0.51$ (as reported by M. Kurata, M. Iwama and K. Kamada, "Polymer Handbook", (J. Brandrup and E.H. Immergut, eds.), Interscience Publishers, New York, 1966, Ch. IV).